

**Svitlana Antoniuk**

**INTERPLAY BETWEEN SEROTONIN 5-HT<sub>1A</sub> AND 5-HT<sub>7</sub>  
RECEPTORS IN STRESS-RELATED DISORDERS**

PhD thesis

Completed in the Laboratory of Cell Biophysics  
of the Nencki Institute of Experimental Biology  
Polish Academy of Sciences

**SUPERVISORS:**

**Prof. J. Wlodarczyk, PhD, DSc.**

**Prof. E. Ponimaskin, PhD, DSc.**

This work has been supported by the European Union's Horizon 2020 research and innovation programme under the Marie Skłodowska-Curie grant agreement no 665735 (Bio4Med).

**Warsaw, 2021**

## AUTHOR'S DECLARATION

I, the undersigned(s) Svitlana Antoniuk consent to the storage and release of my dissertation, titled 'INTERPLAY BETWEEN SEROTONIN 5-HT<sub>1A</sub> AND 5-HT<sub>7</sub> RECEPTORS IN STRESS-RELATED DISORDERS' by the M. Nencki Institute of Experimental Biology PAS Library in a printed form, in a reading room and as a part of interlibrary loans, on the basis of free use.

At the same time I grant the M. Nencki Institute of Experimental Biology PAS a free non-exclusive license to use the above work without time and territorial limitation in the following fields of exploitation:

- 1) placing the content of the thesis as a pdf file together with metadata in the digital repository RCIN (*Digital Repository of Scientific Institutes*, collection: *Institute of Experimental Biology PAS/Dissertations*) located at the following address <https://rcin.org.pl/dlibra/collectiondescription/121>
- 2) digital multiplication of the work (digitalization of the work if it is necessary to scan the printed version)

Warsaw, Poland .....

Signature .....

## ACKNOWLEDGMENTS

I would like to thank Prof. Evgeni Ponimaskin and Prof. Jakub Wlodarczyk for their supervision, support, and constructive criticism throughout my studies. Special thanks should be given to my co-supervisors – Dr. Alexander Wirth and Dr. Monika Bijata for the guidance and inspiration.

Moreover, I want to thank all my colleagues and friends at Hannover Medical School and Nencki Institute of Experimental Biology: Dr. Nataliya Gorinski, Dr. Andre Zeug, Dr. Franziska Mueller, Dr. Josephine Labus, Dalia Abdel Galil, Tania Bunke, Dr. Izabela Figiel, Dr. Monika Zaręba-Kozioł, Ewa Bączyńska, Dr. Adam Krzystyniak, Dr. Marta Magnowska, and Dr. Matylda Roszkowska. All of you have contributed to my project a lot and have always been ready to help me at any time.

Additionally, I would like to appreciate the collaboration with Dr. Ewelina Knapska and the Laboratory of Emotions Neurobiology during performing Ecohab studies.

Furthermore, I am grateful to Prof. Kjell Fuxe and Dr. Dasiel Borroto Escuela for the valuable training of proximity ligation assay technique and hospitality at Karolinska Institute.

I would like to express all my love to my family for their understanding and encouragement, always being for me through ups and downs.

# TABLE OF CONTENTS

<b>LIST OF ABBREVIATIONS</b> .....	6
<b>ABSTRACT</b> .....	8
<b>STRESZCZENIE</b> .....	10
<b>1. INTRODUCTION</b> .....	12
1.1. Serotonergic theory of depression .....	12
1.2. Serotonergic system .....	12
1.3. 5-HT <sub>1A</sub> receptor .....	15
1.4. 5-HT <sub>7</sub> receptor .....	19
1.5. Functional crosstalk between 5-HT <sub>1A</sub> and 5-HT <sub>7</sub> receptors .....	22
1.6. Animal models of depression .....	25
<b>2. AIM OF THE STUDY</b> .....	27
<b>3. MATERIALS</b> .....	28
3.1. Theoretical study based on meta-analysis .....	28
3.1.1. Selection of strategy criteria for assessment of sucrose preference test efficiency for modeling of depressive-like behavior in rodents .....	28
3.1.2. Data extraction and characteristics of the included articles .....	28
3.1.3. Statistical analysis .....	29
3.2. Experimental studies .....	30
3.2.1. Materials .....	30
3.2.1.1. Chemicals and materials .....	30
3.2.1.2. Antibodies .....	31
3.2.1.3. Kits and equipment .....	31
3.2.1.4. Buffers and solutions .....	32
<b>4. METHODS</b> .....	33
4.1. Behavioral studies .....	33
4.1.1. Animals and housing conditions .....	33
4.1.2. Stimulation of 5-HT <sub>1A</sub> and 5-HT <sub>7</sub> receptors <i>in vivo</i> .....	33
4.1.3. Mouse model of depression based on modified CUS protocol .....	33
4.1.4. Sucrose preference test .....	35
4.1.5. Forced swimming test .....	35
4.1.6. Tail suspension test .....	35
4.1.7. Eco-Hab .....	36
4.2. Molecular biology .....	36
4.2.1. Quantitative real-time polymerase chain reaction .....	36
4.2.2. Bicinchoninic acid assay .....	38
4.2.3. Sodium dodecyl sulphate polyacrylamide gel electrophoresis .....	39
4.2.4. Western blotting .....	39
4.3. Histology .....	39
4.3.1. 5-HT <sub>1A</sub> R, 5-HT <sub>7</sub> R, and 5-HT immunohistochemistry .....	40
4.3.2. <i>In situ</i> proximity ligation assay .....	40
4.4. Microscopy and images analysis .....	41

4.5. Bioinformatics .....	42
4.6. Statistical analysis.....	42
<b>5. RESULTS</b> .....	<b>43</b>
5.1. Validation of tools for CUS modeling in rodents based on meta-analysis.....	43
5.2. Role of the 5-HT <sub>1A</sub> R and 5-HT <sub>7</sub> R activation in mouse behavior .....	49
5.3. Assessment of 5-HT <sub>1A</sub> R and 5-HT <sub>7</sub> R protein expression during brain development .....	50
5.4. Investigation of 5-HT <sub>1A</sub> R and 5-HT <sub>7</sub> R heterodimerization profile.....	54
5.4.1. Validation of mouse behavioral profile upon CUS application .....	54
5.4.2. Immunohistological staining of 5-HT <sub>1A</sub> and 5-HT <sub>7</sub> receptors .....	55
5.4.3. 5-HT <sub>1A</sub> R and 5-HT <sub>7</sub> R heterodimerization.....	57
5.5. Effects of CUS on 5-HT <sub>1A</sub> R and 5-HT <sub>7</sub> R expression.....	62
<b>6. DISCUSSION</b> .....	<b>65</b>
6.1. Meta-analysis of chronic unpredictable stress applicability in rodents.....	65
6.2. Role of 5-HT <sub>1A</sub> R and 5-HT <sub>7</sub> R in stress-related disorders .....	66
6.3. Heterodimerization of 5-HT <sub>1A</sub> and 5-HT <sub>7</sub> receptors.....	71
<b>7. SUMMARY AND CONCLUSIONS</b> .....	<b>74</b>
<b>8. REFERENCES</b> .....	<b>75</b>

## LIST OF ABBREVIATIONS

<b>MDD</b>	Major depressive disorder
<b>5-HT</b>	Serotonin
<b>5-HT<sub>1A</sub>R</b>	Serotonin receptor 1A
<b>5-HT<sub>7</sub>R</b>	Serotonin receptor 7
<b>5-HTP</b>	5-hydroxytryptophan
<b>AC</b>	Adenylyl cyclase
<b>Akt</b>	Protein kinase B
<b>AMPA</b>	$\alpha$ -amino-3-hydroxy-5-methyl-4-isoxazolepropionic acid
<b>BCA</b>	Bicinchoninic acid
<b>BDNF</b>	Brain-derived neurotrophic factor
<b>BRET</b>	Bioluminescence resonance energy transfer
<b>CA1</b>	Cornu Ammonis 1
<b>CA3</b>	Cornu Ammonis 3
<b>CAMKII</b>	Calmodulin-dependent protein kinase II
<b>cAMP</b>	Cyclic adenosine monophosphate
<b>cDNA</b>	Complementary deoxyribonucleic acid
<b>CHO cells</b>	Chinese hamster ovary cells
<b>CNS</b>	Central nervous system
<b>CRS</b>	Chronic restraint stress
<b>CSDS</b>	Chronic social defeat stress
<b>CUS</b>	Chronic unpredictable stress
<b>DG</b>	Dentate gyrus
<b>ERK 1/2</b>	Extracellular signal-regulated protein kinases 1 and 2
<b>FGFR1</b>	Fibroblast growth factor receptor 1
<b>FRET</b>	Förster resonance energy transfer
<b>GABA</b>	Gamma-aminobutyric acid
<b>GIRK channels</b>	G protein-coupled inwardly-rectifying potassium channels
<b>GPCRs</b>	G-protein coupled receptors
<b>GTP</b>	Guanosine triphosphate
<b>GSK3<math>\beta</math></b>	Glycogen synthase kinase 3 beta
<b>HPA axis</b>	Hypothalamic-pituitary-adrenal axis

<b>MEK</b>	Mitogen-activated protein kinase
<b>mRNA</b>	Messenger ribonucleic acid
<b>NMDA</b>	N-methyl-D-aspartate
<b>PBS</b>	Phosphate-buffered saline
<b>PDGFR</b>	Platelet-derived growth factor receptor
<b>PET</b>	Positron emission tomography
<b>PIK3</b>	Phosphoinositide 3-kinase
<b>PKA</b>	Protein kinase A
<b>PKC</b>	Protein kinase C
<b>PLA</b>	Proximity ligation assay
<b>PLC</b>	Phospholipase C
<b>qRT-PCR</b>	Quantitative real-time polymerase chain reaction
<b>RGS</b>	Regulators of G protein signaling
<b>SDS PAGE</b>	Sodium dodecyl sulfate polyacrylamide gel electrophoresis
<b>SEM</b>	Standard error of the mean
<b>SMD</b>	Standardized mean difference
<b>SSRI</b>	Selective serotonin reuptake inhibitors
<b>TCA</b>	Tricyclic antidepressants
<b>VDCC</b>	Voltage-dependent calcium channels
<b>VEGF</b>	Vascular endothelial growth factor

## ABSTRACT

Stress-related disorders are highly prevalent diseases all over the world. Accumulating data indicate that the serotonergic system is strongly linked with the pathogenesis of depression. Numerous studies based on molecular biology, genetic, histological, and behavioral approaches have shown that serotonin receptors, in particular 5-HT<sub>1A</sub> and 5-HT<sub>7</sub>, might mediate the stress response in both rodents and humans. However, mechanisms explaining an involvement of 5-HT<sub>1A</sub> and 5-HT<sub>7</sub> receptors in stress-related diseases are not completely understood. Previous studies of our research group have shown that 5-HT<sub>1A</sub> and 5-HT<sub>7</sub> receptors form heterodimers in the recombinant system, in neuronal cultures and in the mouse brain, which in turn leads to changes in the receptor-mediated signaling. In this regard, the aim of this project was to investigate functional implication of 5-HT<sub>1A</sub>R/5-HT<sub>7</sub>R heterodimerization by modeling depression in animals.

First, a theoretical study based on meta-analysis was performed to verify the applicability of the chronic unpredictable stress protocol for modeling depression in different strains of rodents. Using this approach, we have demonstrated that both rats and mice showed anhedonic behavior after implementation of the chronic unpredictable stress protocol. In this study, C57BL/6J mice were chosen as the best model due to their higher susceptibility to stress protocol upon shorter stress duration in comparison to other rodent strains, availability of transgenic lines bred on C57BL/6J genetic background, and lower cost of depression modeling compared to rats. The depressive phenotype was assessed based on anhedonic and despair parameters as well as body weight fluctuation.

Second, the investigation of 5-HT<sub>1A</sub> and 5-HT<sub>7</sub> receptors expression profiles in different mouse brain regions during postnatal development was performed. Thus, our data have shown that the 5-HT<sub>1A</sub>R protein level was upregulated in the prefrontal cortex and hippocampus compared to the raphe nuclei, whereas the level of the 5-HT<sub>7</sub>R did not differ. Additionally, applying qRT-PCR it has been demonstrated that the 5-HT<sub>1A</sub>Rs mRNA is the dominant subpopulation in comparison to the 5-HT<sub>7</sub>Rs mRNA in the prefrontal cortex and hippocampus during brain development.

Third, the interaction between 5-HT<sub>1A</sub> and 5-HT<sub>7</sub> receptors using depression-like model in C57BL/6J mice was investigated. Noteworthy, the most prominent changes in heterodimerization profile of 5-HT<sub>1A</sub> and 5-HT<sub>7</sub> receptors were observed in the medial prefrontal cortex and hippocampal dentate gyrus of C57BL/6J mice. We have obtained a decrease in the number of 5-HT<sub>1A</sub>R/5-HT<sub>7</sub>R heterodimeric complexes in the stressed anhedonic mice in comparison to stressed control and stressed resilient animals. In contrast, no significant changes in the 5-HT<sub>1A</sub>R and 5-HT<sub>7</sub>R heterodimerization profile were detected in the dorsal raphe nuclei.

In conclusion, our data revealed that the chronic unpredictable stress paradigm represents a robust and reproducible model for the depression-like behavior in rodents. Moreover, the number of 5-HT<sub>1A</sub>R/5-HT<sub>7</sub>R heterodimers was decreased in the prefrontal cortex of C57BL/6J mice upon chronic unpredictable stress, suggesting functional role of 5-HT<sub>1A</sub>R and 5-HT<sub>7</sub>R interaction in development of depressive-like behavior.

## STRESZCZENIE

Choroby związane ze stresem są bardzo rozpowszechnione na całym świecie. Dotychczas zgromadzone dane wskazują na istnienie związku pomiędzy układem serotonergicznym a patogenezą depresji. Liczne badania z zastosowaniem technik biologii molekularnej, genetyki, histologii oraz badania behawioralne wykazały, że receptory serotoninowe, w szczególności 5-HT<sub>1A</sub> i 5-HT<sub>7</sub> (5-HT<sub>1A</sub>R i 5-HT<sub>7</sub>R), mogą pośredniczyć w odpowiedzi na stres zarówno u gryzoni, jak i u ludzi. Jednak mechanizmy wyjaśniające udział tych receptorów w chorobach związanych ze stresem nie są do końca poznane. Nasze wcześniejsze badania, przeprowadzone na mózgu myszy oraz w pierwotnych hodowlach komórek nerwowych pokazały, że 5-HT<sub>1A</sub>R i 5-HT<sub>7</sub>R mogą tworzyć heterodimery, co prowadzi do zmian w sygnalizacji serotonergiczej. W związku z tym, celem niniejszego projektu było zbadanie funkcjonalnej implikacji heterodimeryzacji 5-HT<sub>1A</sub>R/5-HT<sub>7</sub>R poprzez modelowanie depresji u zwierząt.

Na wstępie przeprowadzono teoretyczne badania oparte na metaanalizie. Pozwoliło to na zweryfikowanie przydatności protokołu przewlekłego nieprzewidywalnego stresu do modelowania depresji u różnych szczepów gryzoni. Po wdrożeniu tego protokołu zaobserwowaliśmy, że zarówno szczury, jak i myszy wykazywały zachowanie anhedoniczne. Do badań zostały wybrane myszy C57BL/6J, ze względu na ich wyższą podatność na stres w porównaniu z innymi szczepami gryzoni, dostępność linii transgenicznych wyhodowanych na tym samym tle genetycznym oraz niższy koszt modelowania depresji w porównaniu do szczurów. Fenotyp depresyjny oceniano na podstawie trzech parametrów: anhedonii, motywacji oraz spadku masy ciała.

Następnie przeprowadzono badanie profilu ekspresji 5-HT<sub>1A</sub>R i 5-HT<sub>7</sub>R w różnych obszarach mózgu myszy w trakcie rozwoju pourodzeniowego. Wykazano, że poziom białka 5-HT<sub>1A</sub>R był podwyższony w korze przedczołowej i hipokampie w porównaniu z jądrami szwu, natomiast poziom 5-HT<sub>7</sub>R był podobny we wszystkich badanych strukturach. Dodatkowo stosując qRT-PCR pokazano znacznie podwyższony poziom mRNA 5-HT<sub>1A</sub>R w korze przedczołowej i hipokampie, w porównaniu z mRNA kodującym 5-HT<sub>7</sub>R.

Z kolei zbadano interakcję pomiędzy 5-HT<sub>1A</sub>R i 5-HT<sub>7</sub>R w mózgu myszy C57BL/6J poddanych przewlekłemu nieprzewidywalnemu stresowi. Największe zmiany w profilu heterodimeryzacji wspomnianych receptorów zaobserwowano w przyśrodkowej korze przedczołowej i w zakręcie zębatym hipokampa. W tych obszarach mózgu wykazano zmniejszoną liczbę heterodimerycznych kompleksów 5-HT<sub>1A</sub>R/5-HT<sub>7</sub>R u myszy anhedonicznych poddanych stresowi w porównaniu do stresowanych zwierząt kontrolnych i zwierząt opornych na stres (*ang. resilient*). Co ciekawe, nie wykryto znaczących zmian w profilu heterodimeryzacji 5-HT<sub>1A</sub>R i 5-HT<sub>7</sub>R w grzbietowych jądrach szwu.

Podsumowując, nasze badania potwierdziły, że paradygmat przewlekłego nieprzewidywalnego stresu stanowi solidny i powtarzalny model depresji u gryzoni. Pokazaliśmy również spadek liczby heterodimerów 5-HT<sub>1A</sub>R/5-HT<sub>7</sub>R w korze przedczołowej myszy C57BL/6J poddanych stresowi, co sugeruje funkcjonalną rolę interakcji tych receptorów serotoniny w rozwoju zachowań podobnych do objawów depresji.

# 1. INTRODUCTION

## 1.1. Serotonergic theory of depression

A recent report of the World Health Organization has shown that depression affects about 350 million people worldwide, leading to a wide range of disabilities (Li et al., 2017). Although the first description of mood disorders was stated by Hippocrates in the 5th century B.C., the current classification of depressive disorders is generally in line with Hippocrates's definition. Noteworthy, patients are identified both with melancholic and atypical subtypes of depression that complicates the diagnosis (Bosaipo et al., 2017). Although considerable research has been devoted to shed light on the pathophysiology of depression, there is still a lack of widely accepted biological markers of depressive disorders (Horwitz et al., 2017).

The involvement of serotonin (5-HT) in mental disorders was suggested by Wooley and colleagues (Woolley and Shaw, 1954). In further studies, Schildkraut (Schildkraut, 1965) and Coppen (Coppen, 1967) underlined the possible role of serotonin in stress-related disorders. Noteworthy, the 5-HT hypothesis postulated a deficit of serotonin as a primary cause, reversed by antidepressants, which would restore normal function in depressed patients. Interestingly, genetic, neurochemical, neuroimaging, and pharmacological studies have shown that functional deficits of serotonergic neurotransmission in brain circuits are associated with the pathophysiology of major depressive disorder (MDD) (Belmaker, 2008). Additionally, it was demonstrated that relatives of MDD patients are more sensitive to the depletion of tryptophan/5-HT (Benkelfat, 1994). The evidence that altered serotonergic function is present in MDD patients in remission (Bhagwagar et al., 2004) suggests the implication of 5-HT in vulnerability to MDD.

## 1.2. Serotonergic system

Serotonin was discovered in 1937 by Vialli and Erspamer in enterochromaffin cells of the gut and named as 'enteramine'. In 1948, it was identified as a vasoconstrictor in blood serum, where it was mentioned as 'serotonin' (Rapport et al., 1948). Afterwards, scientists recognized that these substances were identical (Erspamer and Asero, 1952). Serotonin was accepted as a neurotransmitter, when it was discovered

in extracts from the mammalian brain (Twarog and Page, 1953), and the existence of three receptor families (5-HT<sub>1-3</sub>) was described.

Serotonin is one of the most preserved biologically active compounds found across all eukaryote kingdoms, including protists, plants, fungi, and animals. It is involved in the regulation of cardiovascular homeostasis, gastrointestinal motility, endocrine functions, thermoregulation, mood, sex, appetite, aggression, sleep/wake cycle, cognition, and memory (Barnes and Sharp, 1999; Nichols and Nichols, 2008). Serotonergic distribution is divided into central and peripheral. The peripheral subsystem includes the gastrointestinal tract, pancreatic tissue, heart, lung, blood vessels, and platelets and contains the greatest concentration (90%) of 5-HT. Conversely, only a relatively small amount of 5-HT is found in the central nervous system. The majority of cell bodies of serotonergic neurons are located in the raphe nuclei, within the reticular formation of the brainstem, whereas their complex axonal systems innervate virtually all CNS regions, including the cerebral cortex, limbic structures, basal ganglia, brainstem regions, and the gray matter of the spinal cord (Bortolato et al., 2013). At the biochemical level, serotonin is derived from L-tryptophan through two enzymatic reactions: hydroxylation of L-tryptophan into 5-hydroxytryptophan (5-HTP) and decarboxylation of 5-HTP resulting in 5-hydroxytryptamine. These reactions are mediated by the tryptophan hydroxylase and aromatic amino acid decarboxylase, respectively. Serotonin is stored in presynaptic vesicles and released from nerve terminals upon neuronal firing (Bortolato et al., 2013).

Serotonin receptors belong to the rhodopsin family of G-protein coupled receptors (GPCRs), except for the 5-HT<sub>3</sub> receptor, which is a ligand-gated ion channel (Fig. 1) (Angers et al., 2002; Berger et al., 2009). Only the 5-HT<sub>1B</sub> and 5-HT<sub>2B</sub> receptors are crystallized, whereas many other crystal structures of serotonin receptors are based on homology modeling using the  $\beta$ 2-adrenergic receptor (Wacker et al., 2013; Wang et al., 2013). The current classification of 5-HT receptors and their subtypes is based on their molecular structure, signal transduction pathway, and operational properties. There are seven classes of 5-HT receptors, with some of these receptor classes being further subdivided into subtypes such as 5-HT<sub>1A</sub>, B, D, E, F (Hoyer et al., 2002). In humans, 15 genes encoding serotonin receptors are known. With additional splice variants, more than 20 different functional receptors are expressed.

GPCRs are the third largest family of genes present in the human genome. It has been estimated that about 50% of all modern drugs and almost one-quarter of the top 200 best-selling drugs in 2000 modulate GPCRs activity (George et al., 2002). GPCRs consist of hydrophobic transmembrane  $\alpha$  helical segments, an extracellular amino terminus, and an intracellular carboxyl terminus. Stimulation of GPCR leads to activation of one or more members of the family of highly homologous heterotrimeric guanine nucleotide-binding proteins (G proteins) (Kobilka, 2007) (Fig. 1).

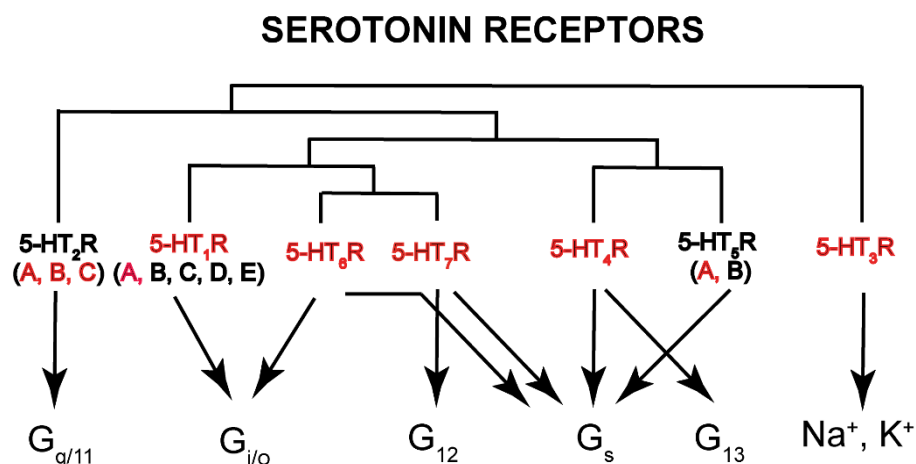


**Fig. 1. Classification of serotonin receptors**

*Serotonin receptors that have been shown to be involved in the pathogenesis of depressive disorders are shown in red*

The G protein  $\alpha$  subunit together with the bound GTP can dissociate from the  $\beta$  and  $\gamma$  subunit. Further, it affects intracellular signaling proteins or targets functional proteins directly depending on the  $\alpha$  subunit type –  $G_{\alpha s}$ ,  $G_{\alpha i/o}$ ,  $G_{\alpha q/11}$ ,  $G_{\alpha 12/13}$ . The G protein subunits modulate the activity of multiple downstream effectors initiating various cellular signaling pathways (Woehler et al., 2009). In particular, the 5-HT<sub>1</sub> receptors (5-HT<sub>1A</sub>, 5-HT<sub>1B</sub>, 5-HT<sub>1D</sub>, 5-HT<sub>1E</sub>, and 5-HT<sub>1F</sub>) couple preferentially to  $G_{i/o}$  with further inhibition of adenylyl cyclase (AC) resulting in reduced cyclic adenosine monophosphate (cAMP) levels. The 5-HT<sub>2</sub> receptors (5-HT<sub>2A</sub>, 5-HT<sub>2B</sub>, and 5-HT<sub>2C</sub>) mediate  $G_{q/11}$  to increase the hydrolysis of inositol phosphates and elevate cytosolic  $[Ca^{2+}]$ . On the contrary, the 5-HT<sub>4</sub>, 5-HT<sub>6</sub>, and 5-HT<sub>7</sub> receptors all couple to  $G_s$  and promote cAMP formation via activation of adenylyl cyclase (Hoyer et al., 2002). Additionally, it has been shown that 5-HT<sub>7</sub>R can couple to  $G_{12}$ , and 5-HT<sub>4</sub>R to  $G_{13}$

proteins which then regulate small GTPases (Kvachnina et al., 2005; Ponimaskin et al., 2002).

### 1.3. 5-HT<sub>1A</sub> receptor

The serotonin receptor 1A (5-HT<sub>1A</sub>) is one of the most extensively characterized members of the serotonin receptor family. Increased interest to the 5-HT<sub>1A</sub> receptor is due to its important role in the regulation of neuronal development, plasticity (Azmitia et al., 2016), functions of 5-HT neurons (Barnes and Sharp, 1999), and involvement in the mechanisms of depression, anxiety, suicide, Parkinson's disease and schizophrenia (Albert and Vahid-Ansari, 2019). The 5-HT<sub>1A</sub> receptor gene was cloned from human, rat, and mouse. It was shown that the 5-HT<sub>1A</sub> receptor gene is localized at the 5th chromosome in humans and at the 13th chromosome in mice and does not contain introns in its coding sequence. The mouse 5-HT<sub>1A</sub> receptor gene shares 94% homology with the rat and 88% homology with the human 5-HT<sub>1A</sub> receptor gene. The 5-HT<sub>1A</sub> receptor protein consists of 422 amino acids. The detailed structure of the 5-HT<sub>1A</sub> receptor gene promoter, including the position of the selective and nonselective enhancer as well as the selective silencer, was also determined (Storring et al., 1999). In addition, several rare single-nucleotide polymorphisms (SNPs) were described for the 5-HT<sub>1A</sub> receptor gene (Naumenko et al., 2014).

In the mammalian brain the 5-HT<sub>1A</sub> receptors exist as two populations – so called autoreceptors (Fig. 2) and heteroreceptors (Fig. 3). Autoreceptors reside on the soma and dendrites of serotonergic neurons in the raphe nuclei, and their activation inhibits neuronal discharges and reduces the release of serotonin (Riad et al., 2000). Heteroreceptors are expressed on non-serotonergic neurons, mainly in the limbic system (hippocampus, lateral septum, and amygdala), as well as in the prefrontal cortex, several hypothalamic and thalamic nuclei, such as the body and dendrites of glutamatergic neurons (Riad et al., 2000), axons of GABAergic neurons (Halasy et al., 1992) or cholinergic neurons (Cassel and Jeltsch, 1995). Receptors located in the medial septum regulate the release of acetylcholine (Jeltsch-David et al., 2008), in the prefrontal cortex – glutamate (López-Gil et al., 2010), and in the midbrain ventral tegmental area – dopamine (Di Matteo et al., 2008).

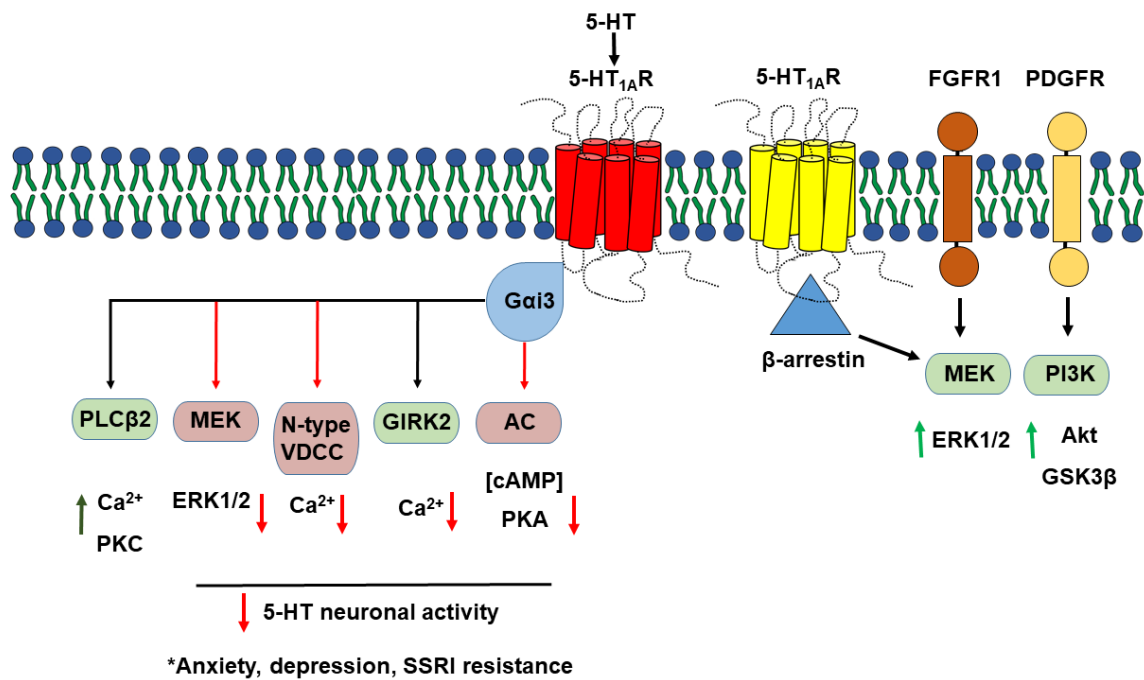


**Fig. 2. 5-HT<sub>1A</sub>R signaling in 5-HT neurons**

The 5-HT<sub>1A</sub> receptor activates various signaling pathways in the raphe nuclei. Upon binding of serotonin to the 5-HT<sub>1A</sub> receptor, G protein transduction is initiated. The G<sub>ai3</sub> subunit coupling leads to inhibition of adenylyl cyclase (AC) and protein kinase A (PKA), and reduction of L-type voltage-dependent Ca<sup>2+</sup> channel (VDCC) opening. Additionally, G<sub>βγ</sub> subunit couples to G protein inward rectifying K<sup>+</sup> (GIRK) channels, inhibits N-type VDCC; extracellular signal-regulated protein kinases 1 and 2 (ERK1/2) signaling, and activates phospholipase C (PLC), and protein kinase C (PKC). Moreover, 5-HT<sub>1A</sub> autoreceptors form hetero-complexes with fibroblast growth factor receptor 1 (FGFR1) and platelet-derived growth factor receptor beta (PDGFR1) that in turn leads to activation of ERK1/2, protein kinase B (Akt) and glycogen synthase kinase 3 beta (GSK3β). The β-arrestin-mediated 5-HT<sub>1A</sub> receptor signaling results in activation of MEK (mitogen-activated protein kinase/ERK 1/2 pathway (Albert and Vahid-Ansari, 2019 with modifications).

The 5-HT<sub>1A</sub> receptor couples to the inhibitory G proteins (G<sub>i</sub>/G<sub>o</sub>), which inhibits adenylyl cyclase, and reduces cAMP levels (Albert and Robillard, 2002). It was demonstrated that knockdown of G<sub>i2</sub> or G<sub>i3</sub> blocked 5-HT<sub>1A</sub> induced inhibition of cAMP in GH4 cells (Liu et al., 1999). More recent studies in Chinese hamster ovary (CHO) cells suggest that 8-OH-DPAT recruits G<sub>i3</sub> at higher potency than G<sub>i2</sub>, but that G<sub>i2</sub> signaling predominates at high receptor expression (Albert and Vahid-Ansari, 2019). In contrast to widely accepted G<sub>i</sub>/G<sub>o</sub>-mediated inhibition of cAMP, the 5-HT<sub>1A</sub> receptor has been shown to constitutively activate AC under certain conditions. In particular, upon co-expression of the 5-HT<sub>1A</sub> receptor and ACII in human embryonic kidney 293 (HEK293) cells, the 5-HT<sub>1A</sub> receptors stimulated cAMP formation via G<sub>βγ</sub> subunits derived from G<sub>i2</sub> (Albert et al., 1999). Additionally, specific knockdown of G<sub>ai1</sub> facilitated 5-HT<sub>1A</sub>-mediated stimulation of cAMP in neuroendocrine GH4 cells that express endogenous ACII (Liu et al., 1999). Taking into account that ACII is enriched in the hippocampus and dorsal raphe nucleus (Furuyama et al., 1993), 5-HT<sub>1A</sub>-ACII coupling may be present in these brain regions.

Interestingly, the 5-HT<sub>1A</sub> receptor coupling to phospholipase C (PLC) was shown in cell lines derived from hippocampus and raphe (Adayev et al., 2003; Kushwaha and Albert, 2005). Although coupling to this pathway has not been shown directly in the brain, the 5-HT<sub>1A</sub> receptors in the prefrontal cortex are associated with PLC<sub>β</sub> coupling and an increase of calcium calmodulin-dependent protein kinase II (CAMKII) activation (Purkayastha et al., 2012). Interestingly, Mogha et al. have shown that the 5-HT<sub>1A</sub> signaling to PKC induces synaptogenesis in the hippocampus during brain development (Mogha et al., 2012). Additionally, some studies (Kushwaha and Albert, 2005; Mogha et al., 2012) suggest that the 5-HT<sub>1A</sub> stimulation of PLC may be restricted to neurons that express PLC<sub>β2/3</sub> in an age-dependent manner.

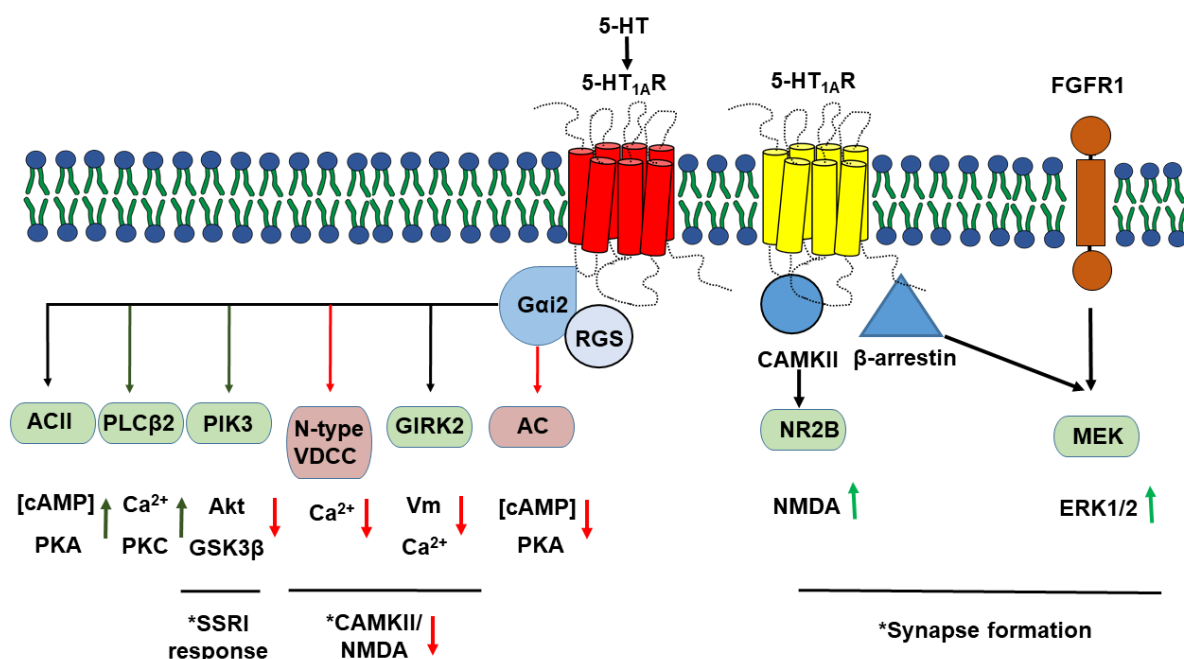


**Fig. 3. 5-HT<sub>1A</sub>R signaling in cortical and hippocampal neurons**

5-HT<sub>1A</sub> heteroreceptors are mainly identified in the hippocampus and prefrontal cortex. Upon serotonin binding to the 5-HT<sub>1A</sub> heteroreceptor, G<sub>αi2</sub> proteins inhibit adenylyl cyclase (AC), which leads to a decrease of cAMP and PKA activity, and reduction of VDCC channels opening. The G<sub>βγ</sub> subunit coupling results in activation of phosphatidylinositol 30-kinase (PI3K) and Akt, opening of GIRK channels and closing of N-type VDCC channels. On the contrary, G<sub>βγ</sub>-mediated signaling leads to activation of ACII/PLCA, PLC<sub>β2</sub>, PKC pathways. In addition, the 5-HT<sub>1A</sub> receptor are involved in the synaptogenesis via activation of CAMKII and increase of NMDA-NR2B subunits; and to the ERK1/2 pathway via dimerization with FGFR1 (Albert and Vahid-Ansari, 2019 with modifications).

Noteworthy, it was demonstrated that 5-HT<sub>1A</sub> auto- and heteroreceptors stimulate ERK1/2 signaling in the opposite manner (Kushwaha and Albert, 2005). Thus, in raphe RN46A differentiated cells the 5-HT<sub>1A</sub> receptors inhibit both adenylyl cyclase and ERK1/2 phosphorylation (Kushwaha and Albert, 2005). On the contrary, the 5-HT<sub>1A</sub> receptors in hippocampal cells increase ERK1/2 phosphorylation (Adayev et al., 2003). Wang et al. have shown that 5-HT<sub>1A</sub> heteroreceptor signaling to ERK1/2 is inhibited by

uncoupling of  $G_{i2}$  by RGS-19 regulator and enhanced by fibroblast growth factor 2 (FGF-2) in SH-SY5Y cells and hippocampal neurons (Wang et al., 2014). It was demonstrated that FGF-2/5-HT<sub>1A</sub> signaling in the raphe tissues and in the raphe cell line increases ERK1/2 activation, indicating that 5-HT<sub>1A</sub> autoreceptor signaling may depend on trophic stimulation and possible FGFR-1/5-HT<sub>1A</sub> receptor heterodimerization (Borroto-Escuela et al., 2013, 2015).

The 5-HT<sub>1A</sub> receptor also activates G protein-gated inwardly rectifying potassium channels (GIRK) via G protein  $\beta\gamma$ -subunits (Liu et al., 1999). This leads to membrane hyperpolarization, reduction of neuronal excitability and inhibition of potential-dependent calcium channels, and as a consequence – decrease of calcium influx (Chen and Penington, 1996). Noteworthy, the 5-HT<sub>1A</sub> receptors coupling to GIRKs declines upon aging and chronic stress exposure (Goodfellow et al., 2009). Although multiple GIRKs may couple the 5-HT<sub>1A</sub> receptors, GIRK2 is considered to be the most prominent. Thus, chronic glucocorticoid treatment led to down-regulation of GIRK2 channels in the raphe nuclei that corresponds to the 5-HT<sub>1A</sub> autoreceptor uncoupling upon inhibition of serotonin neurons firing (Fairchild et al., 2003). Interestingly, 8-OH-DPAT-induced hypothermia mediated by the 5-HT<sub>1A</sub> receptors was blocked in GIRK2<sup>-/-</sup> mice (Costa et al., 2005), that show resistance to depression (Llamosas et al., 2015).

The 5-HT<sub>1A</sub> receptor also couples to voltage-dependent calcium channels (VDCC) via  $G_{\alpha o}$  and  $G_{\beta\gamma}$  subunits. For instance, in the raphe nuclei, 5-HT<sub>1A</sub> receptors couple via  $G_{\beta\gamma}$  subunits to inhibit N-type VDCCs, resulting in decreased excitability (Albert and Vahid-Ansari, 2019). The 5-HT<sub>1A</sub> heteroreceptor has also been shown to reduce ionotropic glutamate receptor function. Thus, upon 5-HT<sub>1A</sub>-mediated inhibition of cAMP formation and CAMKII activity there was observed reduction in AMPA currents in rat cortical neurons (Cai et al., 2002). Similarly, the 5-HT<sub>1A</sub> signaling led to inhibition of NMDA receptor-mediated ionic and synaptic currents in the cortical pyramidal neurons, that was blocked by CaMKII (calcium/calmodulin-dependent kinase II) and MEK/ERK (mitogen-activated protein kinase/extracellular signal-regulated kinase) (Yuen et al., 2005). On the contrary, studies performed in the prefrontal cortical tissue have shown that clozapine prompted a complex formation between 5-HT<sub>1A</sub>/CAMKII and NR2B that increased NMDA currents (Purkayastha et al., 2012). Interestingly, there is an

evidence that 5-HT<sub>1A</sub> receptor activity inhibits CAMKII and reduces NMDA receptor function associated with cognitive impairment and neuroprotection in the hippocampus (Yuen et al., 2008). In line with the above-mentioned, early postnatal blocking of 5-HT<sub>1A</sub> receptors led to activation of the hippocampal CAMKII and anxiety phenotype (Lo Iacono and Gross, 2008).

#### 1.4. 5-HT<sub>7</sub> receptor

The serotonin receptor 7 (5-HT<sub>7</sub>R) was first described by three independent groups in 1993 (Bard et al., 1993; Lovenberg et al., 1993; Ruat et al., 1993). There are five isoforms of the 5-HT<sub>7</sub> receptor (humans and mice: 5-HT<sub>7a</sub>, 5-HT<sub>7b</sub>, 5-HT<sub>7d</sub>; rats: 5-HT<sub>7a</sub>, 5-HT<sub>7b</sub>, 5-HT<sub>7c</sub>, 5-HT<sub>7e</sub>) that differ within the length of the C-terminal tail and expression in different tissues (Heidmann et al., 1998; Krobert et al., 2001; Liu et al., 2001). The 5-HT<sub>7c</sub> splice variant is detectable in rat tissue but is not expressed in humans and mice. Conversely, rats do not express a splice variant 5-HT<sub>7d</sub> as the rat 5-HT<sub>7</sub> gene lacks the exon necessary to encode this isoform. Interestingly, the human 5-HT<sub>7d</sub> receptor isoform possesses a distinct pattern of receptor-mediated signaling: 5-HT<sub>7d</sub> receptors display agonist-independent internalization and internalize even in the presence of antagonist (Guthrie et al., 2005). Numerous studies indicate that, except for 5-HT<sub>7d</sub>, 5-HT<sub>7</sub> splice variants are pharmacologically indistinguishable, and modifications of the carboxyl tail do not influence coupling to adenylyl cyclase (Guthrie et al., 2005; Heidmann et al., 1998; Krobert et al., 2001). The gene encoding the 5-HT<sub>7</sub> receptor is localized at the 19th chromosome in mice and at 7th chromosome in human. Comparison of the amino acid sequence of the transmembrane regions of 5-HT<sub>7</sub> receptors from different species showed 39-50% homology. Interestingly, the homology of the transmembrane domains of 5-HT<sub>7</sub> and 5-HT<sub>1A</sub> receptor gene is relatively high (about 40%), which can partly explain the cross-reactivity of the agonists developed for 5-HT<sub>1A</sub> and 5-HT<sub>7</sub> receptors (Leopoldo et al., 2011).

The 5-HT<sub>7</sub> receptor is widely expressed in the central nervous system. The highest density of this receptor was detected in spinal cord, thalamus and hippocampus (Dogrul and Seyrek, 2006), raphe nuclei and the suprachiasmatic nucleus (Leopoldo et al., 2011), whereas cortex, putamen and cerebellum demonstrated relatively low level of the 5-HT<sub>7</sub> receptor (Barnes and Sharp, 1999; Horisawa et al., 2013). The

5-HT<sub>7</sub> receptor has been primarily identified in smooth muscle cells of blood vessels (Schoeffter et al., 1996) and in the gastrointestinal tract, where it is involved in peristalsis regulation (Tuladhar et al., 2003). The 5-HT<sub>7</sub> receptor is associated with numerous physiological and pathological responses, including serotonin-induced phase shifting of the circadian rhythm (Lovenberg et al., 1993) and age-dependent changes of the circadian timing (Duncan and Congleton, 2010). There are some data implicating 5-HT<sub>7</sub> receptors in the control of memory (Cifariello et al., 2008), emotionality, locomotor and exploratory activity (Liu and Jordan, 2005; Takeda et al., 2005). A large body of evidence indicates the involvement of the 5-HT<sub>7</sub> receptors in anxiety and depression, and recent studies suggest that the 5-HT<sub>7</sub> receptor can be highly relevant for the treatment of major depressive disorders (Gellynck et al., 2013). At the cellular level, the 5-HT<sub>7</sub> receptors are coupled to both G<sub>s</sub> and G<sub>12</sub> proteins (Fig. 4) (Wirth et al., 2017).

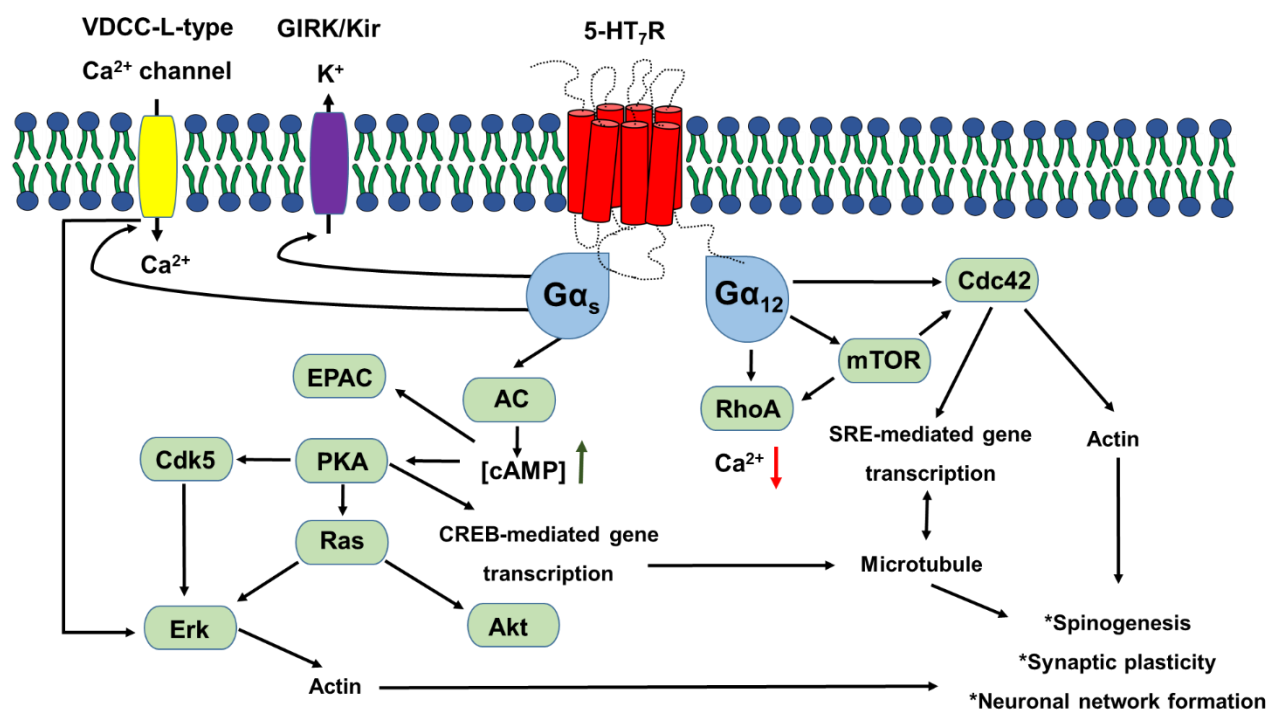


**Fig. 4. Signal transduction of the 5-HT<sub>7</sub> receptor**

At the cellular level, the 5-HT<sub>7</sub> receptor signaling is mediated both via G<sub>s</sub> and G<sub>12</sub> subunits. G<sub>s</sub> coupling leads to AC activation and cAMP formation, which in turn renders PKA, Erk, Akt activation. Additionally, the 5-HT<sub>7</sub> receptor facilitates EPAC-mediated cAMP formation. The 5-HT<sub>7</sub>R/G<sub>12</sub> pathway protein results in selective activation of small guanosine triphosphatases (GTPases) (RhoA and Cdc42) and promotes the mTOR-mediated phosphorylation (Wirth et al., 2017 with modifications).

Upon cloning of the 5-HT<sub>7</sub> receptor (Shen et al., 1993), it was first established that it binds to the G<sub>s</sub> protein, leading to stimulation of adenylyl cyclase and, consequently, to an increase in intracellular cAMP and activation of protein kinase A (PKA). PKA triggers phosphorylation of downstream targets and modulates the signaling cascades

of the extracellular regulated kinase (Erk) and protein kinase B (Akt) pathways (Errico et al., 2001; Johnson-Farley et al., 2005). Interestingly, in the case of the 5-HT<sub>7</sub> receptor, it has been demonstrated that G<sub>s</sub> protein-mediated ERK activation is independent of PKA, but still sensitive to AC activation and remains dependent on cAMP guanine nucleotide exchange factors such as Epac1 and Epac2 (Lin et al., 2003). It has also been demonstrated that the 5-HT<sub>7</sub> receptors can stimulate intracellular calcium release in cell lines (Baker et al., 1998). Additionally, the 5-HT<sub>7</sub> receptor is coupled to the G<sub>12</sub> protein that activates RhoGEFs (Kvachnina et al., 2005). Functionally, G<sub>12</sub> proteins have been shown to interact with the regulator of G protein signaling (RGS) family members, non-receptor tyrosine kinases (nRTKs), ezrin-radixin-moesin (ERM) proteins, A-kinase anchoring proteins (AKAPs), and heat shock protein 90 (Hsp90) (Hiley et al., 2006). Kvachnina et al. have shown that 5-HT<sub>7</sub> receptor stimulation was associated with G<sub>α12</sub> protein-mediated activation of gene transcription by serum response element (SRE) *via* Rho GTPases (Kvachnina et al., 2005). Furthermore, stimulation of the 5-HT<sub>7</sub> receptor/G<sub>α12</sub> pathway promotes dendritic spine outgrowth and synaptogenesis, resulting in increased spontaneous synaptic activity (Kobe et al., 2012).

Noteworthy, activation of the 5-HT<sub>7</sub> receptor also leads to Erk- and Cyclin-dependent kinase 5 (Cdk5)-dependent outgrowth of neurites in striatal and cortical neurons (Speranza et al., 2013). This activation of Erk might also be crucial for hippocampal function and depression. Taken together, activation of 5-HT<sub>7</sub>R/G<sub>12</sub> signaling pathways participates in the growth of new synapses and the formation of initial neuronal circuits related to plasticity-dependent networks (Citri and Malenka, 2008). In addition, Bijata and colleagues (Bijata et al., 2017) have recently demonstrated an existence of the 5-HT<sub>7</sub>R/MMP-9/CD44/Cdc42 signaling module. This study has demonstrated that stimulation of the 5-HT<sub>7</sub>R increases MMP-9 activity and leads to dendritic spine elongation and impairment of long-term potentiation (LTP). Noteworthy, it has been found that the inverse agonist properties of 5-HT<sub>7</sub> receptor ligands can lead to heterologous desensitization of other G protein-coupled receptor families (Krobert et al., 2006). Additionally, it has been shown that the constitutive activity of the 5-HT<sub>7</sub> receptor is regulated by the palmitoylation. In particular, the 5-HT<sub>7</sub> receptor has been found to be palmitoylated in an agonist-dependent manner at cysteine residues 404, 438, and 441, located in the C-terminal receptor domain (Kvachnina et al., 2009).

## 1.5. Functional crosstalk between 5-HT<sub>1A</sub> and 5-HT<sub>7</sub> receptors

The hypothesis of G protein-coupled receptor dimerization was first proposed by Zoli and colleagues (Zoli et al., 1993). Since then, dimerization has progressively been studied and accepted by numerous research groups (Bai, 2004; Bouvier, 2001; Breitwieser, 2004; Bulenger et al., 2005; Devi, 2001; Kroeger et al., 2003). Oligomerization can occur between identical receptors (homodimerization) (Bulenger et al., 2005), different receptors belonging to the same (Panetta and Greenwood, 2008) or distinct (Trifilieff et al., 2011) GPCR families, and different families (heteromerization). Moreover, results of multiple biochemical, structural, and functional studies point to the functional importance of dimerization to all aspects of GPCR function, including synthesis, ligand binding, G protein-coupling, receptor trafficking, and internalization (Angers et al., 2002; Borroto-Escuela et al., 2017a; Milligan, 2007). Interestingly, heterodimerization may change receptor pharmacology both by modulation of ligand binding on individual monomers and by formation of new binding sites (Franco et al., 2007; Fuxe et al., 2005; Gomes et al., 2000; Hornigold et al., 2003; Israilova et al., 2004; Jordan et al., 2003; Marshall et al., 1999; Rozenfeld and Devi, 2010), which can lead to a switch in G protein coupling (Lee et al., 2004). The clinical significance of GPCR oligomerization has also become more evident during recent years, leading to the identification of receptor oligomers as novel therapeutic targets (George et al., 2002; González-Maeso et al., 2008; Holliday et al., 2011; Milligan et al., 2014; Waldhoer et al., 2005). Nowadays, various approaches are used to study dimerization. In particular, they are based on biochemical, biophysical, physiological, computational methods, X-ray crystallography, and sequence-based techniques (Calebiro and Sungkaworn, 2018; Guo et al., 2017).

Numerous reports have identified that dysfunction of the GPCR heteroreceptor complexes that can lead to neurological diseases. For instance, antagonistic A<sub>2A</sub>-D<sub>2</sub> intramembrane receptor interaction was shown to be associated with Parkinson's disease (PD), and the development of potent A<sub>1</sub> and A<sub>2A</sub> dual antagonists is considered as a promising strategy for treatment of PD since it will also allow an enhancement of D<sub>1</sub> and D<sub>2</sub> signaling (Fuxe et al., 2008). Additionally, another strategy for the treatment of PD is based on the development of mGluR5 antagonists and enhancement of D<sub>2</sub> signaling in the dorsal striatopallidal GABA pathway by removing the antagonistic

mGluR5/D<sub>2</sub> interaction (Conn et al., 2005). It should be noted that the effect of mGluR5 antagonists is dependent on A<sub>2A</sub>/D<sub>2</sub>/mGluR5 interaction (Kachroo et al., 2005), where A<sub>2A</sub>/mGluR5 complex synergizes to counteract D<sub>2</sub> signaling (Schwarzschild et al., 2006). At the same time, A<sub>2A</sub> and mGluR5 agonists with the addition of a low dose of D<sub>2</sub> antagonist in A<sub>2A</sub>/D<sub>2</sub>/mGluR5 complex formation were shown to be an effective novel strategy for the treatment of schizophrenia (Díaz-Cabiale et al., 2000). The D<sub>2</sub>/NR2B heterodimerization has also been shown to be sufficient in cocaine treatment (Caine et al., 1999; Liu et al., 2006). Interestingly, the 5-HT<sub>1A</sub> receptor heterocomplexes were recently found to be a new target for the treatment of depression (Borrito-Escuela et al., 2018). It was shown that 5-HT<sub>1A</sub>-FGFR1 heteroreceptor complexes synergistically enhanced neuroplasticity both in the hippocampus and in the dorsal raphe serotonergic nerve cells (Borrito-Escuela et al., 2013, 2015). Stimulation of the 5-HT<sub>1A</sub> receptor activated FGFR1 signaling in wild-type rats. Additionally, disturbances in 5-HT<sub>1A</sub>-FGFR1 heterodimerization in the raphe-hippocampal serotonergic projection were observed in Flinders sensitive rat line – a rat genetic model of depression. It was suggested that the inability of co-treatment with FGFR1 and 5-HT<sub>1A</sub>R agonists to produce antidepressant-like effects in FSL rats could be caused by blocking of uncoupling of the 5-HT<sub>1A</sub> post-junctional receptors and autoreceptors from the hippocampal and dorsal raphe GIRK channels. This could lead to inhibition of hippocampal pyramidal nerve cell and dorsal raphe serotonergic nerve cell firing (Borrito-Escuela et al., 2017b). Moreover, 5-HT<sub>1A</sub>-5-HT<sub>2A</sub> heterocomplexes were recently shown in the hippocampus and limbic cortex (Borrito-Escuela et al., 2017c). The authors suggested that their role in depression is mediated via 5-HT<sub>2A</sub>R signaling, which led to inhibition of 5-HT<sub>1A</sub>R recognition and signaling. Finally, galanin (1–15) was reported to enhance the antidepressant effects of fluoxetine through the putative formation of GalR1-GalR2-5-HT<sub>1A</sub> heteroreceptor complexes (Borrito-Escuela et al., 2017a). Moreover, Renner and colleagues have shown that the 5-HT<sub>1A</sub>R and 5-HT<sub>7</sub>R can form homo- and heterooligomers (Renner et al., 2012). Notably, by the use of Förster resonance energy transfer (FRET) technique, it has been demonstrated that 5-HT<sub>1A</sub> receptors can form homodimers at the plasma membrane (Kobe et al., 2008; Woehler et al., 2009). Additionally, FRET efficiency of the 5-HT<sub>1A</sub> receptor oligomers was significantly decreased in response to agonist stimulation. Previous studies suggest that the effect was mediated by the accumulation of FRET-negative complexes rather than by dissociation of oligomers to monomers. Formation

of 5-HT<sub>1A</sub>R homooligomers was further confirmed by several publications (Ganguly et al., 2011; Paila et al., 2011). Furthermore, a combination of computational protein-protein docking, site-directed mutagenesis, and FRET-based analysis has demonstrated that transmembrane domains TM4/TM5 are essential in the formation of 5-HT<sub>1A</sub> receptor dimers and indicate that specific amino acids interactions maintain the interface (Gorinski et al., 2012).

Although the existence of GPCR heterooligomers has been generally accepted, their physiological role and functional importance are under numerous debates (Borroto-Escuela et al., 2017a; Trifilieff et al., 2011). Interestingly, previous studies have suggested functional crosstalk between 5-HT<sub>1A</sub> and 5-HT<sub>7</sub> receptors (Prasad et al., 2019; Renner et al., 2012). It was shown that 5-HT<sub>1A</sub> receptor stimulation induced hypothermic response in rats upon intraperitoneal (Goodwin et al., 1987) and subcutaneous (Hjorth, 1985) administration of 8-OH-DPAT, an agonist of both 5-HT<sub>1A</sub> and 5-HT<sub>7</sub> receptors. Moreover, intracerebroventricular administration of selective 5-HT<sub>7</sub> receptor agonist LP44 produced a considerable hypothermic response in mice, indicating the involvement of central 5-HT<sub>7</sub> receptors in thermoregulation.

Additionally, it was shown that hippocampal neurons express both 5-HT<sub>1A</sub> and 5-HT<sub>7</sub> receptors, and these receptors are highly co-localized at the plasma membrane. Functional analysis of oligomerization between 5-HT<sub>1A</sub> and 5-HT<sub>7</sub> receptors revealed that heterooligomers decreased the 5-HT<sub>1A</sub> receptor-mediated activation of G<sub>i</sub> protein without affecting 5-HT<sub>7</sub> receptor-mediated G<sub>s</sub> protein activation (Renner et al., 2012, Prasad et al 2019). In addition it was also demonstrated that heterodimerization is involved in agonist-mediated internalization of the 5-HT<sub>1A</sub> receptor, highly resistant to internalization when expressed alone. Once internalized, the 5-HT<sub>1A</sub> receptor can activate G protein-independent signaling pathways such as a  $\beta$ -arrestin-mediated coupling to mitogen-activated protein kinase (MAPK) (Renner et al., 2012). Thus, depending on the relative amount of 5-HT<sub>1A</sub> receptors participating in heterooligomers, the same ligand (serotonin) can activate distinct ERK-mediated pathways (i.e., G protein-dependent or  $\beta$ -arrestin dependent). The above-mentioned has raised the possibility that conditions selectively promoting or inhibiting heterodimerization may be of significant physiological importance.

## 1.6. Animal models of depression

The literature review has shown that studies of the pathogenesis of depression and mechanisms of antidepressant action are mainly based on the implementation of numerous animal models of major depressive disorders (MDD) (Czéh et al., 2016; Duman, 2010). Noteworthy, since a minimum of criteria should be met for an animal model to be considered reasonable, rodent models of affective illness may not be completely corresponding to the human condition. Initially, modeling depression in animals was based on the surgical approach (e.g., olfactory bulbectomy; Cairncross et al., 1978) or acute stress-induced protocols (tail suspension (Steru et al., 1985), learned helplessness (Overmier and Seligman, 1967) and forced swimming (Porsolt et al., 1977). Interestingly, the direct link between olfactory bulbectomy and human depressive phenotype is rather controversial and less invasive, and more ethologically relevant models have been proposed (Czéh et al., 2016; Duman, 2010; Slattery and Cryan, 2017). Chronic paradigms, such as chronic restraint stress (CRS; (Renaud, 1959), chronic social defeat stress (CSDS; (Blanchard et al., 1998), and chronic unpredictable stress (CUS; (Katz et al., 1981; Willner, 1997) are considered to be more reliable and effective in comparison to procedures that rely on short-term stress exposure. It is widely accepted that chronic stress facilitates numerous impairments in mood, cognition, and memory (Qiao et al., 2014) and may lead to the development of systemic inflammation, type 2 diabetes, Alzheimer's disease, Parkinson's disease, gastric ulceration, and cancer (Han et al., 2015). Additionally, the consequences of unpredictable stress include cortical and limbic brain region atrophy (Marsden, 2013), decrease in hippocampal neurogenesis (Schoenfeld et al., 2017), sensitization of the serotonergic system (Pereira et al., 2019), excessive activation of the noradrenergic system (Pereira et al., 2019), increase in hippocampal inflammatory proteins (Yirmiya and Goshen, 2011), microglial proliferation and activation (Wang et al., 2017), and hypothalamic-pituitary-adrenal (HPA) axis disturbances (Ménard et al., 2017). Interestingly, in contrast to chronic stress exposure, acute stress leads to the differentiation of stem cells into new nerve cells that improve cognitive performance in rats and increase neurogenesis in the dentate gyrus (Kirby et al., 2013).

Although numerous studies were based on the investigation of stress consequences, the obtained results are still rather controversial (Marsden, 2013). For instance, the

possible correlation between hippocampal volume reduction and depression is currently under debate due to the evidence (Masi and Brovedani, 2011) supporting the lower hippocampal volume in high-risk patients even before the occurrence of early-onset depressive symptoms. Noteworthy, both hippocampal volume reduction and decreased neurogenesis are not specific only to depression – these effects have also been reported in other psychiatric disorders, such as schizophrenia and bipolar disorder (Han et al., 2015; Scheltens, 1999). Additionally, HPA axis function dysregulation in either directions can result in a depressive phenotype (Krishnan and Nestler, 2010; Zunszain et al., 2011). Nowadays, a wide range of depression-inducing protocols is developed, and the choice of the appropriate paradigm relies on various factors. For instance, CRS model is widely used to study depression because of its relative workflow simplicity, but it is frequently criticized for low efficacy. Chronic social defeat stress models of depression are mainly limited to using male rodents. At the same time, chronic unpredictable stress procedures overcome the possible habituation to stress and sex specificity. Noteworthy, stressors combination leads to representative predictive, face, and construct validity of depression protocols and produces the most consistent results in terms of behavioral, neurochemical, neuroendocrine, and neuroimmune alterations.

## 2. AIM OF THE STUDY

Previous studies have shown that both 5-HT<sub>1A</sub> and 5-HT<sub>7</sub> receptors are involved in the pathogenesis of depression. Moreover, studies *in vitro* have demonstrated that 5-HT<sub>1A</sub> and 5-HT<sub>7</sub> receptors form heterodimers that change receptors signaling cascades.

Thus, the aims of the study are the following:

- ❖ Verification of the applicability of the chronic unpredictable stress protocol for modeling depression in different strains of rodents based on the sucrose preference test.
- ❖ Determination of 5-HT<sub>1A</sub> and 5-HT<sub>7</sub> receptors expression profile in different brain regions as underlying cause of heterodimerization between these serotonin receptors.
- ❖ Determination of the possible involvement of 5-HT<sub>1A</sub> and 5-HT<sub>7</sub> receptors heterodimerization in the pathogenesis of depression using model for the depressive-like behavior in mice.

## 3. MATERIALS

### 3.1. Theoretical study based on meta-analysis

The present meta-analysis was performed according to recommendations of Preferred Reporting Items for Systematic Reviews and Meta-analyses (PRISMA) guidelines (Moher et al., 2010). The randomized controlled trials were assessed by following the checklist that includes the title, abstract, introduction, methods, results, discussion, and funding that are reported in a specific and systematic manner.

#### 3.1.1. Selection of strategy criteria for assessment of sucrose preference test efficiency for modeling of depressive-like behavior in rodents

The literature screening was performed using the PubMed database, including studies published from January 1, 1998 to September 31, 2018. The search strategy was based on using of the following keywords and terms in the title abstract: “animal model” and “chronic unpredictable/mild stress”. The meta-analysis was conducted independently by two researchers (Svitlana Antoniuk and Monika Bijata). The studies were included upon meeting the following criteria: (1) original article, (2) implementation of CUMS protocol; (3) depressive-like behavior was assessed based on a sucrose preference test (calculated according to the following formula: sucrose preference [%] = [sucrose intake / total fluid intake] × 100), sucrose intake (calculated as the weight of sucrose solution (g) (4) using of rodents that were not genetically modified or subjected to prenatal stress or sterilization. The search was based on papers published in English.

#### 3.1.2. Data extraction and characteristics of the included articles

The following data were screened and the studies characteristics were assessed according to the following checklist: (1) name of the first author and year of publication, (2) rodent characteristics, (3) stress model design, (4) details of the sucrose preference protocol, (5) mean, standard error of the mean, and sample size (n) of each stress and control group. The meta-analysis was performed after collecting a minimum of 3 studies per group and availability of mean sucrose preference, standard error or standard deviation of the mean and sample size.

### 3.1.3. Statistical analysis

The efficiency of CUMS protocol for modelling depressive-like behavior in rodents was assessed by evaluation of sucrose preference (%) in rodents. The meta-analysis and graphical visualization of forest plots was performed using RevMan 5.3 software (Nordic Cochrane Center). Meta-analysis was based on the calculation of weighted mean effect sizes (i.e., standardized mean difference (SMD), 95% confidence interval,  $I^2$  heterogeneity value, and p value) using the fixed-effect model. The effect size is represented as the SMD. It represents the degree of difference between the stress control groups and was calculated according to the following formula:

*SMD = (M1 – M2)/SD, where M1-M2 shows difference in means, and SD is the pooled and weighted standard deviation*

Statistical heterogeneity ( $I^2$ ) was assessed using the Higgins recommendations (Higgins and Thompson, 2002). This approach represents the variation between studies, with values between 0% and 100% ( $I^2=0%$  demonstrates statistical homogeneity, whereas  $I^2>50%$  shows substantial statistical heterogeneity).  $I^2$  was calculated as  $I^2=100% \times (Q - df)/Q$ , where Q is Cochran's heterogeneity statistics, and df is the degrees of freedom. Cochran's Q shows the weighted sum of squared differences between individual effects and the pooled effect across studies, with weights from the pooling method. The outcomes of the meta-analysis are depicted as forest plots. Error bars in the forest plots indicate the 95% confidence intervals of the effect size. A vertical midline divides the diagram into the parts that favor the stress and control group. Central vertices of a black diamond represent the average mean effect size of all of the studies, whereas the outer vertices indicate the 95% confidence intervals. The influence of the study on the overall results of the meta-analysis is represented as weight (%). The weight of a study on the overall results is calculated by the study's sample size and precision of the study's results, indicated by confidence intervals. The overall effect is based on Z statistics based on p values that indicated the level of statistical significance.

## 3.2. Experimental studies

### 3.2.1. Materials

#### 3.2.1.1. Chemicals and materials

**Table 1. Summary of used chemicals and materials**

Chemical/material	Supplier	Catalogue #
5-CT maleate (5-Carboxamidotryptamine maleate)	Tocris Bioscience	458
Acrylamide solution	Roth	3029.1
APS (Ammonium peroxodisulphate)	Roth	9592.2
Bromphenol blue	Roth	512.1
BSA (Bovine serum albumin fraction V)	Roth	8076.4
DMSO (Dimethyl sulfoxide)	Roth	A994.1
EDTA·2Na <sub>2</sub> H <sub>2</sub> O (Ethylenediaminetetraacetic acid disodium dehydrate)	Roth	8043.2
EGTA (ethylene glycol-bis(β-aminoethyl ether)- <i>N,N,N,N</i> -tetraacetic acid)	Roth	3054.1
EtOH (Ethanol)	Roth	9065.4
Glycine	Sigma	50046
HEPES ( <i>N</i> -2-Hydroxyethylpiperazine- <i>N</i> -2-ethane sulphononic acid)	Roth	9105.3
K <sub>2</sub> HPO <sub>4</sub> (Potassium dihydrogen phosphate)	Roth	P018.1
KCl (Potassium chloride)	Roth	6781.1
KOH (Potassium hydroxide)	Roth	7986.1
LP-211 (4-[1,1'-biphenyl]-2-yl-N-[(4-cyanophenyl)methyl]-1-piperazinehexanamide)	Sigma	SML1561
MeOH (Methanol)	Roth	8388.2
Milk powder	Frema	0203 V04
Na <sub>2</sub> HPO <sub>4</sub> ·2H <sub>2</sub> O (Disodium hydrogen phosphate dehydrate)	Roth	T879.1
NaCl (Sodium chloride)	Roth	3957.5
Nitrocellulose Blotting Membrane (0.45 μm)	GE Healthcare	10600003
Formaldehyde solution (4%; ph 6.9)	Merck	1004969010
SDS (Sodium dodecyl sulfate)	Serva Electrophoresis	20765.02
Sucrose D-(+)-Glucose	Sigma	G-7021
TEMED (Tetramethylethylenediamine)	Roth	2367.1
Tris (Tris(hydroxymethyl)aminomethane)	Serva	37190.03
Tris hydrochloride	Sigma	T5941
Tri-sodium citrate (dihydrate)	Fluka	71402
Tween®20	Roth	9127.2
Urea	Roth	2317.1
β-ME (β-mercaptoethanol)	Roth	4227.1

### 3.2.1.2. Antibodies

**Table 2. Summary of primary antibodies**

Target	Host species	Dilution	Dissolvement	Supplier	Catalogue #
5-HT <sub>1A</sub> R	Rabbit	1:250	BSA	Alomone	ASR-021
5-HT <sub>1A</sub> R	Mouse	1:100	BSA	Millipore	MAB11041
GAPDH	Mouse	1:10000	Milk	Millipore	MAB374
5-HT <sub>7</sub> R	Rabbit	1:1000	BSA	Abcam	AB128892
5-HT <sub>7</sub> R	Rabbit	1:100	BSA	Immunostar	24430
5-HT	Goat	1:1000	BSA	Abcam	AB66047

**Table 3. Summary of secondary antibodies**

Target	Conjugate	Dilution	Dissolvement	Supplier	Catalogue #
Mouse	Alexa-488	1:400	BSA	Jackson ImmunoResearch	715-545-150
Goat	Alexa-488	1:1000	BSA	Thermo Fischer	A11055
Rabbit	Alexa-594	1:400	BSA	Jackson ImmunoResearch	711-585-152
Goat	Alexa-647	1:400	BSA	Jackson ImmunoResearch	705-607-003
Rabbit	Oligonucleotide plus	1:200	BSA	Sigma	DUO92002
Mouse	Oligonucleotide minus	1:200	BSA	Sigma	DUO92004

### 3.2.1.3. Kits and equipment

**Table 4. Summary of used kits**

Kit	Supplier	Catalogue #
BCA protein kit	Thermo Fisher	23225
RNeasy® Plus Mini Kit	Qiagen	74134
SuperScript®III First-Strand Synthesis System for RT-PCR	Life Technologies	18080-051
TaqMan® Universal PCR Master Mix	Life Technologies	4324018
Duolink In situ Detection Reagents Red	Sigma	DUO92008

**Table 5. List of qRT-PCR probes**

Probe	Supplier	Catalogue #/Sequence
5-HT <sub>1A</sub> R	Life Technologies	4331182; Mm00434106_s1
5-HT <sub>7</sub> R	Life Technologies	4448892; Mm01204045_m1
GAPDH	Sigma	fw 5'-TGCACCACCAACTGCTTAGC-3', rev 5'-GGCATGGACTGTGGTCATGAG-3', probe 5'-6-FAM-CCCTGGCCAAGGTCATCCATGACAAC-TAM-3'

**Table 6. List of equipment**

Equipment	Supplier
Centrifuge 5417R	Eppendorf
Fusion SL	Peqlab
NanoDrop 2000	Peqlab
OptimaTMTLX Ultracentrifuge 120000 RPM	Beckman coulter
PCR System 9400	Applied Biosystems
StepOnePlus thermocycler	Applied Biosystems
Zeiss LSM 780	Carl Zeiss

### 3.2.1.4. Buffers and solutions

**Table 7. Summary of used buffers and solutions**

Buffer	Composition
Stacking gel	5% Acrylamide solution (29:1); 0.125 M Tris; 0.1 % SDS; 0.25% TEMED; 0.15% APS
Separation gel (12%)	12% Acrylamide solution (29:1); 0.375 M Tris; 0.1 % SDS; 0.1% TEMED; 0.05% APS
4xTris-HCl/SDS buffer pH 6.8	0.5 M Tris; 0.4% SDS; pH 6.8
4xTris-HCl/SDS buffer pH 8.8	1.5 M Tris; 0.4% SDS; pH 8.8
Running buffer	192 mM Glycine; 25 mM Tris; 0.1% SDS
Transfer buffer	192 mM Glycine; 25 mM Tris; 0.1% SDS; 20% Methanol
Phosphate buffer saline (PBS)	1.37 M NaCl; 100 mM Na <sub>2</sub> HPO <sub>4</sub> ; 27mM KCl; 18 mM KH <sub>2</sub> PO <sub>4</sub> ; pH 7.4
Thorner buffer (TB)	Urea 8 M; SDS 5%; Tris 40 mM; EDTA 0.1 mM; Bromphenol blue 0.6 mM; pH 6.8
Tris-buffered saline + Tween® 20	20 mM Tris; 150 mM NaCl; 0.05% Tween 20; pH 7.4
Homogenization buffer	10 mM HEPES; 5 mM EGTA; 1 mM EDTA; 0.32 M Sucrose
Sodium citrate buffer	10 mM Tri-sodium citrate (dihydrate); pH 9.0
Lysis buffer	150 mM NaCl; 50 mM Tris-Cl; 5 mM EDTA; 0.1% SDS; 0.2% Triton 100
Buffer A	150 mM NaCl; 10 mM Tris; 0.05% Tween 20; pH 7.4
Buffer B	100 mM NaCl; 35 mM Tris; 165 mM Tris-HCl; pH 7.5

## 4. METHODS

### 4.1. Behavioral studies

#### 4.1.1. Animals and housing conditions

Male 3-month-old C57BL/6J mice (Charles Rivers; Białystok, Poland) were individually housed with food and water available *ad libitum*. Rodents exposed to 5-CT, LP-211 injections were housed at standard 12 h/12h light/dark cycle (lights on at 8:00 AM), whereas animals subjected to chronic stress protocol were housed under reverse 12 h/12h light/dark cycle (lights on at 8:00 PM). Male CD1 mice (Charles Rivers; Sulzfeld, Germany) were used as intruders in the social defeat stress procedure. Exposure to male Wistar rats (Warsaw, Poland) was part of the predator stress. Animal experiments were approved by the I Warsaw Ethical Committee on animal research (Permissions no. 132/2016 and 248/2017).

#### 4.1.2. Stimulation of 5-HT<sub>1A</sub> and 5-HT<sub>7</sub> receptors *in vivo*

5-CT and LP-211 (10 mg/kg) were administered 30 min before the behavioral tests. The dose was chosen based on their effectiveness in other behavioral and thermoregulation experiments (Hedlund et al., 2004, 2005). Ligands were dissolved according to manufactures' recommendations: 5-CT was dissolved in saline solution and LP-211 – in DMSO (3.3% in saline solution). For behavioral testing, mice were handled for at least 7 days in order to minimize stress effects. Each animal was only used for one test.

#### 4.1.3. Mouse model of depression based on modified CUS protocol

Mouse model of depression was established according to previously described CUS protocol (Krzystyniak et al., 2019; Strekalova and Steinbusch, 2010). After 1 week of acclimatization and 1 week of handling, the mice were weighed and tested for baseline sucrose preference. Further, they were assigned to a control and stress group and housed in separate rooms. The CUS procedure consisted of 2 weeks of stress exposure (Fig. 5).

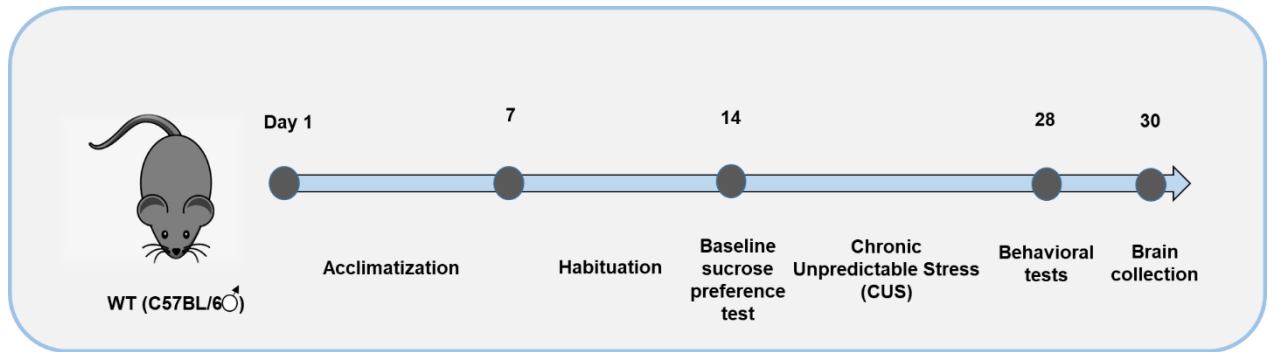


*Fig 5. Experimental timeline*

The stressors were applied daily in a semi-random order during the dark and light phases of the light/dark cycle (Krzystyniak et al., 2019; Strekalova and Steinbusch, 2010). All the stressing procedures, except for rat exposure, were performed during the dark phase of the light/dark cycle.

- ❖ Restraining stress was based on placing animals inside a plastic tube (26 mm internal diameter) for 2 h.
- ❖ The mice were subjected to the tail suspension using adhesive tape for 40 min. To prevent climbing, plastic cylinders (0.5 cm\*4 cm) were used at the base of mice tails.
- ❖ Social defeat stress was based on the defeat of C57BL/6J mice by aggressive CD1 mouse strain. During 30 min social defeat session, aggressive CD1 rodents were placed in the home cages of C57BL/6J mice. CD1 mice were selected based on their ability to attack C57BL/6J mice in less than 60 s without injuring them. C57BL/6J mice showed the following signs of social defeat stress: fight response, submissive posture, and vocalization. Upon physical harm of stressed animals, CD1 individuals were immediately removed from the cage of the C57BL6J resident mice.
- ❖ In order to perform exposure to rats, mice were individually placed into transparent, well-ventilated cylinders (15 cm\*8 cm) with food and some bedding. The cylinders were positioned for 12 h (08:00 P.M.–08:00 A.M.) into the cage with a rat.

For the rest of the day (08:00 A.M.–08:00 P.M.), the mice were housed in the home cages in the same experimental room. In order to stabilize glucocorticoid levels, mice were left undisturbed (16 h, overnight) after the last stressor and further were subsequently subjected to 8 h sucrose preference test and the forced swim test. All of the mice were sacrificed 24 h after the last sucrose preference test.

#### 4.1.4. Sucrose preference test

The sucrose preference test is based on the free-choice access to sucrose solution (1%) and water for 8 h provided in identical bottles. The percentage of sucrose preference was calculated according to the following formula:

$$\text{Sucrose Preference [\%]} = \left[ \frac{\text{Sucrose solution Weight}}{\text{Sucrose solution Weight} + \text{Water Weight}} \right] * 100\%$$

Water and sucrose solution consumption was assessed simultaneously in control and experimental groups. Twenty-four hours before the baseline sucrose preference test, sucrose solution (2.5%) was given to the mice for 2 h in order to prevent possible effect of taste neophobia. To eliminate the possible bias of side preferences, the bottles positions were switched each 4 h. A sucrose preference <70% in mice in the stress group measured after the 8-h sucrose preference test (24 h after cessation of the stress procedure) was the criterion for “anhedonia” defined by difference between control and stressed group.

#### 4.1.5. Forced swimming test

In order to perform the forced swimming test, cylindrical glass containers (20 cm\*40 cm) were filled with warm water (~30°C) to a depth of 15 cm. The swimming pattern of mice that underwent CUS protocol was assessed under the red light during the dark phase of the light/dark cycle. Each mouse was placed in the container filled with water for 6 min session. The latency to the first episode of floating (no body or head movements for more than 2 s) and the sum of floating time during the last 4 min were measured by visual scoring.

#### 4.1.6. Tail suspension test

The procedure followed in this study was previously described by Cryan (Cryan et al., 2005). Mice were suspended by their tails with tape in such a position that allows to prevent escape and proper holding to nearby surfaces. During the test, 6 minutes in duration, the resulting escape oriented behaviors were quantified.

#### 4.1.7. Eco-Hab

Eco-Hab test was established according to a previously described protocol by Puscian and colleagues (Puścian et al., 2016). Briefly, prior to the behavioral testing, subjects were housed together and grouped appropriately for their respective experiment. In order to individually identify animals in Eco-HAB, all mice were subcutaneously injected with glass-covered microtransponders (9.5 mm length, 2.2 mm diameter, RFIP Ltd) under brief isoflurane anesthesia. After the injection of transponders, subjects were moved to the experimental rooms and adapted to the shifted light/dark cycle of their new environment (12.00 A.M.–12.00 P.M.). Cohorts consisting of mice were subjected to 72 h Eco-HAB testing procedure that was divided into an adaptation (48 h) and experimental phase (post-injection of LP-211 and SB-266970) (24 h) with unrestricted food and water access. Mice could freely explore both testing compartments for 24 h. Compartments crossing was recorded using Eco-HAB.rfid software. Locomotor activity after 30 min from the injections was used for statistical analysis. Relative locomotor activity was defined as the ratio of total number of compartments crossing in the corresponding compartments of the apparatus.

## 4.2. Molecular biology

### 4.2.1. Quantitative real-time polymerase chain reaction

The mRNA was purified using the RNeasy® Plus Mini Kit. Briefly, brain tissue from different regions (prefrontal cortex, hippocampus, and raphe nuclei) was lysed in 350 µl RLT lysis buffer containing DTT. Further steps were performed according to the manufacturer's instruction. mRNA concentration was measured using the NanoDrop 2000. Isolated mRNA was transcribed into cDNA using the SuperScriptIII First-Strand Synthesis System (reverse transcription) according to the manufacturer's protocol (Table 8). Thus, for one reaction 2 µg of total mRNA was used. An mRNA/hexamer/dNTP mix was incubated at 65°C for 5 minutes in the GeneAmp PCR system 9700 (Applied Biosystems). Then, the mix was kept on ice for one minute and the cDNA synthesis mix containing RT buffer/MgCl<sub>2</sub>/DTT/RNaseOUT/SuperScript was added. The following steps were proceeded in the GeneAmp PCR system 9700 as described in step 3 of Table 9. The synthesized cDNA was stored at -20°C.

**Table 8. Pipetting scheme for cDNA synthesis**

Component	Volume/reaction
mRNA/hexamer/dNTP mix	
mRNA	2 µg/ul
Random hexamer (50 ng/µl)	1 µl
dNTPs (10 mM)	1 µl
cDNA synthesis mix	
10XRT buffer	2 µl
MgCl <sub>2</sub> (25 mM)	4 µl
DTT (0,1 M)	2 µl
RNaseOUT™ (40U/µl)	1 µl
SuperScript® III RT (200U/µl)	1 µl

**Table 9. Steps for cDNA synthesis**

Step	Temperature, °C	Time	Components
1	65	5 minutes	mRNA/hexamer/dNTP mix
2	1 minute	Combining cDNA synthesis mix with mRNA/hexamer/dNTP mix	
3	25	10 minutes	
4	50	50 minutes	
5	85	5 minutes	
6	37	20 minutes	Adding 1 µl of RNase H

The qRT-PCR was performed in order to quantify the amount of mRNA encoding proteins of interest. Sequence-specific DNA probes labeled with fluorescent dye and quencher at opposing ends (TaqMan® probes) were used to detect cDNA molecules. The reaction is based on the specific hybridization of fluorescently labeled oligonucleotides with complementary sequences and elongation by Taq polymerase. The 3'-5' exonuclease activity of the polymerase leads to the excision of quencher-carrying nucleotides resulting in an accumulation of fluorescence according to the corresponding mRNA concentration. Thus, 2 µl of the obtained cDNA was mixed 10 µl of Master Mix, 5 µl PCR grade water, and 1 µl of corresponding primer/TaqMan probes. The qRT-PCR was carried out with a Step One Plus PCR system. The qRT-PCR cycle conditions (N=40) are described in the Table 10.

**Table 10. qRT-PCR cycle conditions**

Step	Temperature, °C	Time
1	50	2 min
2	95	10 min
3	95	15 sec
4	60	1 min

The data were collected using Step one plus 2.1 software. Relative changes of genes expression were analyzed implementing the comparative  $2^{-\Delta\Delta Ct}$  method (Livak and Schmittgen, 2001). The threshold cycle (Ct) indicates the cycle number at which the amplified target reaches a fixed threshold as a result of the significant fluorescence increase. The relative value for the expression level of each gene was calculated by the equation  $Y = 2^{-\Delta\Delta Ct}$ , where  $\Delta Ct$  is the difference between target and housekeeping (GAPDH) product i.e.  $\Delta Ct = Ct (\text{target}) - Ct (\text{housekeeping})$ .

#### 4.2.2. Bicinchoninic acid assay

Brain tissue from the prefrontal cortex, hippocampus, and raphe nuclei was homogenized in the Homogenization buffer (see section 3.2.1.4 for details). The membrane fraction and soluble fraction have been separated by applying the following centrifugation steps: 300xg (5 min at 4 °C); 800xg (5 min at 4 °C); 20.000xg (1 h at 4 °C). The obtained pellet was lysed using the Lysis buffer (see section 3.2.1.4 for details). Protein concentration was measured using bicinchoninic acid (BCA) assay, based on the reduction of copper (II) to copper (I) by protein peptide bonds in alkaline solution followed by chelation of copper (I) by bicinchoninic acid resulting in a purple complex. Therefore, 5  $\mu$ l of protein lysate and 200  $\mu$ l of BCA working solution, composed of 98% BCA assay solution A and 2% BCA assay solution B, were combined in a 96-well plate and incubated at 37°C for 30 minutes. Afterward, the absorbance of the bicinchoninic assay copper (I) complex was measured at 562 nm wavelength. The protein concentrations of the lysates were calculated by linear fitting of protein standards with concentrations ranging from 0  $\mu$ g/ml to 2 mg/ml BSA.

#### 4.2.3. Sodium dodecyl sulphate polyacrylamide gel electrophoresis

Proteins were separated using sodium dodecyl sulfate polyacrylamide gel electrophoresis (SDS PAGE) applying the Biometra SDS-PAGE system. The protocol was based on cell lysis and further treatment with SDS containing buffers, which form micelles wrapping the proteins according to their molar mass. In this way, different proteins were separated by their molecular mass using 5% (v/v) bis-/acrylamide stacking gels and 12% (v/v) bis-/acrylamide separation gels (section 3.2.1.4). Protein stacking and separation was performed at 70V and 140V, respectively.

#### 4.2.4. Western blotting

SDS PAGE separated proteins were transferred using the semi-dry western blot system. Negatively charged proteins are transferred from the SDS gel to nitrocellulose membranes (2 mA/cm<sup>2</sup> per gel, 1 hour), which can be afterward detected with antibodies. Membranes were blocked in the non-fatty dry milk or bovine serum albumin (see section 3.2.1.1 for detailed information) in TBST for 1 hour at room temperature with agitation. Afterward, membranes were incubated with primary antibodies (see section 3.2.1.2 for detailed information) at 4°C overnight and secondary antibodies (see section 3.2.1.2 for detailed information) at room temperature for 1 hour. Membranes were washed three times with TBST after incubation with primary and secondary antibodies. Membranes were developed with SuperSignal Femto chemoluminescence substrate and imaged with the FUSION XL Imager (PeqLab), further quantified was performed using MatLab.

### 4.3. Histology

C57BL/6J mice were anesthetized and perfused intracardially with 4% (w/v) paraformaldehyde. Brains were removed, post-fixed (mouse brain), or immersed directly (human brain) in 4% paraformaldehyde, cryoprotected in 30% (m/v) sucrose solution. Brain coronal sections (30 µm) were cut on a cryostat and processed for free-floating histochemistry.

#### 4.3.1. 5-HT<sub>1A</sub>R, 5-HT<sub>7</sub>R, and 5-HT immunohistochemistry

The sections were pre-incubated in the sodium citrate buffer (80 °C; 30 min) and methanol (20 °C; 5 min). Brain slices were incubated in a blocking buffer containing 0.1% (w/v) Triton-100 and 5% (w/v) donkey serum. After 30 min incubation at room temperature, the sections were labeled with the primary antibodies using the following primary antibodies for 48 hours at +4 C. Control experiments employed only secondary antibodies. Primary antibodies were extensively washed, and stained with the indicated fluorescence-labeled secondary antibodies. The primary antibodies were the following (see section 3.2.1.2 for detailed information): mouse monoclonal anti-5-HT<sub>1A</sub> receptor (Millipore); rabbit monoclonal anti-5-HT<sub>7</sub> receptor (Immunostar); goat monoclonal anti-serotonin (Abcam). The secondary antibodies (see section 3.2.1.2 for detailed information) were applied for 1 h at room temperature (Alexa Fluor 488-conjugated donkey anti-mouse IgG (1:400; Jackson ImmunoResearch); Alexa Fluor 594-conjugated donkey anti-rabbit IgG (1:400; Jackson ImmunoResearch); Alexa Fluor 488-conjugated donkey anti-goat (1:2000; Invitrogen). The sections were mounted in the fluoroshield mounting medium with DAPI (Abcam).

#### 4.3.2. *In situ* proximity ligation assay

To study the 5-HT<sub>1A</sub>-5-HT<sub>7</sub> receptor interaction, the *in situ* proximity ligation assay (PLA) was performed according to the previously described protocol (Borroto-Escuela et al., 2015) with minor modifications. Briefly, brain sections were incubated with the primary antibodies as specified above (see section 4.3.1 for detailed information). Afterward, the slices were washed 3 times with PBS and incubated with secondary antibodies conjugated to Plus and Minus PLA oligonucleotide arms for 2 h at 37 °C in a humidity chamber. The unbound proximity probes were removed by washing the slides 3 times with PBS at room temperature under gentle agitation. Further, sections were incubated with the hybridization-ligation solution (0.025 U/μL) and the amplification mixture (125 units/μl) and incubated in a humidity chamber at 37 °C for 60 and 100 min, respectively. The excess of the ligation solution was removed by applying the washing buffer A. In the last step, the sections were washed twice in the dark, 10 min each, with the washing buffer B at room temperature. The free-floating sections were mounted on a microscope slide in the mounting medium containing

DAPI (VectaShield, Sigma). The coverslips were placed on the section and sealed with the nail polish. The sections were protected from light and stored for several days at  $-20\text{ }^{\circ}\text{C}$  before confocal microscopy analysis.

#### 4.4. Microscopy and images analysis

All data were collected on a Zeiss LSM 780 microscope controlled with ZEN 2012 software. The imaging was performed in the lambda mode resulting in emission spectra collection. This approach enables to unmix the different fluorophore spectra directly during the measuring. Images were acquired in online fingerprinting mode. DAPI, Alexa 488, Alexa 594, Alexa 647, Texas Red, autofluorescence reference spectra were used. Z-stacks were collected in order to get even information about the signal distribution, and maximum projection was applied for analysis. Immunohistochemical stainings were collected applying the following configurations: a)  $40\times/1.2$  NA water immersion objective (bit depth 16-bit, zoom 2.0,  $30.00\text{ }\mu\text{m}$ ); b)  $20\times/0.8$  NA air immersion objective (bit depth 16-bit, zoom 0.7,  $20.00\text{ }\mu\text{m}$ ). Images processing was performed using Fiji software.

The number of cell bodies and serotonergic cells was calculated using the Cell Counter plugin upon manual marking. The number of 5-HT<sub>1A</sub>R-5-HT<sub>7</sub>R hetero-complex blobs was automatically evaluated by applying the function “Analyze particles.” Image processing included the following steps: a) background setting; b) threshold adjustment; c) defining particles size; d) assessment of the number of 5-HT<sub>1A</sub>R-5-HT<sub>7</sub>R hetero-complex blobs. The final calculation was performed according to the formulas:

$$a) \text{ Blobs/cell} = 5\text{-HT}_{1A}\text{R-5-HT}_{7}\text{R hetero-complex blobs number/cell bodies number}$$

$$b) \text{ Blobs/serotonergic neuron} = 5\text{-HT}_{1A}\text{R-5-HT}_{7}\text{R hetero-complex blobs number/serotonergic neurons cell number}$$

#### 4.5. Bioinformatics

The obtained data were analysed using the following software (Table 11).

**Table 11. Summary of used software**

Software	Analysis
MatLab	Western blots evaluating
GraphPad Prism 7	Data visualization, statistics
Adobe Photoshop CS3	Image processing
Adobe Illustrator CS5	Figures preparation
Fiji	Image processing, western blot analysis

#### 4.6. Statistical analysis

Statistical differences were calculated using GraphPad Prism7 software. Details of the statistical analysis are specified in the figure legends. In order to analyze statistical differences in behavioral, microscopic, and molecular biology experiments, t-test and two-way ANOVA with the Tukey post-hoc test were applied, if not indicated differently. In general, qRT-PCR and western blots were analyzed and normalized taking into account the sum of replicates (Degasperi et al., 2014). The intensity of the band was divided by the sum of all band intensities on the blot of interest. Protein and mRNA expression signals were normalized to the loading control and housekeeping gene, respectively. For relative comparisons, the control mean was set equal to one. The mean + SEM per experiment was used for statistical analyses. Statistical significance is annotated as \* $p < 0.05$ , \*\* $p < 0.01$ , \*\*\* $p < 0.001$ , \*\*\*\* $p < 0.0001$ . Data were considered significantly different when  $p < 0.05$ .

## 5. RESULTS

### 5.1. Validation of tools for CUS modeling in rodents based on meta-analysis

Recent reports have shown that both preclinical and clinical studies widely used the meta-analysis to validate the efficiency of the treatment protocols. Since the primary goal of our project was to investigate the cross-talk between 5-HT<sub>1A</sub>R and 5-HT<sub>7</sub>R in stress-related disorders in animals, in this work, we have conducted the meta-analysis in order to verify the applicability of rodents in the chronic unpredictable stress paradigm and sucrose preference test (Fig. 6).

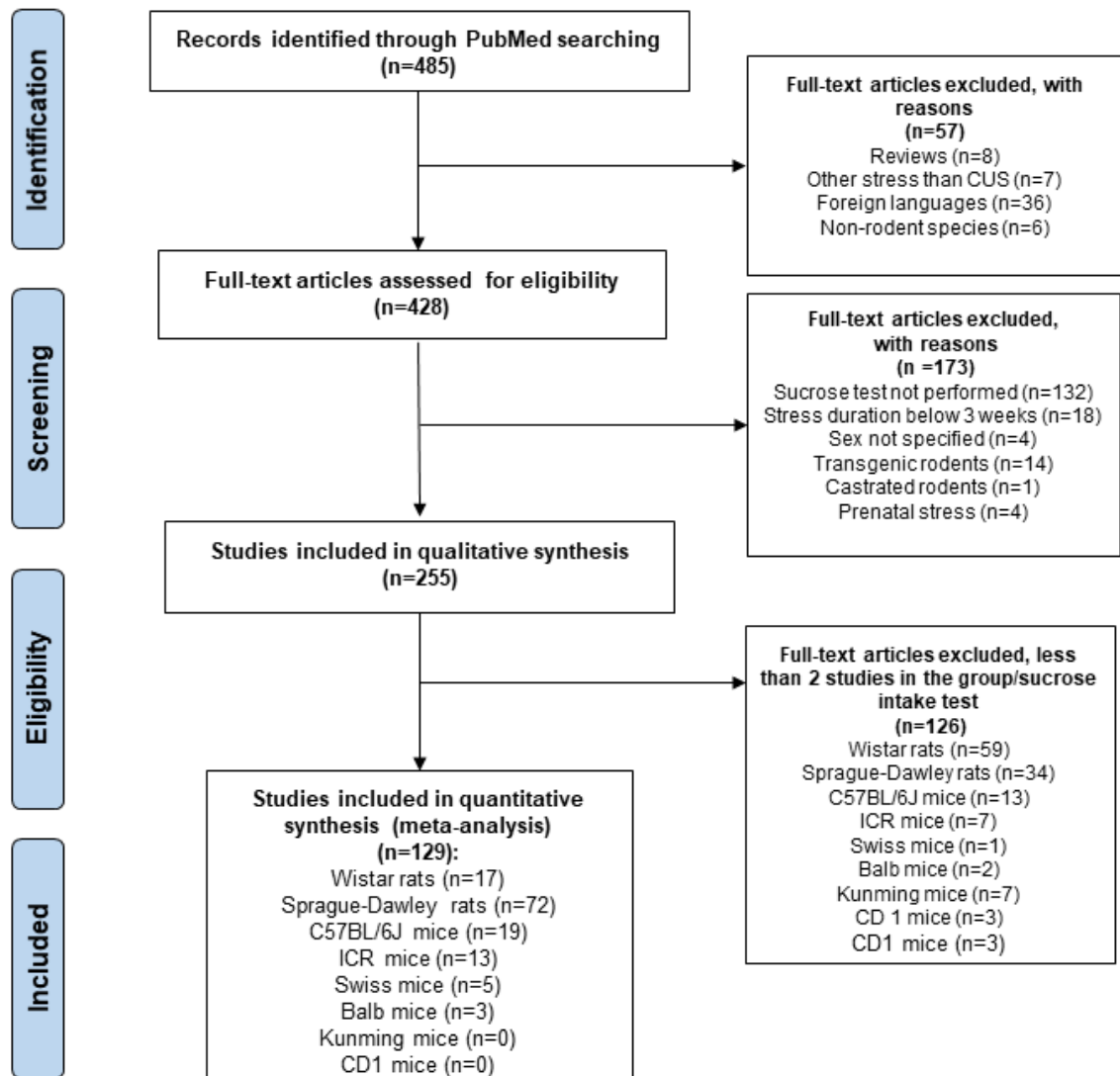
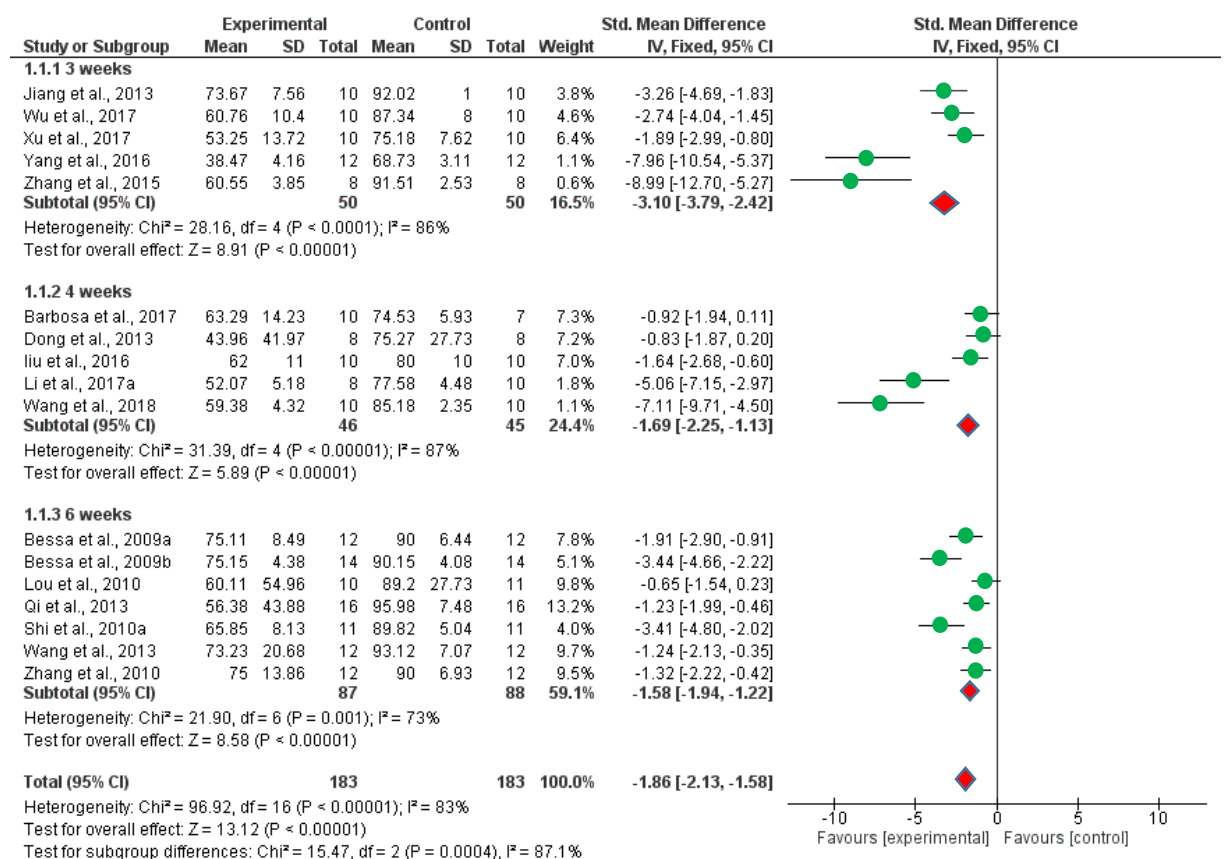


Fig. 6. Studies selection process

Upon the initial literature search, 485 papers were selected for general screening. Further, 428 studies were included for full-text assessment. As a result, 299 papers did

not meet the inclusion criteria and 129 papers were selected for the final qualitative and quantitative synthesis. Detailed analysis of the CUS protocols has demonstrated that stress modeling was mainly based on the circadian rhythm modification, cage titling, soiled bedding, food, and water deprivation. Interestingly, restraining, exposure to foreign objects, and tail suspension were used more often as stressors in mice in comparison to rats. Noteworthy, the pooled estimation of the included studies showed the significant induction of anhedonic behavior in rodents upon implementation of the CUS protocol (Figs. 7-12). Thus, experiments performed with both rats (Figs. 7-8) and mice (Figs. 9-12) demonstrated a sufficient effect size (SMD).



**Fig. 7. Forest plots of standardized mean differences in sucrose preference (%) in Wistar rats following implementation of the CUMS protocol.** The effect size was determined by calculating the standardized mean difference (SMD) and associated 95% confidence intervals. The size of the shaded square is proportional to the percent weight of each study. Horizontal lines represent 95% confidence intervals. The diamond data markers indicate the SMD.

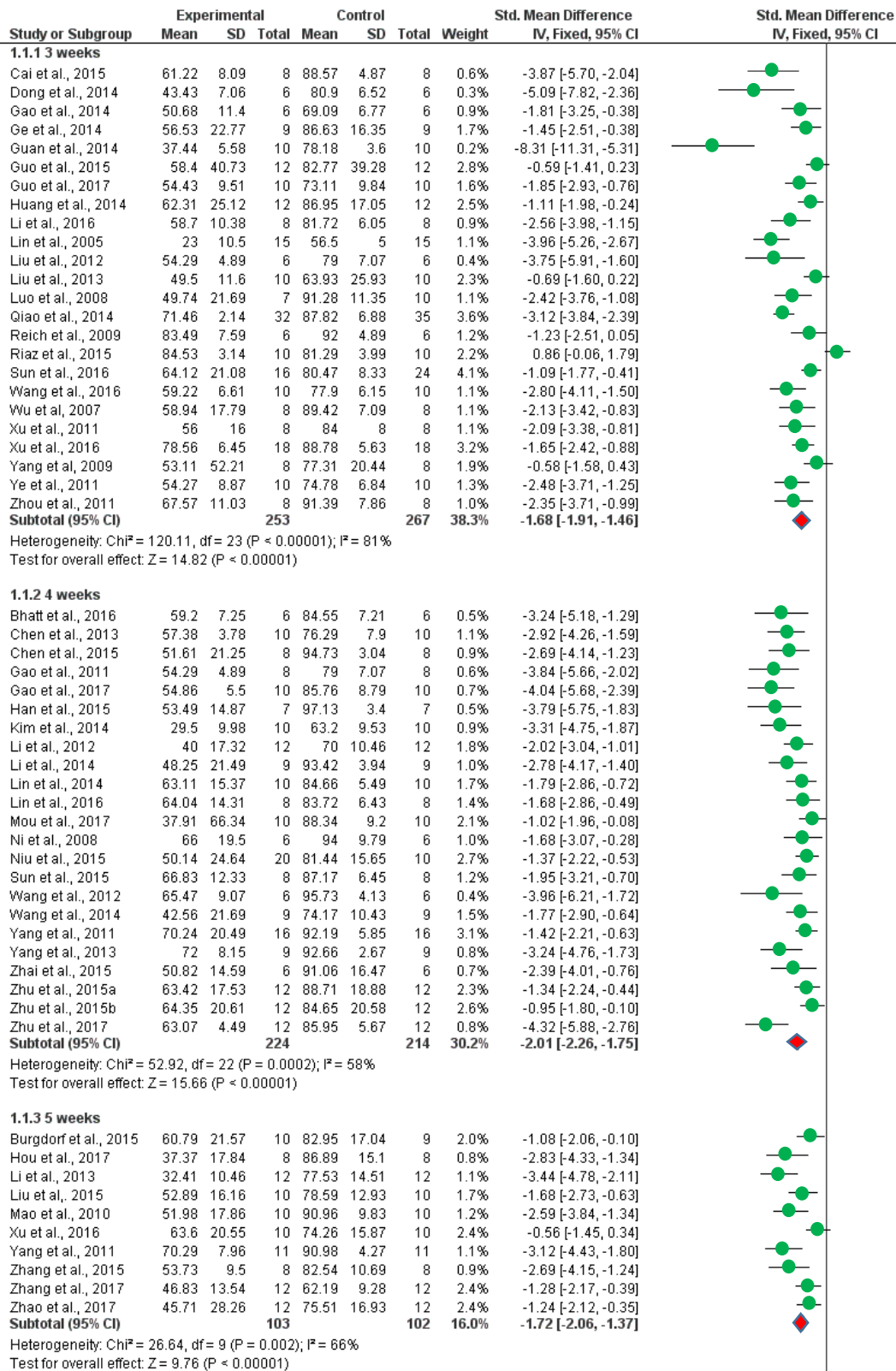


**Fig. 8. Forest plots of standardized mean differences in sucrose preference (%) in Sprague-Dawley rats following implementation of the CUMS protocol.**

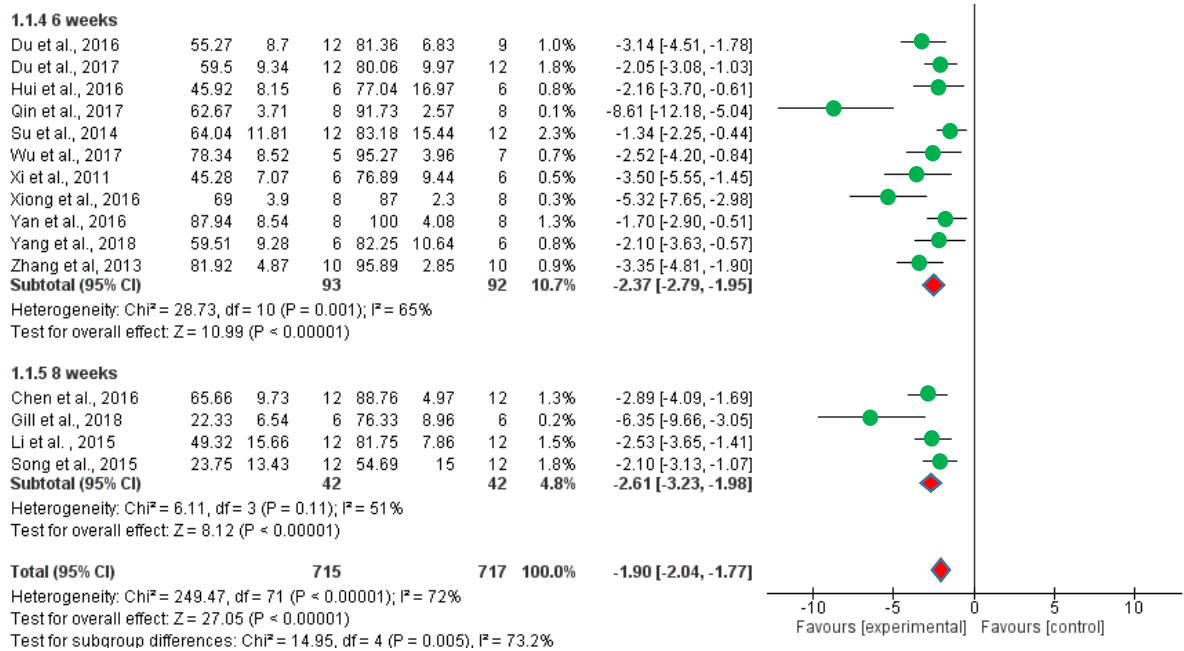


**Fig. 8. Continuation. Forest plots of standardized mean differences in sucrose preference (%) in Sprague-Dawley rats following implementation of the CUMS protocol.** The effect size was determined by calculating the standardized mean difference (SMD) and associated 95% confidence intervals. The size of the shaded square is proportional to the percent weight of each study. Horizontal lines represent 95% confidence intervals. The diamond data markers indicate the SMD.

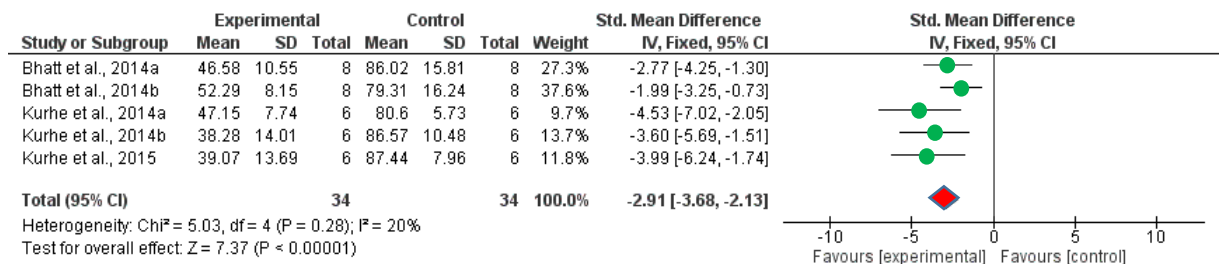


**Fig. 9. Forest plots of standardized mean differences in sucrose preference (%) in Swiss mice following implementation of the CUMS protocol (4 weeks).** The effect size was determined by calculating the standardized mean difference (SMD) and associated 95% confidence intervals. The size of the shaded square is proportional to the percent weight of each study. Horizontal lines represent 95% confidence intervals. The diamond data markers indicate the SMD.

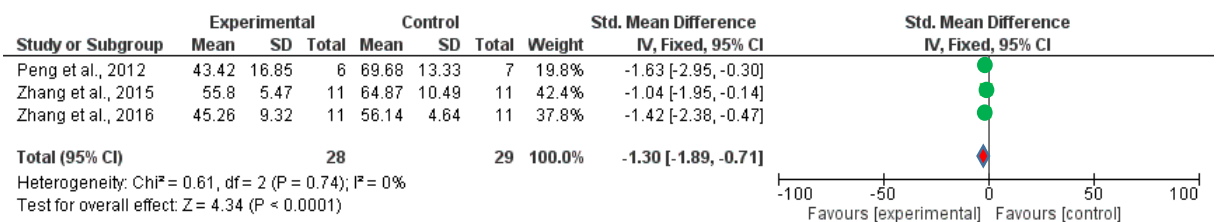


**Fig. 10. Forest plots of standardized mean differences in sucrose preference (%) in Balb mice following implementation of the CUMS protocol (4 weeks).** The effect size was determined by calculating the standardized mean difference (SMD) and associated 95% confidence intervals. The size of the shaded square is proportional to the percent weight of each study. Horizontal lines represent 95% confidence intervals. The diamond data markers indicate the SMD.

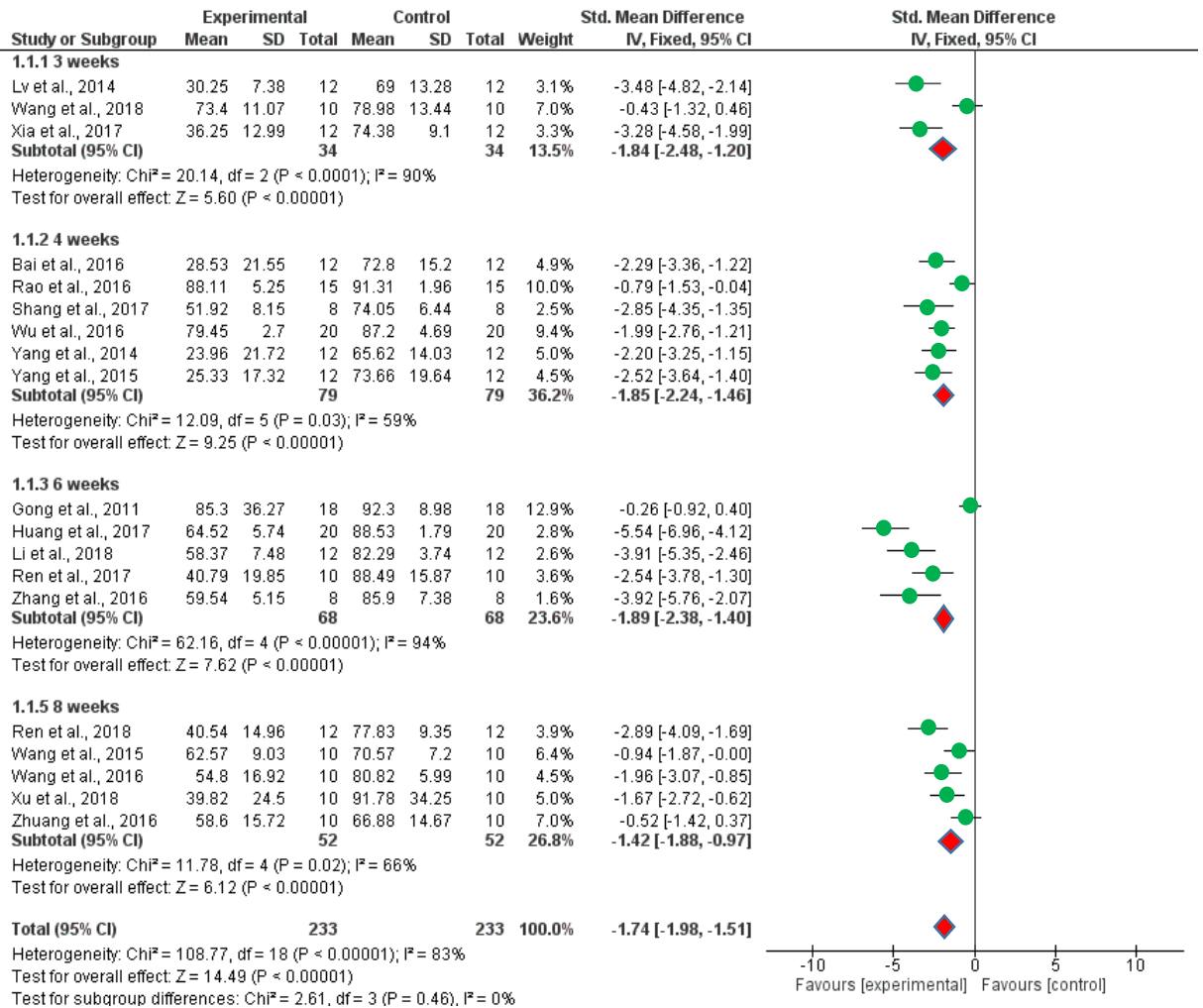


**Fig. 11. Forest plots of standardized mean differences in sucrose preference (%) in C57BL/6J mice following implementation of the CUMS protocol.** The effect size was determined by calculating the standardized mean difference (SMD) and associated 95% confidence intervals. The size of the shaded square is proportional to the percent weight of each study. Horizontal lines represent 95% confidence intervals. The diamond data markers indicate the SMD.

Noteworthy, the total effect size of the sucrose preference test (%) for Wistar rats (Fig. 7) (SMD= -1.86 [-2.13, -1.58]; Z=13.12 (P<0.00001); I<sup>2</sup>=83%) was in line with the results of the sucrose preference (%) obtained for Sprague-Dawley rats (Fig. 8) (SMD= -1.90 [-2.04, -1.77]; Z=27.05 (P<0.00001); I<sup>2</sup>=72%). Additionally, the analogous parameters for stressed mice were the following: C57BL/6J mice (Fig. 11) (SMD=-1.74 [-1.98, -1.51]; Z=14.49 (P < 0.00001); I<sup>2</sup>=83%), ICR mice (Fig. 12) (SMD= -1.83 [-2.14, -1.51]; Z=11.36 (P < 0.00001); I<sup>2</sup>=68%), Swiss mice (Fig. 9) (SMD= -2.91 [-3.68, -2.13]; Z=7.37 (P < 0.00001); I<sup>2</sup>=20%), Balb mice (Fig. 10) (SMD= -1.30 [-1.89, -0.7]; Z=4.34 (P < 0.0001); I<sup>2</sup>=0%).

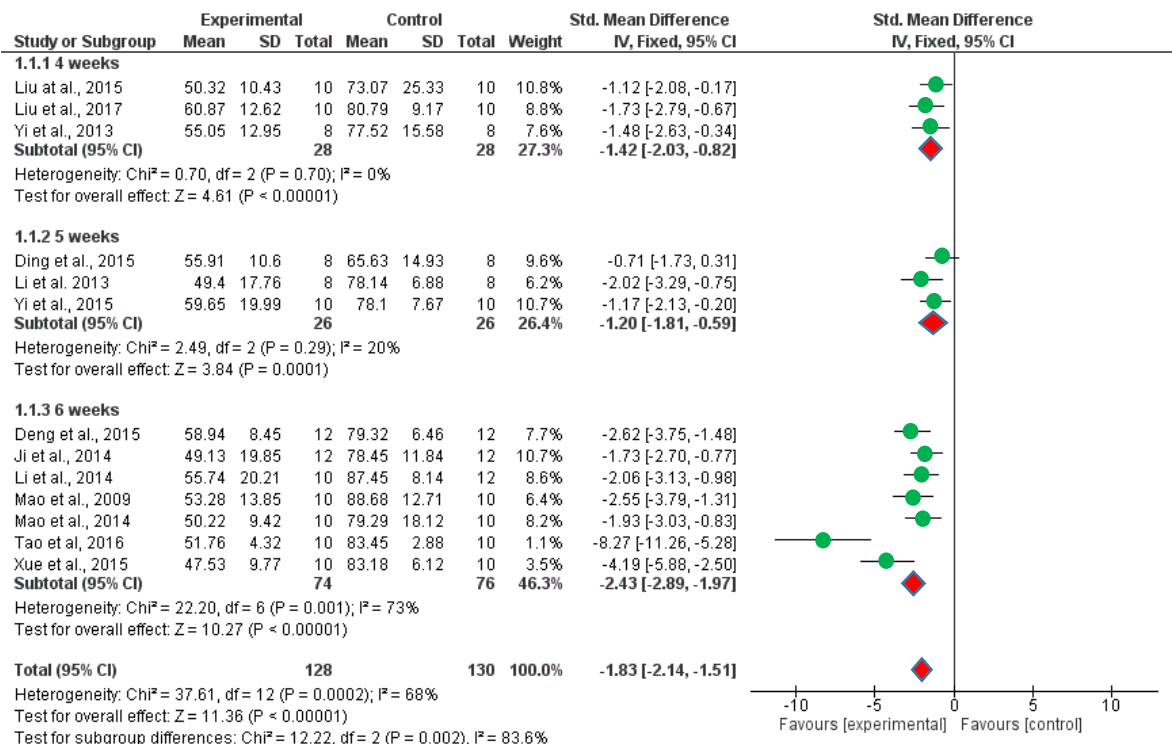


**Fig. 12. Forest plots of standardized mean differences in sucrose preference (%) in ICR mice following implementation of the CUMS protocol.** The effect size was determined by calculating the standardized mean difference (SMD) and associated 95% confidence intervals. The size of the shaded square is proportional to the percent weight of each study. Horizontal lines represent 95% confidence intervals. The diamond data markers indicate the SMD.

Interestingly, rodents showed different sensitivity to stress upon prolonging the CUS protocol. For instance, for SD rats (Fig. 8), the SMD value was determined to be approximately 140% higher for 6 and 8 weeks in comparison to 3, 4, and 5 weeks of exposure. Similar tendency was observed for ICR mice (Fig. 12), the implementation of a longer exposure of stress resulted in an approximately 190% stronger behavioral effect (6 weeks in comparison to 4 and 5 weeks). Additionally, the analysis has revealed an opposite effect for Wistar rats (Fig. 7): the anhedonic effect was decreased by about 50% upon extending 3-weeks strong protocol to 6 weeks. Similarly, CUS protocol efficiency for C57BL/6J mice (Fig. 11) was not associated with the stress duration. Thus, the SMD value after 8 weeks of stress decreased by 25% compared to 3 weeks of stress exposure. Since the SMD value for Swiss (Fig. 9) and Balb (Fig. 10) mice is shown for a single time point (4 weeks), the comparative analysis is impossible for these mouse strains. Taking into account the high susceptibility of C57BL/6J mice to CUS implementation upon short stress protocol duration, availability of transgenic lines bred on C57BL/6J genetic background, and lower cost of depression modeling in mice in comparison to rats, our further experiments were based on using of C57BL/6J mice for study of involvement 5-HT<sub>1A</sub> and 5-HT<sub>7</sub> receptors in depressive disorders.

## 5.2. Role of the 5-HT<sub>1A</sub>R and 5-HT<sub>7</sub>R activation in mouse behavior

It has been reported previously that 5-HT<sub>1A</sub>R and 5-HT<sub>7</sub>R are strongly associated with the pathogenesis of depressive disorders. In order to verify the behavioral profile of C57BL/6J mice after stimulation of 5-HT<sub>1A</sub>R and 5-HT<sub>7</sub>R, we have performed 5-carboxamidotryptamine (5-CT, high-affinity agonist of 5-HT<sub>7</sub>R and 5-HT<sub>1A</sub>R) (10 mg/kg; s.c.) or LP-211, high-affinity agonist of 5-HT<sub>7</sub>R (10 mg/kg; i.p.) injections and evaluated behavior using the tail suspension test. In these experiments, an 80% increase in immobility in the 5-CT group ( $153.80 \pm 20.55$  sec, n=4) in comparison to control ( $276.30 \pm 43.88$  sec, n=3) rodents injected with saline solution points to a despair behavior after 30 min of 5-CT administration (Fig. 13 A). Figure 13 B depicts that upon 30 min stimulation of 5-HT<sub>7</sub>R with LP-211 mice ( $198.30 \pm 13.76$  sec, n=6) showed an immobility rate increased by 25% compared to animals injected with the vehicle ( $245.00 \pm 12.58$  sec, n=6). To further assess the possible influence of disturbances in locomotion during the analysis of rodents movements during the tail suspension, the Eco-hab test was chosen. Noteworthy, despair behavior was not associated with changes in locomotor activity upon LP-211 administration (Fig. 13 C) (control group ( $0.25 \pm 0.06$ , n=7) and LP-211 ( $0.15 \pm 0.03$ , n=10). In conclusion, our results demonstrate that stimulation of 5-HT<sub>1A</sub>R and 5-HT<sub>7</sub>R *in vivo* leads to depressive phenotype in C57BL/6J mice, and this effect is not associated with changes in motor activity.

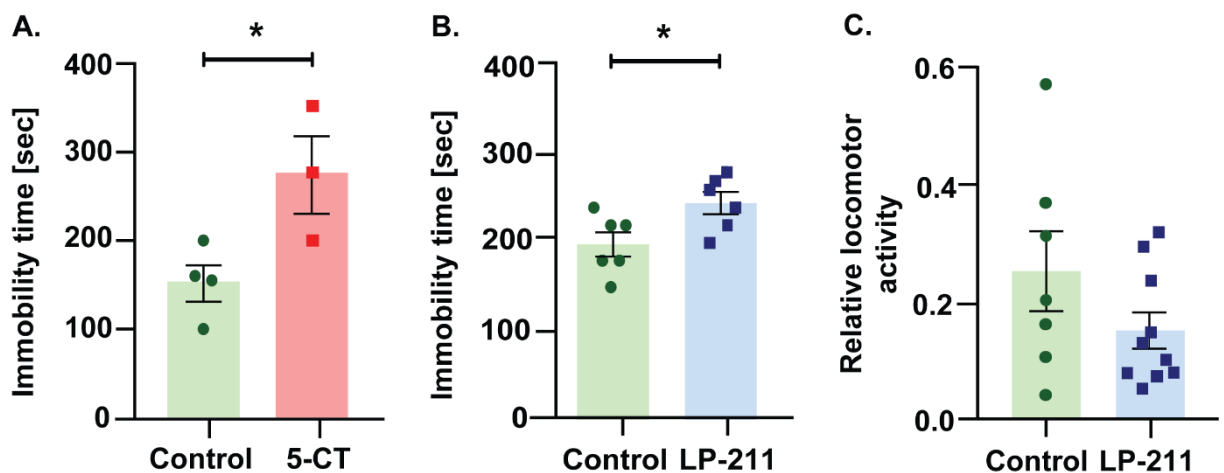


**Fig. 13. Stimulation of 5-HT<sub>1A</sub>R and 5-HT<sub>7</sub>R *in vivo*:** (A.) Tail suspension test upon injection of 5-CT (10 mg/kg; s.c.; 30 min; N≥3). There was observed a significant increase in immobility time in the 5-CT group in comparison to control animals (Unpaired *t* test, Two-tailed,  $t=2.784$ ,  $df=5$ ,  $p=0.039$ ); (B.) Tail suspension test upon injection of LP-211 (10 mg/kg; i.p.; 30 min; N=6). There was shown a significant increase in immobility time in the LP-211 group in comparison to control animals (Unpaired *t* test, Two-tailed,  $t=2.502$ ,  $df=10$ ,  $p=0.031$ ); (C.) Eco-hab upon injection of LP-211 (10 mg/kg; i.p.; 30 min; N≥7). No differences were found between the control and LP-211 groups (Unpaired *t* test, Two-tailed,  $t=1.499$ ,  $df=15$ ,  $p=0.155$ ). Results are represented as Mean  $\pm$  SEM.

### 5.3. Assessment of 5-HT<sub>1A</sub>R and 5-HT<sub>7</sub>R protein expression during brain development

Numerous studies based on autoradiography, *in situ* hybridization, positron emission tomography, and qRT-PCR have shown that 5-HT<sub>1A</sub>R and 5-HT<sub>7</sub>R are highly enriched in the cortical, brainstem, and limbic areas (Leopoldo et al., 2011; Renner et al., 2012). Therefore, we verified the 5-HT<sub>1A</sub>R and 5-HT<sub>7</sub>R mRNA (Fig. 14, 15) and protein level (Fig. 16) in the above-mentioned brain regions during brain development at postnatal days 2, 12, and 90. Thus, the 5-HT<sub>1A</sub> mRNA was overexpressed in the hippocampus in comparison to the prefrontal cortex and raphe nuclei during brain development. At the same time, the 5-HT<sub>7</sub> mRNA level was the highest in the raphe nuclei in comparison to the prefrontal cortex and hippocampus at day 2 and 12, whereas the 5-HT<sub>7</sub> mRNA expression was at the same level in all the studied brain structures at day 90. Using the same data set, we then determined the ratio of 5-HT<sub>1A</sub> and 5-HT<sub>7</sub> receptors in different brain region during development (Fig. 15). In particular, there was observed overexpression of the 5-HT<sub>1A</sub> mRNA both in the prefrontal cortex and hippocampus at days 2, 12, and 90. On the contrary, in the raphe nuclei the 5-HT<sub>7</sub>R mRNA expression was higher compared to 5-HT<sub>1A</sub>R mRNA.

Interestingly, Western blot analysis (Fig. 16) has shown that the most robust changes were observed for the 5-HT<sub>1A</sub> receptors, whereas the level of the 5-HT<sub>7</sub>R did not differ within the studied brain structures. Thus, at day 2 of postnatal development the relative expression of the 5-HT<sub>1A</sub> receptors was  $2.09 \pm 0.25$  (n=6) in the prefrontal cortex,  $3.10 \pm 0.46$  (n=6) in the hippocampus, and  $1.00 \pm 0.13$  (n=6) in the raphe nuclei. The 5-HT<sub>7</sub>R protein level was  $2.33 \pm 0.47$  (n=6) in the prefrontal cortex,  $1.73 \pm 0.46$  (n=6) in the hippocampus, and  $1.00 \pm 0.26$  (n=6) in the raphe nuclei. In respect to day 12, the expression of the 5-HT<sub>1A</sub> receptors was double as high in the prefrontal cortex ( $2.38 \pm 0.23$  (n=6) and hippocampus ( $2.08 \pm 0.18$  (n=6) as in the raphe nuclei ( $1.00 \pm 0.16$  (n=6), whereas the 5-HT<sub>7</sub>R level was  $1.44 \pm 0.20$  (n=6) in the prefrontal cortex,  $1.55 \pm 0.22$  (n=6) in the hippocampus, and  $1.00 \pm 0.16$  (n=6) in the raphe nuclei. Additionally, at day 90 of postnatal development the relative expression of the 5-HT<sub>1A</sub> receptors is the lowest in the raphe nuclei and the highest in the prefrontal cortex and hippocampus (RN:  $1.00 \pm 0.23$  (n=6); PFC:  $3.21 \pm 0.48$  (n=6); HIP:  $3.92 \pm 0.66$  (n=6). The 5-HT<sub>7</sub>R protein level was  $2.03 \pm 0.45$  (n=6) in the prefrontal cortex,  $1.95 \pm 0.39$  (n=6) in the hippocampus, and  $1.00 \pm 0.29$  (n=6) in the raphe nuclei.

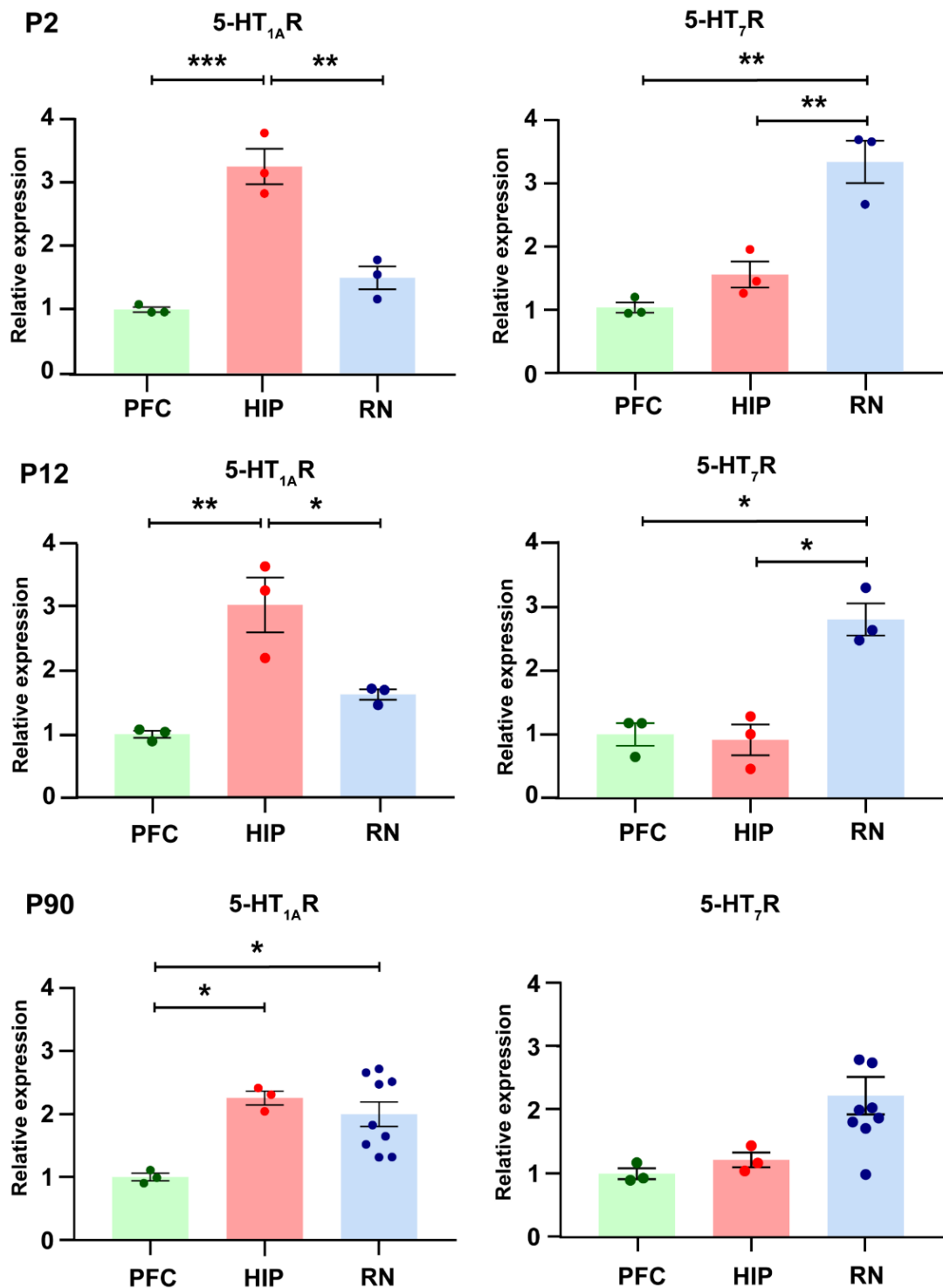


**Fig. 14.** 5-HT<sub>1A</sub>R and 5-HT<sub>7</sub>R mRNA expression in the C57BL/6J mouse brain at day 2, 12 and 90 of the postnatal development using real-time PCR and  $\Delta\Delta CT$  method. **P2:** 5-HT<sub>1A</sub>R relative expression was determined as significantly higher in the hippocampus (HIP) in comparison to the prefrontal cortex (PFC) and raphe nuclei (RN) (One-way ANOVA:  $F(2,6) = 37.29$ ,  $p = 0.0004$ ; Tukey's Multiple comparisons: PFC vs. HIP:  $p = 0.0004$ ; HIP vs. RN:  $p = 0.002$ ); 5-HT<sub>7</sub>R relative expression was determined as significantly higher in the raphe nuclei (RN) in comparison to the prefrontal cortex (PFC) and hippocampus (HIP) (One-way ANOVA:  $F(2,6) = 27.05$ ,  $p = 0.001$ ; Tukey's Multiple comparisons: PFC vs. RN:  $p = 0.001$ ; HIP vs. RN:  $p = 0.004$ ). **P12:** Significant differences were observed for 5-HT<sub>1A</sub>R expression (One-way ANOVA:  $F(2,6) = 16.66$ ,  $p = 0.004$ ; Tukey's Multiple comparisons: PFC vs. HIP:  $p = 0.003$ ; HIP vs. RN:  $p = 0.02$ ) and 5-HT<sub>7</sub>R expression (One-way ANOVA:  $F(2,6) = 22.31$ ,  $p = 0.002$ ; Tukey's Multiple comparisons: PFC vs. RN:  $p = 0.003$ ; HIP vs. RN:  $p = 0.003$ ). **P90:** Significant differences were observed for 5-HT<sub>1A</sub>R expression (One-way ANOVA:  $F(2,12) = 4.84$ ,  $p = 0.0156$ ; Tukey's Multiple comparisons: PFC vs. HIP:  $p = 0.0211$ ; PFC vs. RN:  $p = 0.0244$ ) and 5-HT<sub>7</sub>R expression (One-way ANOVA:  $F(2,12) = 1.32$ ,  $p = 0.0389$ ; Tukey's Multiple comparisons: PFC vs. HIP:  $p = 0.9298$ ; PFC vs. RN:  $p = 0.0641$ ; HIP vs. RN:  $p = 0.1361$ ).

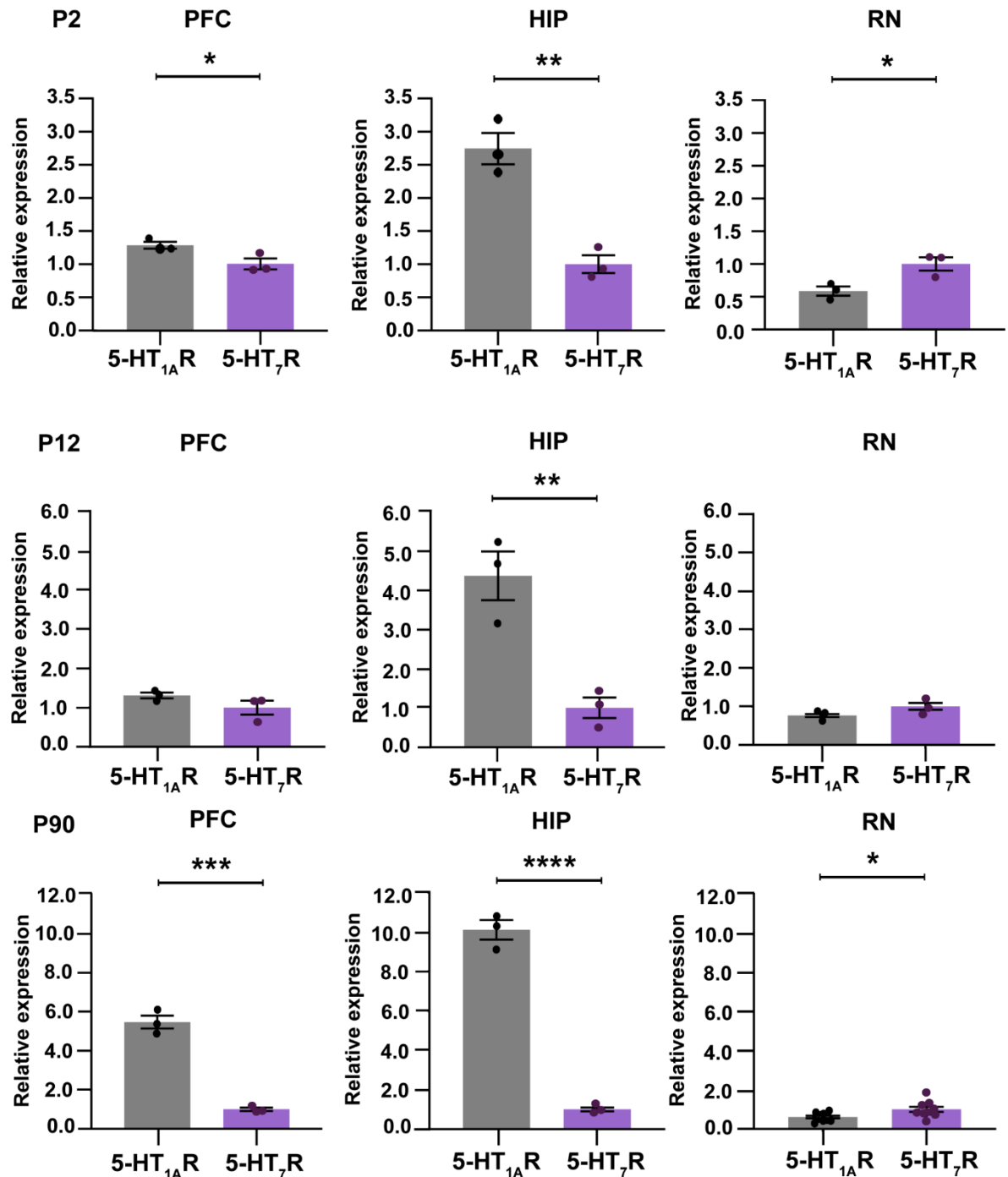


**Fig. 15. 5-HT<sub>1A</sub>R and 5-HT<sub>7</sub>R mRNA expression in the C57BL/6J mouse brain at day 2, 12 and 90 of the postnatal development using real-time PCR and  $\Delta\Delta CT$  method:** **P2: (PFC)** It was determined that the 5-HT<sub>1A</sub>R was overexpressed in comparison to the 5-HT<sub>7</sub>R in the prefrontal cortex (Unpaired *t* test, Two-tailed,  $t=2.891$ ,  $df=4$ ,  $p=0.045$ ); **(HIP)** Significant differences of the 5-HT<sub>1A</sub>R/5-HT<sub>7</sub>R relative expression were shown in the hippocampus (Unpaired *t* test, Two-tailed,  $t=6.422$ ,  $df=4$ ,  $p=0.003$ ); **(RN)** Significant changes of 5-HT<sub>1A</sub>R/5-HT<sub>7</sub>R relative expression in the raphe nuclei were observed (Unpaired *t* test, Two-tailed,  $t=3.361$ ,  $df=4$ ,  $p=0.028$ ). Results are represented as Mean  $\pm$  SEM ( $N=3$ ). **P12: (PFC)** No significant differences were observed for 5-HT<sub>1A</sub>R/5-HT<sub>7</sub>R relative expression in the prefrontal cortex (Unpaired *t* test, Two-tailed,  $t=1.623$ ,  $df=4$ ,  $p=0.179$ ). **(HIP)** Significant differences were observed for 5-HT<sub>1A</sub>R/5-HT<sub>7</sub>R relative expression in the hippocampus (Unpaired *t* test, Two-tailed,  $t=4.989$ ,  $df=4$ ,  $p=0.008$ ). **(RN)** No significant differences were observed for 5-HT<sub>1A</sub>R/5-HT<sub>7</sub>R relative expression in the raphe nuclei (Unpaired *t* test, Two-tailed,  $t=2.417$ ,  $df=4$ ,  $p=0.073$ ). Results are represented as Mean  $\pm$  SEM ( $N=3$ ). **P90: (PFC)** Significant differences were observed for 5-HT<sub>1A</sub>R/5-HT<sub>7</sub>R relative expression in the prefrontal cortex (Unpaired *t* test, Two-tailed,  $t=13.14$ ,  $df=4$ ,  $p=0.0002$ ). **(HIP)** Significant differences were observed for 5-HT<sub>1A</sub>R/5-HT<sub>7</sub>R relative expression in the hippocampus (Unpaired *t* test, Two-tailed,  $t=18.04$ ,  $df=4$ ,  $p=0.0001$ ). **(RN)** Significant differences were observed for 5-HT<sub>1A</sub>R/5-HT<sub>7</sub>R relative expression in the raphe nuclei (Unpaired *t* test, Two-tailed,  $t=2.671$ ,  $df=16$ ,  $p=0.0167$ ). Results are represented as Mean  $\pm$  SEM ( $N=9$ ).

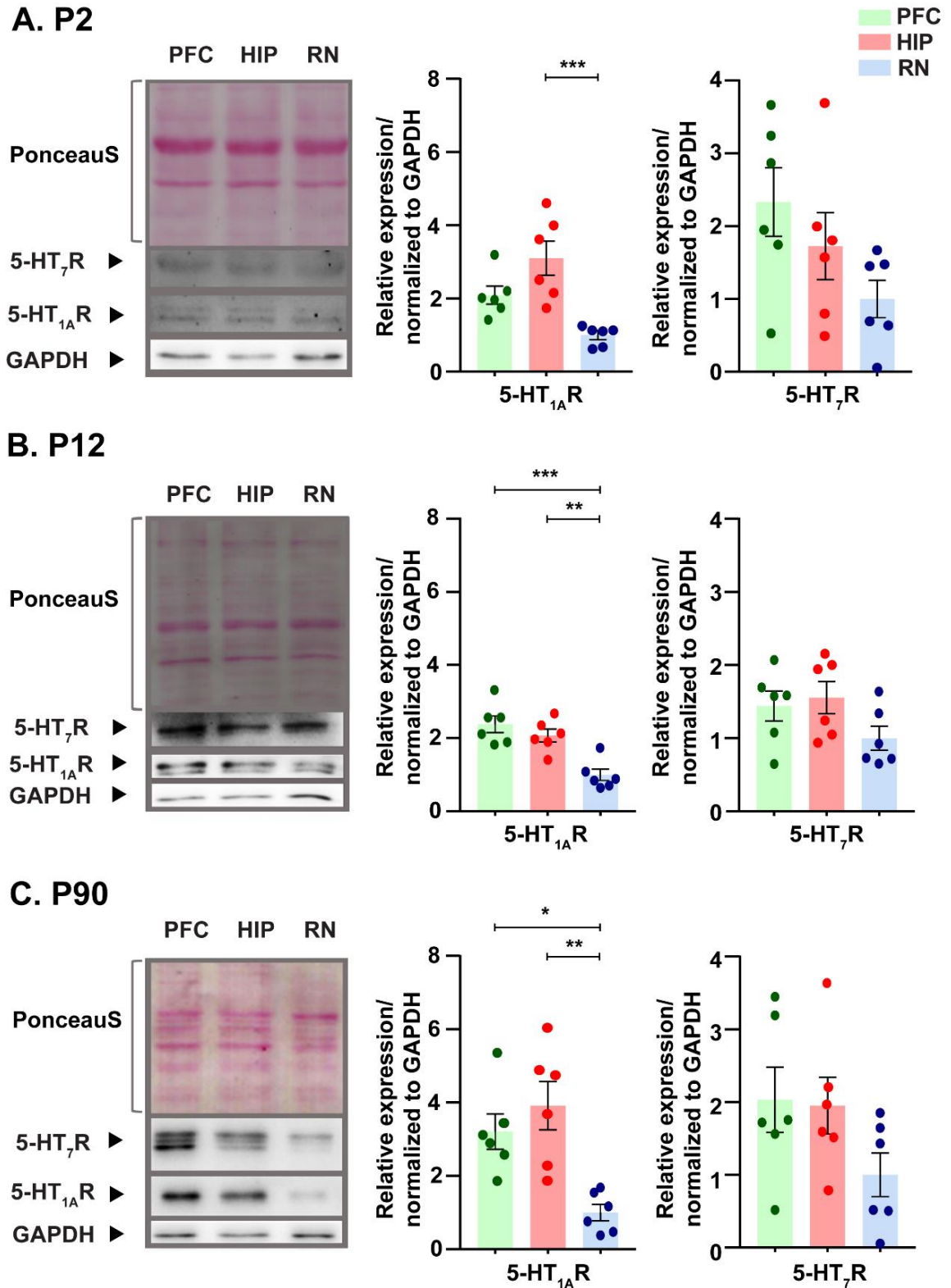


**Fig. 16. Western blot analysis of 5-HT<sub>1A</sub>R and 5-HT<sub>7</sub>R protein levels in the developing brain of C57BL/6J mice:** Significant differences were found for the 5-HT<sub>1A</sub>R protein level at the postnatal day 2 (P2) (**A.**) (One-way ANOVA:  $F(2, 15) = 11.38$ ,  $p = 0.001$ ; Tukey's Multiple comparisons: HIP vs. RN:  $p = 0.0007$ ); postnatal day 12 (P12) (**B.**) (One-way ANOVA:  $F(2, 15) = 14.59$ ,  $p = 0.0003$ ; Tukey's Multiple comparisons: PFC vs. RN:  $p = 0.0003$ ; HIP vs. RN:  $p = 0.003$ ), and postnatal day 90 (P90) (**C.**) (One-way ANOVA:  $F(2, 15) = 9.659$ ,  $p = 0.002$ ; Tukey's Multiple comparisons: PFC vs. RN:  $p = 0.02$ ; HIP vs. RN:  $p = 0.002$ ). No changes were found for the 5-HT<sub>7</sub>R protein level at the postnatal day 2 (P2) (**A.**) (One-way ANOVA:  $F(2, 15) = 2.673$ ,  $p = 0.101$ ); postnatal day 12 (P12) (**B.**) (One-way ANOVA:  $F(2, 15) = 2.202$ ,  $p = 0.145$ ), and postnatal day 90 (P90) (**C.**) (One-way ANOVA:  $F(2, 15) = 2.224$ ,  $p = 0.143$ ). Results are represented as Mean  $\pm$  SEM ( $N = 6$ ).

## 5.4. Investigation of 5-HT<sub>1A</sub>R and 5-HT<sub>7</sub>R heterodimerization profile

### 5.4.1. Validation of mouse behavioral profile upon CUS application

Taking into account a functional role of heterodimerization between 5-HT<sub>1A</sub>R and 5-HT<sub>7</sub>R obtained from *in vitro* experiments (Prasad et al., 2019; Renner et al., 2012), we investigated whether the level of heterodimerization can be changed upon stressful condition. To this end, we combined a chronic unpredictable stress procedure in C57BL/6J mice followed by using a proximity ligation assay. CUS protocol efficiency was verified by monitoring body weight, sucrose preference test and forced swimming test (Fig. 17).

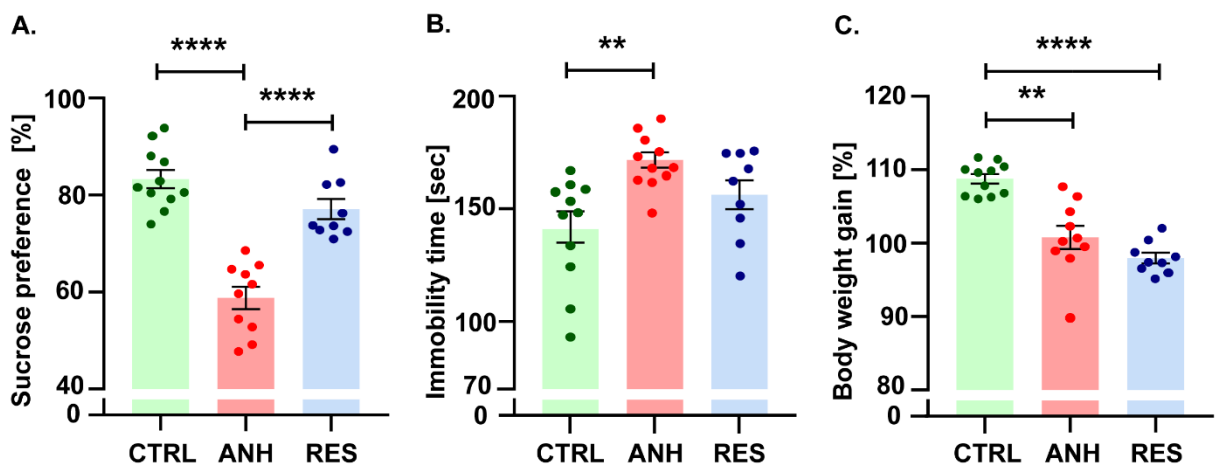


**Fig. 17. Assessment of chronic unpredictable mild stress efficiency:** (A.) Significant differences were found in sucrose consumption in the sucrose preference test (One-way ANOVA:  $F(2, 27) = 38.12, p < 0.0001$ ; Tukey's Multiple comparisons: CTRL vs. ANH:  $p < 0.0001$ ; ANH vs. RES:  $p < 0.0001$ ); (B.) Significant differences were found in immobility in the forced swimming test (One-way ANOVA:  $F(2, 28) = 7.12, p = 0.003$ ; Tukey's Multiple comparisons: CTRL vs. ANH:  $p = 0.002$ ); (C.) There was observed a significant difference in the body weight (One-way ANOVA:  $F(2, 27) = 28.01, p < 0.0001$ ; Tukey's Multiple comparisons: CTRL vs. ANH:  $p < 0.0001$ ; CTRL vs. RES:  $p < 0.0001$ ). Results are represented as Mean  $\pm$  SEM (C57BL/6J (P110;  $N \geq 9$ )).

Anhedonic animals were selected based on lower sucrose consumption in comparison to control and stress-resistant animals. Thus, sucrose preference (%) for control animals was observed at the level of  $83.27 \pm 1.89\%$  ( $n=11$ ); for anhedonic animals –  $58.78 \pm 2.31\%$  ( $n=10$ ); for resilient animals –  $77.11 \pm 2.08\%$  ( $n=9$ ) (Fig. 17 A). The anhedonic phenotype that was assessed by the sucrose preference test, was additionally verified by performing a forced swimming test in order to check for signs of despair in rodents. In line with the results obtained in the sucrose preference test, the immobility of anhedonic mice ( $171.70 \pm 3.44$  sec,  $n=11$ ) was increased compared to non-stressed animals ( $141.90 \pm 6.97$  sec,  $n=11$ ) (Fig. 17 B). Noteworthy, both sucrose consumption and the behavioral pattern during the swimming test of stress-

resilient mice were similar to unstressed control animals, but changes in their body weight ( $97.95 \pm 0.73$  g,  $n=9$ ) were in line with the stress-susceptible group ( $100.80 \pm 1.58$  g,  $n=10$ ) (Fig. 17 C).

#### 5.4.2. Immunohistological staining of 5-HT<sub>1A</sub> and 5-HT<sub>7</sub> receptors

Since the success of the PLA protocol implementation is strongly dependent on the specificity of immunohistological stainings, we optimized and adopted the staining protocol for all antibodies to PLA conditions. By omitting primary antibodies (Fig. 18), we did not observe the specific signals upon applying secondary antibodies only (Fig. 18 D, F).

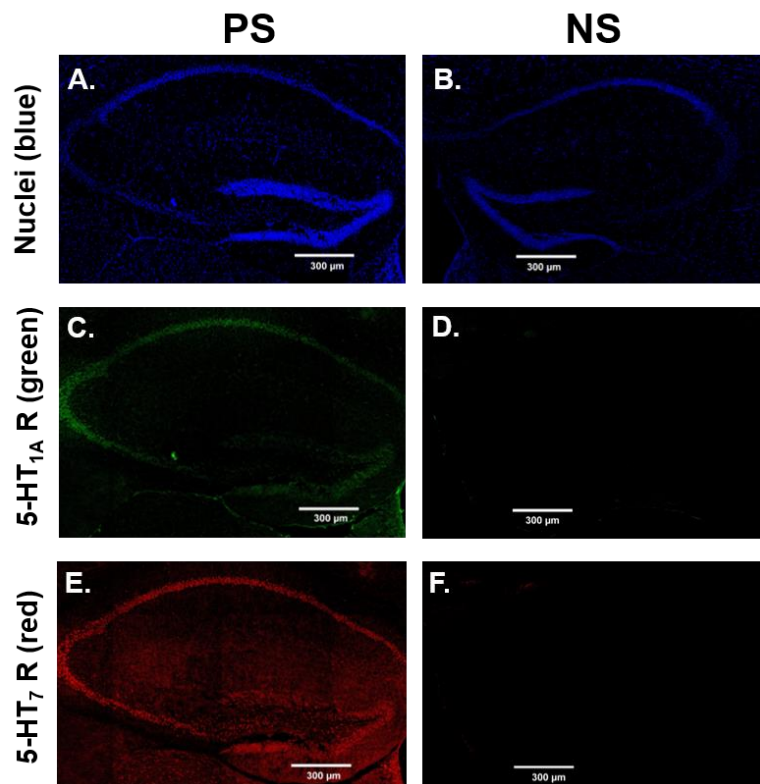


**Fig. 18. Immunostaining of 5-HT<sub>1A</sub> and 5-HT<sub>7</sub> receptors immunolabeling in the mouse hippocampus:** (A, B) DAPI-stained cell nuclei; (C, D) Immunodetection of 5-HT<sub>1A</sub> R (green) and (E, F) 5-HT<sub>7</sub> (red) are demonstrated in positive (PS) and negative (NS) stainings. Negative controls omit the primary antibodies.

As illustrated in Fig. 19, both the 5-HT<sub>1A</sub> and 5-HT<sub>7</sub> receptors are expressed within the prefrontal cortex, hippocampus, and raphe nuclei. The distribution of the 5-HT<sub>1A</sub>R and 5-HT<sub>7</sub>R in the above-mentioned structures becomes clearly visible in higher-magnification images. Moreover, by merging 5-HT<sub>1A</sub>R (in green) and 5-HT<sub>7</sub>R (in red) stainings, clustering of the 5-HT<sub>1A</sub>R and 5-HT<sub>7</sub>R in the same cells becomes obvious (Figs. 19, indicated in yellow).

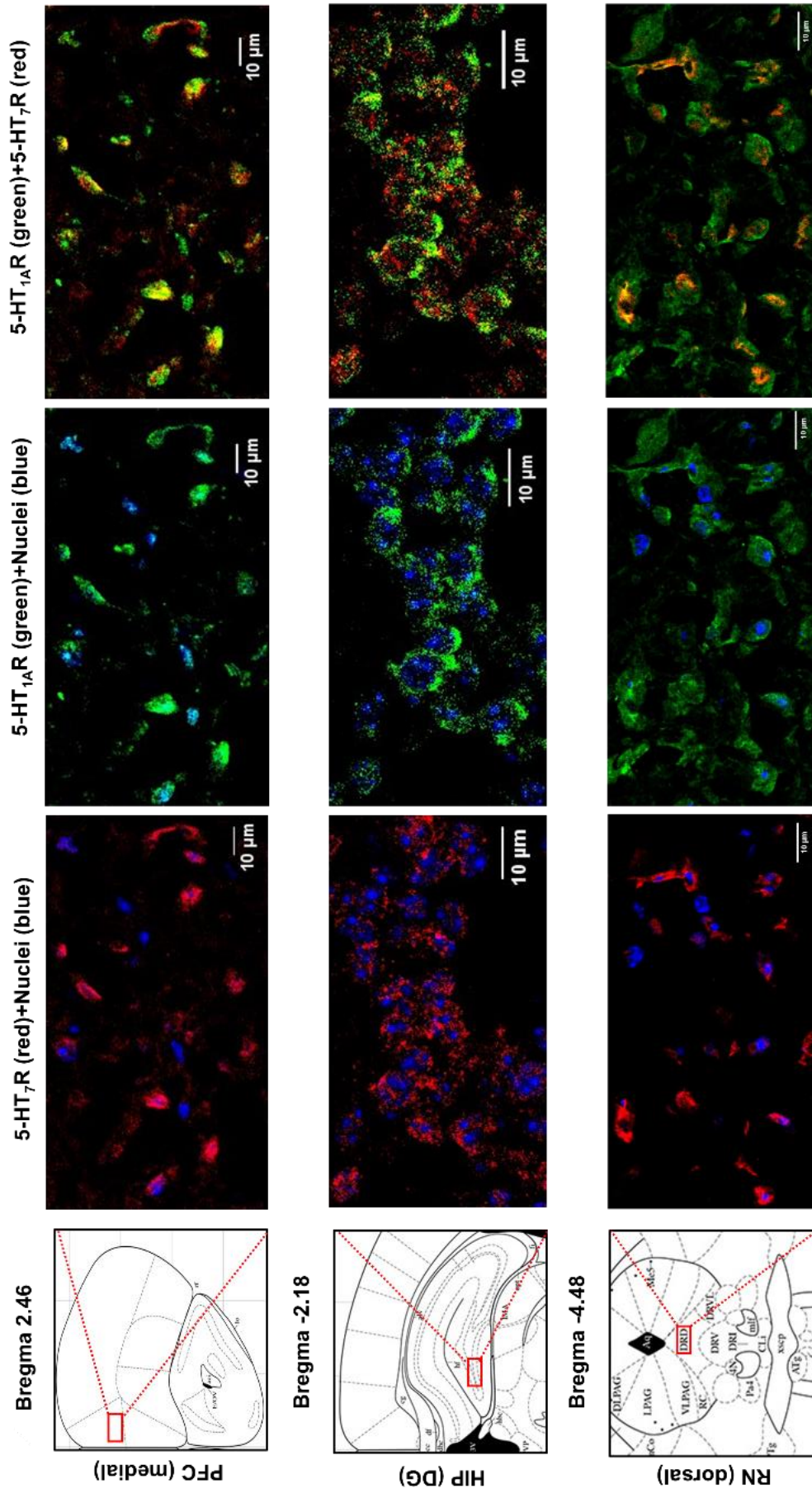


**Fig. 19. Immunostaining of 5-HT<sub>1A</sub>-5-HT<sub>7</sub> receptors immunolabeling in the mouse brain: (PFC medial) Bregma 2.46 ; (HIP, DG) Bregma -2.18; (RN dorsal) Bregma -4.48. DAPI-stained cell nuclei are shown in blue; 5-HT<sub>1A</sub>R – in green and 5-HT<sub>7</sub>R – in red. Merged images of 5-HT<sub>1A</sub>R and 5-HT<sub>7</sub>R show double immunostaining of both receptors in yellow.**

### 5.4.3. 5-HT<sub>1A</sub>R and 5-HT<sub>7</sub>R heterodimerization

Since the prefrontal cortex is strongly involved in the pathogenesis of depression, we analyzed changes in heterodimerization ratio of 5-HT<sub>1A</sub>R and 5-HT<sub>7</sub>Rs in the medial prefrontal cortex after stressful conditions (Fig. 20).

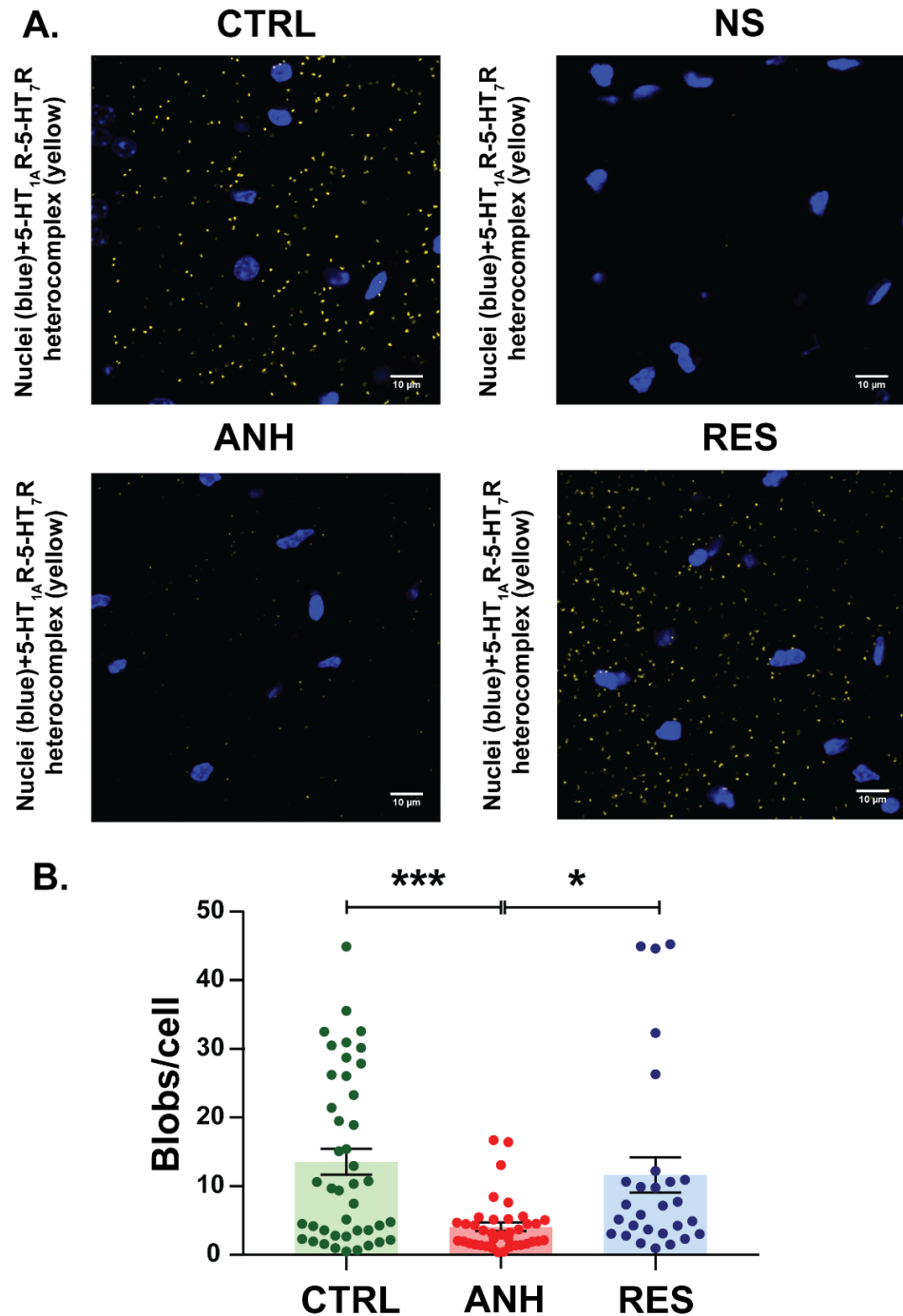


**Fig. 20. 5-HT<sub>1A</sub>R and 5-HT<sub>7</sub>R heterocomplex formation in the medial prefrontal cortex of C57BL/6J mice upon stress implementation: (A.)** Representative images of proximity ligation assay staining of control (CTRL), anhedonic (ANH), and resilient (RES) groups are shown as the single Z-stack (1  $\mu$ m). The nuclei are shown in blue, PLA blobs – in yellow. Negative staining (NS) was performed omitting primary antibodies; **(B.)** Evaluation of 5-HT<sub>1A</sub>R/5-HT<sub>7</sub>R heterodimers density has shown significant difference between investigated groups (One-way ANOVA:  $F(2, 106) = 8.595, p = 0.0003$ ; Tukey's Multiple comparisons: CTRL vs. ANH:  $p = 0.0003$ ; ANH vs. RES:  $p = 0.014$ ). Each dot represents the ROI value for the tested condition. Results are represented as Mean  $\pm$  SEM ( $N \geq 5$ ).

The quantification of PLA-positive blobs per cell (Fig. 20 B) indicates that the number of 5-HT<sub>1A</sub>R/5-HT<sub>7</sub>R heterodimers decreased significantly in stress-susceptible animals to nearly one third ( $4.08 \pm 0.63$ , ROI n=38) in comparison to control ( $13.54 \pm 1.88$ , ROI n=43) and one fourth in stress-resilient groups ( $11.63 \pm 2.58$ , ROI n=28), whereas there was no significant different observable between control animals and resilient animals. Fig. 20 A presented representative images of 5-HT<sub>1A</sub>R/5-HT<sub>7</sub>R heterodimers density in control, anhedonic, and resilient rodents. Additionally, to proof our hypothesis of 5-HT mediated contribution to depression, we were able to shown that beside the mouse brain, 5-HT<sub>1A</sub>R/5-HT<sub>7</sub>R heterodimerization also occurs in the human prefrontal cortex (Fig. 21).

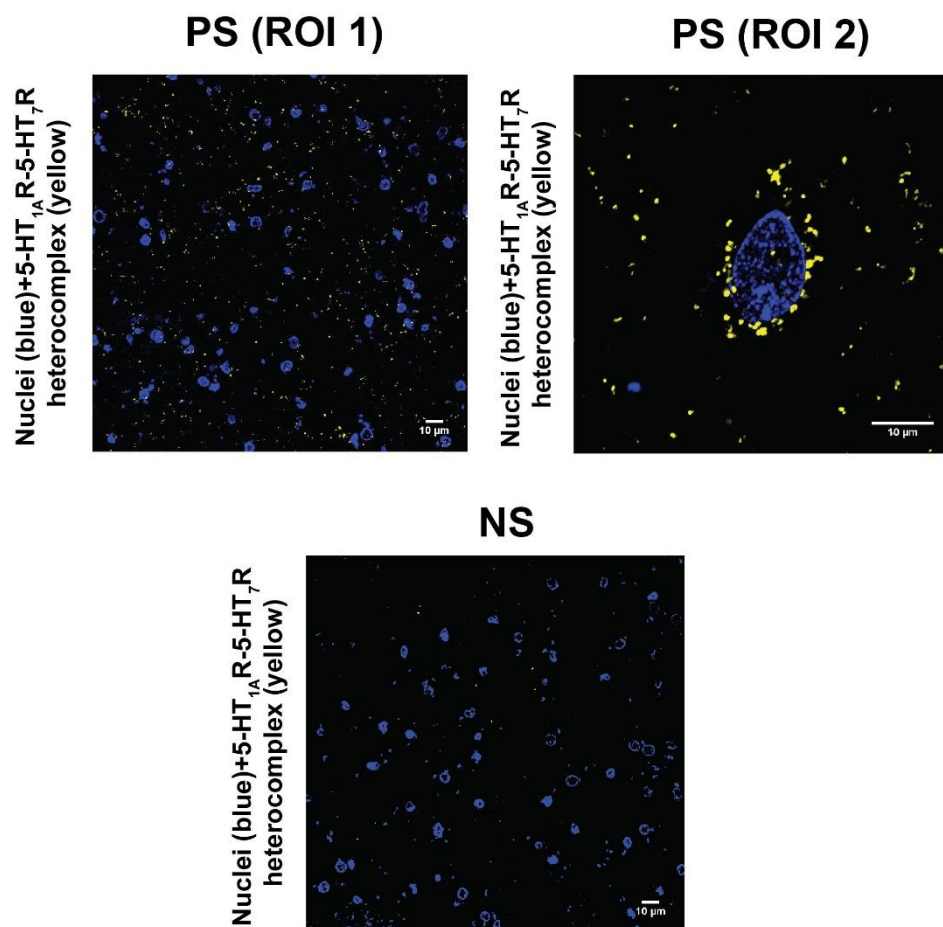


**Fig. 21. 5-HT<sub>1A</sub>R and 5-HT<sub>7</sub>R heterocomplex formation in the human prefrontal cortex.** The representative images are shown as the single z-plane (1 µm). The nuclei are shown in blue, PLA blobs – in yellow. Positive stainings (PS) are demonstrated in low (ROI 1) and high (ROI 2) magnification. Negative staining (NS) is performed omitting primary antibodies.

Additionally, we have observed that 5-HT<sub>1A</sub>R and 5-HT<sub>7</sub>R heterodimerization was decreased in the dentate gyrus (DG) region (Fig. 22) of the hippocampus of stress-susceptible C57BL/6J mice ( $0.29 \pm 0.06$ , ROI n=18) compared to stress-resilient animals ( $0.97 \pm 0.33$ , n=14). Noteworthy, the density of 5-HT<sub>1A</sub>R/5-HT<sub>7</sub>R

heterocomplexes under basal condition in the hippocampus was approximately 25 times lower in comparison to the medial prefrontal cortex.

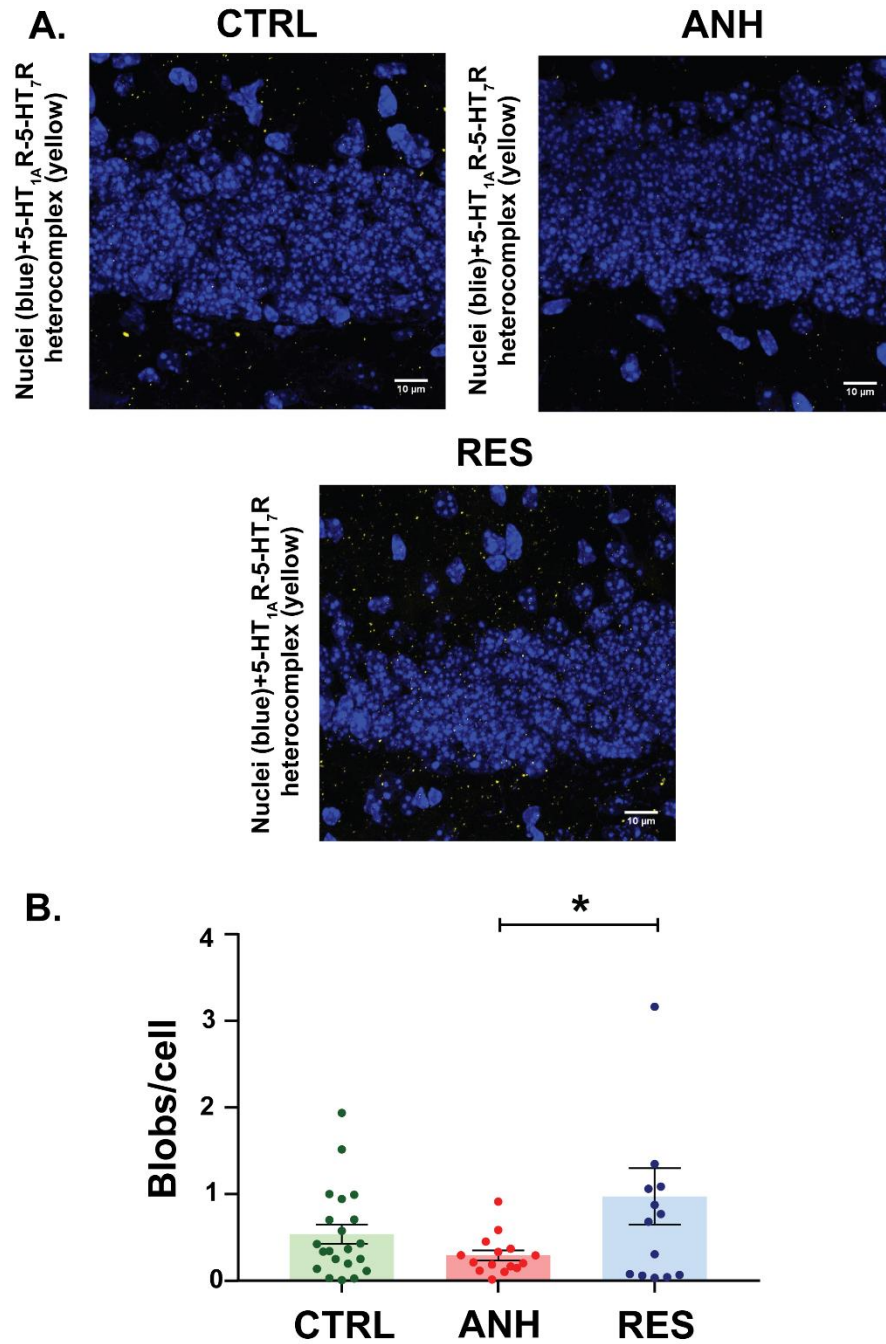


**Fig 22. 5-HT<sub>1A</sub>R and 5-HT<sub>7</sub>R heterocomplex formation in dentate gyrus region of the hippocampus of C57BL/6J mice after stress implementation:** (A.) Representative images of proximity ligation assay staining of control (CTRL), anhedonic (ANH), and resilient (RES) groups are shown as the maximum intensity projection (30 µm). The nuclei are shown in blue, PLA blobs – in yellow; (B.) Evaluation of 5-HT<sub>1A</sub>R/5-HT<sub>7</sub>R heterodimers density has shown significant difference between the anhedonic, and resilient groups (One-way ANOVA:  $F(2,47) = 3.23$ ,  $p = 0.048$ ; Tukey's Multiple comparisons: ANH vs. RES:  $p = 0.041$ ). Each dot represents the ROI value for the tested condition. Results are represented as Mean  $\pm$  SEM ( $N \geq 5$ ).

To verify the level of 5-HT<sub>1A</sub>R/5-HT<sub>7</sub>R heterocomplexes formation in the midbrain, we have focused on the dorsal raphe nuclei region (Fig. 23). Taking into account that serotonergic cell bodies are located in the raphe nuclei, additional serotonergic staining was performed.

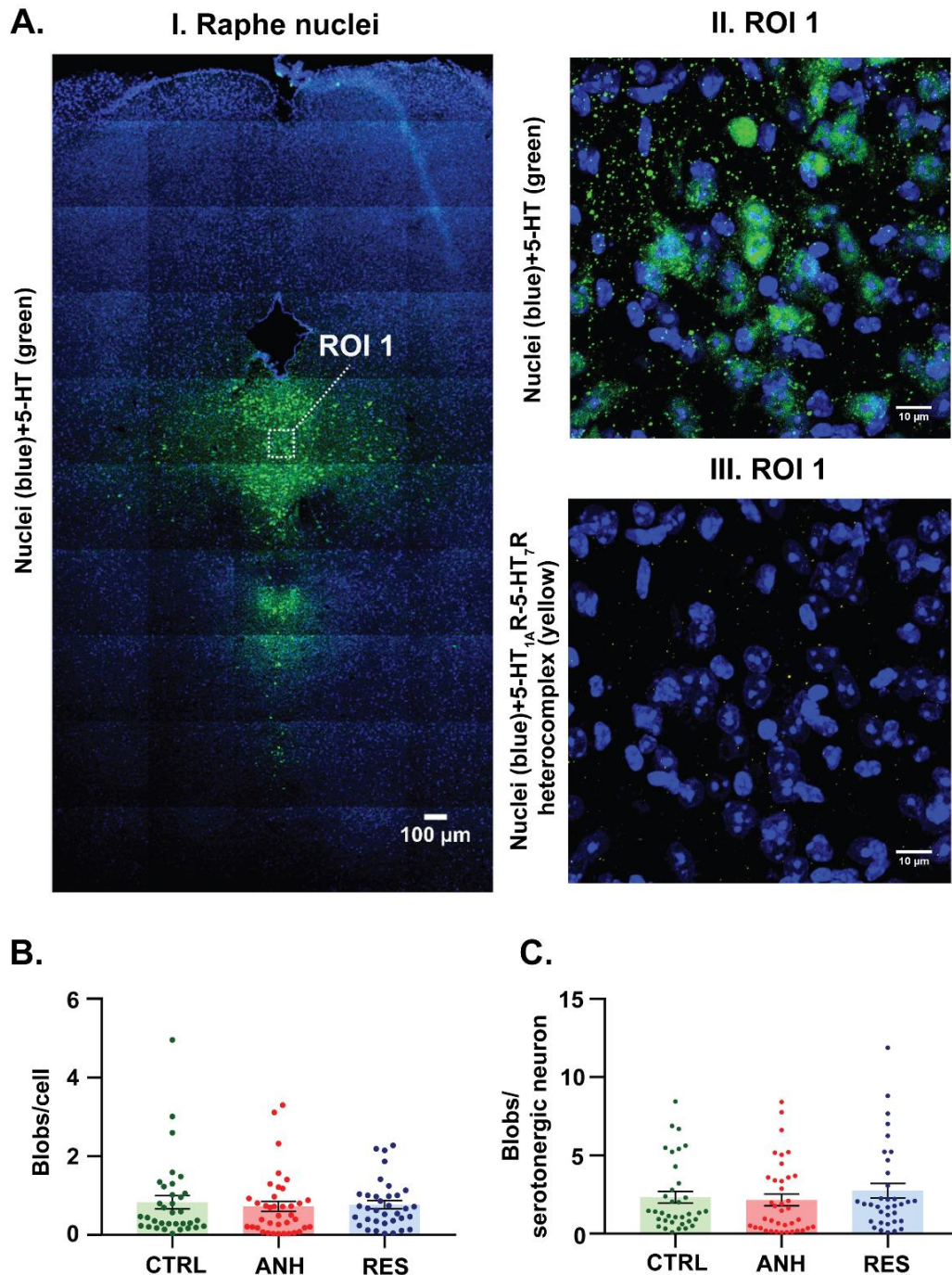


**Fig. 23. 5-HT<sub>1A</sub>R and 5-HT<sub>7</sub>R heterocomplex formations in the dorsal raphe nuclei of C57BL/6J mice after stress implementation:** Distribution of serotonergic neurons in the raphe nuclei in the overview (A. I) and upon scaling (A. II) 5-HT<sub>1A</sub>R/5-HT<sub>7</sub>R heterodimers blobs localization; (A. III) The nuclei are shown in blue, serotonergic neurons – in green, 5-HT<sub>1A</sub>R/5-HT<sub>7</sub>R heterodimers blobs – in yellow. The representative images (A. II, III) are shown as the maximum intensity projection (30  $\mu$ m); (B.) Evaluation of 5-HT<sub>1A</sub>R/5-HT<sub>7</sub>R heterodimers density upon normalization to the general number of cells. No differences were found between control, anhedonic, and resilient animals (One-way ANOVA:  $F(2, 105) = 0.161, p = 0.851$ ); (C.) Evaluation of 5-HT<sub>1A</sub>R/5-HT<sub>7</sub>R heterodimers density upon normalization to the general number of serotonergic neurons. No differences were found between control, anhedonic, and resilient animals (One-way ANOVA:  $F(2, 105) = 0.568, p = 0.568$ ). Each dot represents the ROI value for the tested condition. Results are represented as Mean  $\pm$  SEM ( $N \geq 5$ ).

There were not observed significant changes in 5-HT<sub>1A</sub>R/5-HT<sub>7</sub>R oligomerization after both normalization of the 5-HT<sub>1A</sub>R/5-HT<sub>7</sub>R blobs number to the total number of cells in the field of view (Fig. 23 B) and to serotonergic neurons (Fig. 23 C) between different groups. Noteworthy, the average number of PLA blobs per cell in the raphe nuclei was  $0.80 \pm 0.17$  (ROI n=35);  $0.69 \pm 0.13$  (ROI n=38) and  $0.74 \pm 0.10$  (ROI n=35) for control, anhedonic, and resilient animals, respectively. Although the 5-HT<sub>1A</sub>R and 5-HT<sub>7</sub>R heterodimerization in the dorsal raphe nuclei was by 17 times lower in comparison to the medial prefrontal cortex of control rodents, the number of the 5-HT<sub>1A</sub>R and 5-HT<sub>7</sub>R heterodimers in the raphe nuclei was by 50% higher than in the hippocampus.

## 5.5. Effects of CUS on 5-HT<sub>1A</sub>R and 5-HT<sub>7</sub>R expression

Further, we assessed changes of 5-HT<sub>1A</sub>R and 5-HT<sub>7</sub>R expression both on mRNA (Figs. 24) and protein levels (Fig. 25) in C57BL/6J mice upon exposure to CUS.

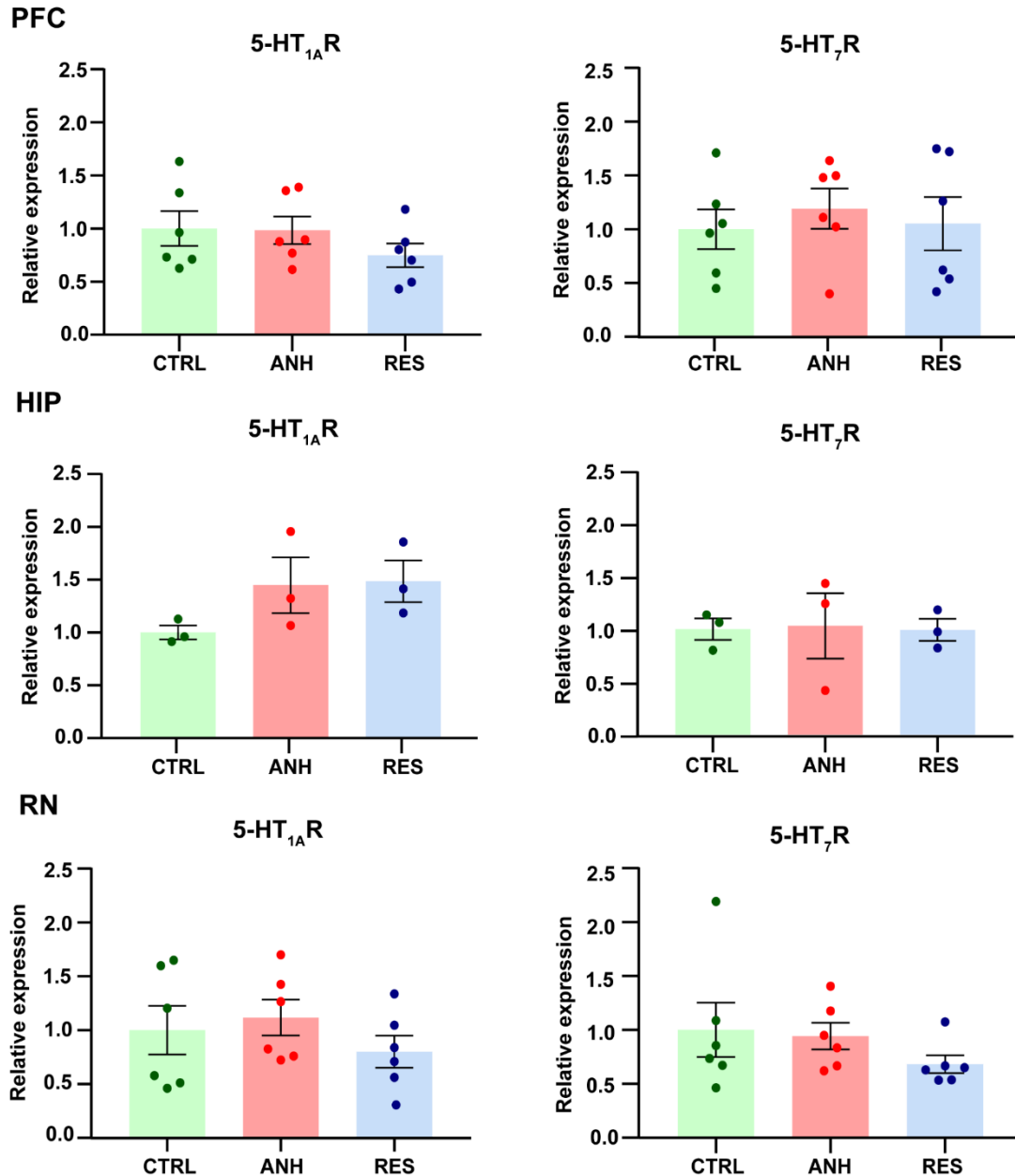
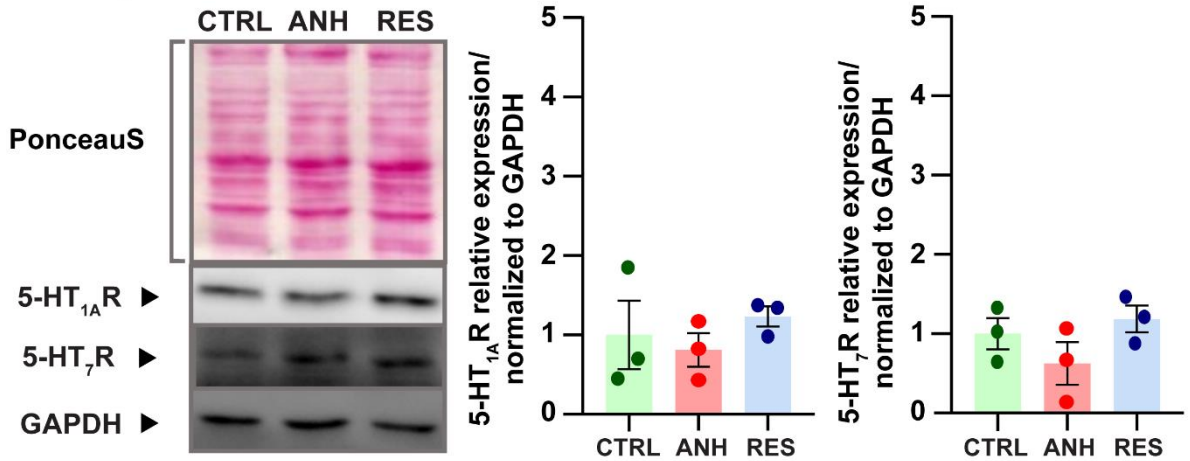
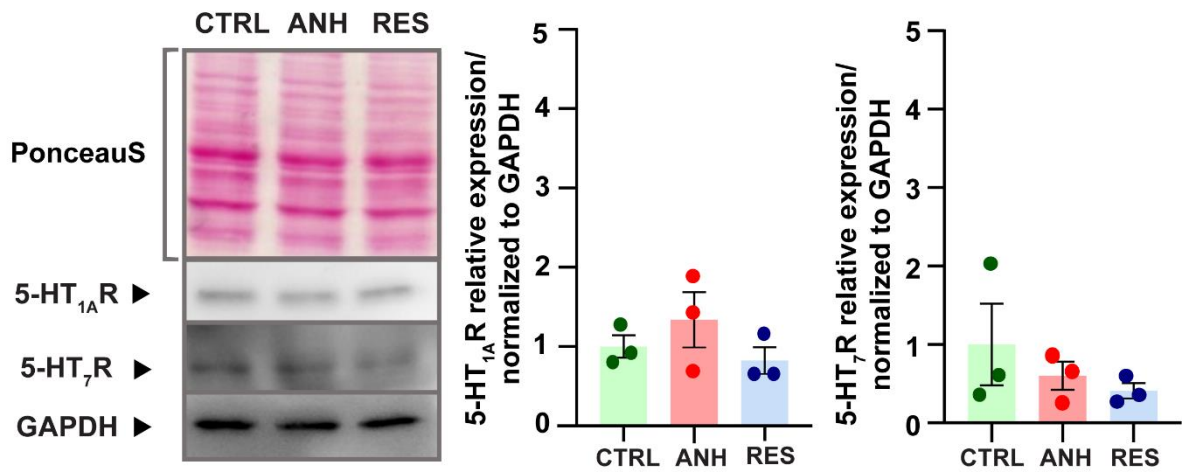


**Fig. 24.** 5-HT<sub>1A</sub>R and 5-HT<sub>7</sub>R mRNA expression in C57BL/6J mice after implementation of chronic unpredictable stress in different brain regions using qRT-PCR and  $\Delta\Delta C_t$  method: No significant differences of 5-HT<sub>1A</sub>R and 5-HT<sub>7</sub>R mRNA expression were observed in the prefrontal cortex (PFC): 5-HT<sub>1A</sub>R (One-way ANOVA:  $F(2, 15) = 1.066, p = 0.369$ ); 5-HT<sub>7</sub>R (One-way ANOVA:  $F(2, 15) = 0.225, p = 0.802$ ); hippocampus (HIP): 5-HT<sub>1A</sub>R (One-way ANOVA:  $F(2, 6) = 1.935, p = 0.225$ ); 5-HT<sub>7</sub>R (One-way ANOVA:  $F(2, 6) = 0.010, p = 0.989$ ); and raphe nuclei (RN): 5-HT<sub>1A</sub>R (One-way ANOVA:  $F(2, 15) = 0.767, p = 0.482$ ); 5-HT<sub>7</sub>R (One-way ANOVA:  $F(2, 15) = 1.008, p = 0.389$ ).

## A. PFC



## B. HIP



## C. RN

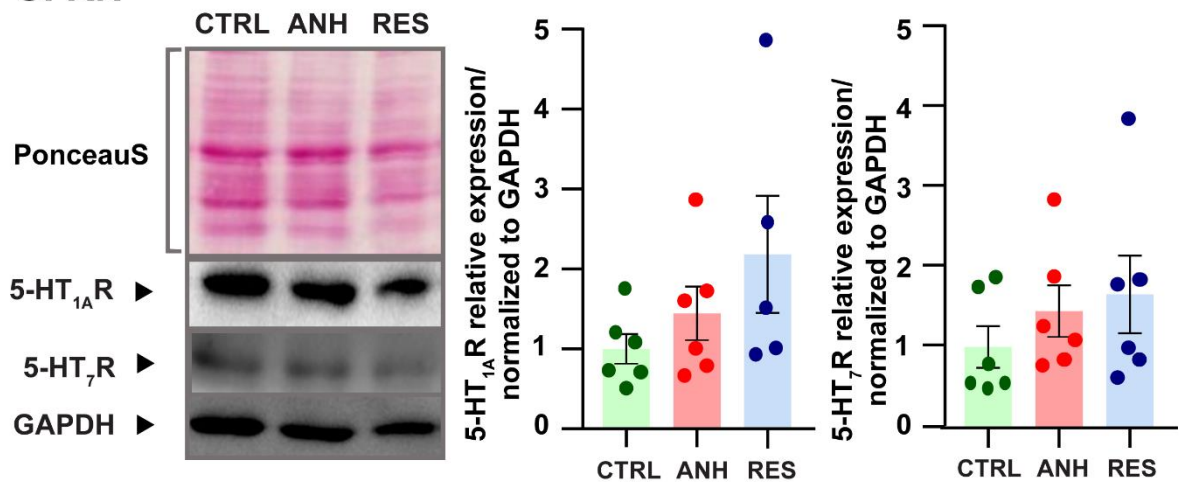


**Fig 25. 5-HT<sub>1A</sub>R and 5-HT<sub>7</sub>R protein level in C57BL/6J mice after implementation of chronic unpredictable mild stress in different brain regions using Western blot:** No differences were detected for 5-HT<sub>1A</sub>R and 5-HT<sub>7</sub>R protein level in the prefrontal cortex (A.): 5-HT<sub>1A</sub>R (One-way ANOVA:  $F(2,6) = 0.544, p = 0.607$ ); 5-HT<sub>7</sub>R (One-way ANOVA:  $F(2,6) = 1.744, p = 0.253$ ); hippocampus (B.): 5-HT<sub>1A</sub>R (One-way ANOVA:  $F(2,6) = 1.195, p = 0.366$ ); 5-HT<sub>7</sub>R (One-way ANOVA:  $F(2,6) = 0.869, p = 0.466$ ); and raphe nuclei (C.): 5-HT<sub>1A</sub>R (One-way ANOVA:  $F(2,14) = 1.780, p = 2.205$ ); 5-HT<sub>7</sub>R (One-way ANOVA:  $F(2,15) = 0.828, p = 0.456$ ). Results are represented as Mean  $\pm$  SEM. C57BL/6J (P120; N=3-6).

Our studies have shown that chronic unpredictable stress did not lead to changes in the 5-HT<sub>1A</sub>R and 5-HT<sub>7</sub>R mRNA expression (Fig. 24). Thus, there were observed no significant differences of 5-HT<sub>1A</sub>R and 5-HT<sub>7</sub>R mRNA expression in the prefrontal cortex: 5-HT<sub>1A</sub>R (One-way ANOVA:  $F(2,15) = 1.066$ ,  $p = 0.369$ ); 5-HT<sub>7</sub>R (One-way ANOVA:  $F(2,15) = 0.225$ ,  $p = 0.802$ ); hippocampus (HIP): 5-HT<sub>1A</sub>R (One-way ANOVA:  $F(2,6) = 1.935$ ,  $p = 0.225$ ); 5-HT<sub>7</sub>R (One-way ANOVA:  $F(2,6) = 0.010$ ,  $p = 0.989$ ); and raphe nuclei (RN): 5-HT<sub>1A</sub>R (One-way ANOVA:  $F(2,15) = 0.767$ ,  $p = 0.482$ ); 5-HT<sub>7</sub>R (One-way ANOVA:  $F(2,15) = 1.008$ ,  $p = 0.389$ ). Even though not significant as well, we observed tendencies in changes of protein levels, mostly for the anhedonic group (Fig. 25). In particular, a decrease of the 5-HT<sub>7</sub>R protein expression in the prefrontal cortex (CTRL:  $1.00 \pm 0.185$  (n=6); ANH:  $1.19 \pm 0.186$  (n=6); RES:  $1.051 \pm 0.247$  (n=6) and an increase in 5-HT<sub>1A</sub>R expression within the hippocampus (CTRL:  $1.00 \pm 0.065$  (n=3); ANH:  $1.45 \pm 0.264$  (n=3); RES:  $1.49 \pm 0.197$  (n=3) was detected.

## 6. DISCUSSION

### 6.1. Meta-analysis of chronic unpredictable stress applicability in rodents

The present study provides verification of CUS protocol for modeling depressive-like behavior in rodents assessed by sucrose preference test . Thus, the meta-analysis has shown that the CUS protocol is a reliable approach for modeling depression in rodents because it is strongly associated with anhedonic behavior. Interestingly, difficulties in reproducing the protocol by different research groups were observed due to the high heterogeneity of the anhedonic effect in rodents in the single-group analysis (Figs. 7-12). Noteworthy, the heterogeneous responses to stress in animal studies go in line with research in humans (Matar et al., 2013). It should be taken into account that the nature of the stressors (e.g., intensity, controllability, and chronicity; (Benelli et al., 1999; Hennessy et al., 1979; Odio and Maickel, 1985; Pacák et al., 1995), housing conditions (Baker et al., 1998), and features of the organisms (e.g., species, strain, age, genetics, sex, and physical activity), are essential in designing experiments (Czéh et al., 2016; Duman, 2010; Slattery and Cryan, 2017). Additionally, differences in stress response could be observed due to ordering animals from different suppliers, genetic drift or differences in rearing procedures.

Different stressors have been demonstrated to activate various molecular pathways. For instance, social stress, exposure to cold temperature, physical immobilization were accepted as primarily physiological stressors (Blanchard et al., 1998; Odio and Maickel, 1985). Exposure of rats to a novel environment, electric foot shock, or restraining propagated different patterns of changes in hypothalamic norepinephrine and prohormone convertases (Keim and Sigg, 1976) and brain cGMP, pituitary cAMP and circulating prolactin levels (Lenox et al., 1980). Additionally, Dauchy and colleagues have shown that the light cycle modifications significantly disrupted biologic rhythms and, as a result, potentially altered the endocrine physiology of experimental animals (Dauchy et al., 2010). Interestingly, some stressors (white noise, novel odors, and foreign objects) have been suggested as insufficient for modeling stressful conditions (Benelli et al., 1999). Thus, in our studies we applied immobilization, social stress, rat exposure and light cycle modification to model depression in rodents.

Although the sucrose consumption test is a reliable approach for assessment of hedonic behavior, the protocol of this test differs significantly between studies. Noteworthy, the initial protocol developed by Willner was implemented upon prior food and water restriction for 20 h and included further using of a 1% sucrose solution for 1 h (Muscat and Willner, 1992). In general, the majority of experiments listed in the meta-analysis were based on the analogous protocols, and only some researchers have modified sucrose solution concentration. According to Papp's recommendations, a pioneer in the field, sucrose concentration should be in the range of 1 – 2% (Wistar or Lister rats), but should not exceed 2% (Papp, 2012). Noteworthy, the outcome of the sucrose consumption test can be dependent on the circadian rhythms. Taking into account that rodents are nocturnal species, the peak of locomotor activity takes place at the beginning of the dark cycle. Differences in the sucrose consumption after CUS have been shown (D'Aquila et al., 1997; Papp, 2012) for Wistar rats: an insufficient response was noted upon test performing during the light and strong decrease in sucrose consumption when tested at the start of the dark phase. Importantly, individual housing prior to the CUMS was reported as the stimulator for modelling depressive behavior (Willner, 1997, 2017). Similarly, food and water withdrawal before sucrose testing may act as an additional stressor and, as a result, facilitate the anhedonic response. For instance, overnight food and water deprivation increases fluids consumptions of rodents during the light cycle. Moreover, stress-resilient animals demonstrated stronger decrease in sucrose consumption in comparison to stress-susceptible and control rodents upon food and water restriction. Regarding our project, the sucrose preference test was performed using 1% sucrose solution without applying previous food and water deprivation. Thus, the present meta-analysis gave us an insight into the applicability of different strains of rodents for modeling depressive-like phenotype.

## 6.2. Role of 5-HT<sub>1A</sub>R and 5-HT<sub>7</sub>R in stress-related disorders

In the present study (Fig. 13) we have demonstrated that both the activation of 5-HT<sub>1A</sub> as well as the activation of 5-HT<sub>7</sub> receptors *in vivo* leads to despair behavior, measured by an increase in immobility time during the tail suspension test. Our findings are in accordance with the previously published studies that show involvement of both 5-HT<sub>1A</sub> and 5-HT<sub>7</sub> receptors in the pathogenesis of stress-related disorders and

antidepressants treatment (Hedlund, 2009; Leopoldo et al., 2011; Savitz et al., 2009). The role of 5-HT<sub>1A</sub> receptors in modulation of anxiety was confirmed using tissue-specific and conditional 5-HT<sub>1A</sub>R rescue mouse models (Gross et al., 2002). Additionally, both pharmacological blocking and genetic knockout of the 5-HT<sub>7</sub>R in rodents results in anti-depressive phenotype (Guscott et al., 2005; Hedlund et al., 2005; Wesółowska et al., 2006).

We would like to outline that our experiments indicate a stronger induction of despair behavior upon injection of 5-CT in comparison to LP-211 (Fig. 13). Notably, the inhibitory constant (K<sub>i</sub>) of 5-CT for the 5-HT<sub>1A</sub>R and 5-HT<sub>7</sub>R is 0.3 and 0.4, respectively (Latacz et al., 2018). As a result, despair behavior readout detected during applying the tail suspension test upon 5-CT injection is mediated via the stimulation of both 5-HT<sub>1A</sub>R and 5-HT<sub>7</sub>R. At the same time, the radioligand binding screening confirmed that LP-211 binding affinity to the 5-HT<sub>7</sub>R is 25 times higher (K<sub>i</sub>=15 nM) in comparison to the 5-HT<sub>1A</sub>R (K<sub>i</sub>=379 nM) (Hedlund et al., 2010), meaning that LP-211 stimulation activates the 5-HT<sub>7</sub>R only. Previously, it was shown that on the cellular level, 5-CT stimulation led to adenylyl cyclase activation in guinea-pig hippocampal membranes (Thomas et al., 1999). Interestingly, the selective 5-HT<sub>7</sub>R antagonist SB-258719 blocked the response to 5-CT. At the same time, neither WAY-100635 nor cyanopindolol (antagonists of the 5-HT<sub>1A</sub>R) significantly altered basal AC activity. Although 5-HT<sub>1A</sub>R activation in guinea-pig hippocampus did not directly stimulate adenylyl cyclase activity, it might boost G<sub>s</sub> coupled receptor response, since it has been shown that activation of adenylyl cyclase isoform 2 can be supported by βγ subunits released upon the activation of the 5-HT<sub>1A</sub>R/G<sub>i</sub>-signaling (Tang and Gilman, 1991). Additionally, Tang and colleagues have reported that LP-211 induced 5-HT<sub>7</sub>R-mediated stimulation of adenylate cyclase and an increase in cAMP levels (Tang and Trussell, 2015). Moreover, several experimental data have indicated that 5-CT activation of the 5-HT<sub>7</sub>R/G<sub>12</sub> signaling pathway resulted in Rho-dependent activation in the hippocampus (Bijata et al., 2017; Kvachnina et al., 2005). Thus, Bijata and colleagues have shown that upon stimulation of the 5-HT<sub>7</sub>R *in vitro* in the mouse hippocampal dissociated culture there was observed MMP-9 activation with further cleavage of CD44, facilitating spine elongation. Since MMP-9 has been considered as a potent marker of depression in humans (Bobińska et al., 2016), 5-HT<sub>7</sub>R/G<sub>12</sub>/MMP-9 signaling may lead to despair behavior detected in the tail suspension test. Further

studies are needed in order to understand the precise mechanism of 5-HT<sub>1A</sub> and 5-HT<sub>7</sub> receptors activation and its functional consequences.

Since their discoveries, the distribution of 5-HT<sub>1A</sub> and 5-HT<sub>7</sub> receptors has been extensively studied in both humans and non-human species. Although some differences were observed in the density of the 5-HT<sub>1A</sub>R and 5-HT<sub>7</sub>R in the brain, it might be associated with limited sensitivity of various techniques (autoradiography, Northern blot, *in situ* hybridization, immunohistochemistry, radiolabeling, qRT-PCR, and PET) or a small population of cells of the region of interest (Leopoldo et al., 2011; Savitz et al., 2009). Our experiments (Fig. 16) have shown that in adult C57BL/6J mice protein levels of the 5-HT<sub>1A</sub> receptors were higher in the prefrontal cortex and hippocampus in comparison to the raphe nuclei. Similar distribution of the 5-HT<sub>1A</sub>R in the brain has been mapped by receptor autoradiography using a wide range of ligands including [<sup>3</sup>H]- 5-HT, [<sup>3</sup>H]-8-OH-DPAT, [<sup>3</sup>H]-ipsapirone, [125I]-BH-8-MeO-N-PAT, [125I]- p-MPPI, and [<sup>3</sup>H]-WAY 100 635 (humans (Arango et al., 2001; Chalmers and Watson, 1991; Hall et al., 1997; Stockmeier et al., 1998), monkeys (Lidow et al., 1989), rats (Matthiessen et al., 1992) and mice (Laporte et al., 1994) and *in situ* hybridization (rat: Chalmers and Watson, 1991; Wright et al., 1995); human (human brain: Burnet et al., 1995). On the protein level no significant changes of the 5-HT<sub>7</sub>R were observed in studied brain structures. Interestingly, numerous studies have shown the 5-HT<sub>7</sub>R mRNA expression differs within the brain of rodents (Table 12). Duncan and colleagues have performed autoradiography in the brains of male Syrian hamsters using [<sup>3</sup>H] 8- OH-DPAT ligand in combination with 5-HT<sub>1A</sub>R and 5-HT<sub>7</sub>R agonists (Duncan et al., 1999). Results of this study showed that the 5-HT<sub>1A</sub> receptor subtype was more abundant in the medial and dorsal raphe nuclei in comparison to 5-HT<sub>7</sub> receptors. At 17–19 months of age, a 50% decrease of the 5-HT<sub>7</sub> receptors was found in the DRN in comparison to 3-4 months old animals; no significant age-related changes of the 5-HT<sub>1A</sub> receptors density were observed.

**Table 12. Abundance of the 5-HT<sub>7</sub> receptor mRNA in the rodent brain**

Technique	Species	Abundance	Reference
RT-PCR	Mouse	Forebrain <sup>***</sup> , brain stem <sup>***</sup> , cerebellum <sup>**</sup>	(Plassat et al., 1993)
	Rat	Hypothalamus	(Shimizu et al., 1996)
Northern blot	Mouse	Not detected	(Plassat et al., 1993)
	Rat	Hypothalamus <sup>***</sup> , hippocampus <sup>**</sup> , mesencephalon <sup>**</sup> , cortex <sup>**</sup> , olfactory bulb <sup>*</sup>	(Shen et al., 1993)
		Hypothalamus <sup>***</sup> , brainstem <sup>***</sup> , hippocampus <sup>***</sup>	(Ruat et al., 1993)
<i>In situ</i> hybridization	Mouse	Data not available	
	Rat	Cortex <sup>***</sup> , hippocampus <sup>***</sup> , hypothalamus <sup>***</sup> , thalamus <sup>***</sup> , raphe nucleus <sup>*</sup>	(Ruat et al., 1993) (Meyerhof et al., 1993)

Notes: <sup>\*\*\*</sup> - high expression; <sup>\*\*</sup> - medium expression; <sup>\*</sup> - low expression.

Noteworthy, both on mRNA (Fig. 24) and protein (Fig. 25) level, the amount of 5-HT<sub>1A</sub> and 5-HT<sub>7</sub> receptors were not altered upon CUS implementation. In line with our studies, Gorinski and colleagues observed no changes in Wistar rats in respect to the expression of the 5-HT<sub>1A</sub> mRNA after exposure to stress (Gorinski et al., 2012). Interestingly, PET imaging based on binding of [carbonyl-C-11]-WAY-100635 to 5-HT<sub>1A</sub>R indicated that male MDD subjects had higher binding potential in the cortical areas, hippocampus, amygdala, and raphe nuclei compared to male controls. Furthermore, on control males there was a more pronounced 5-HT<sub>1A</sub> PET labeling compared to control females across all the above-mentioned regions (Kaufman et al., 2015; Takano et al., 2011). On the contrary, some PET studies have shown a reduced binding of [carbonyl-C-11]-WAY-100635 to 5-HT<sub>1A</sub>R in MDD in humans (Bhagwagar et al., 2004; Sargent et al., 2000) and depressed submissive monkeys (Shively et al., 2006). However, some reports (Hesselgrave and Parsey, 2013; Parsey et al., 2010; Savitz et al., 2009) have outlined that the differences may be due to the fact that depressed individuals exposed to antidepressant medications exhibit stronger binding and the choice of reference region greatly affects the outcome. It should be mentioned that in humans ligands binding to the 5-HT<sub>1A</sub> receptor in the brain is decreased upon electroconvulsive therapy in the brain regions consistently reported to be altered in major depression (Lanzenberger et al., 2013). Additionally, observations in depressed

patients point to a misbalance of pre- and post-synaptic 5-HT<sub>1A</sub>Rs. Studies showed an increased density of presynaptic 5-HT<sub>1A</sub> receptors, accompanied by a decrease of the postsynaptic population (Drevets et al., 2000; López-Figueroa et al., 2004; Sargent et al., 2000). Moreover, post mortem analysis of human brains of depressed subjects revealed a specific upregulation of 5-HT<sub>1A</sub> autoreceptors in the raphe area in comparison to controls, with no changes in the postsynaptic 5-HT<sub>1A</sub> receptor sites (Stockmeier et al., 1998). Some studies (Drevets et al., 2000; Hesselgrave and Parsey, 2013; Hsiung et al., 2003) have shown a decrease in postsynaptic 5-HT<sub>1A</sub> receptor expression in suicide patients. In respect to the 5-HT<sub>7</sub> receptor, upregulated mRNA levels in the hippocampus and hypothalamus, but not in the cortex were shown, in rats exposed to chronic unpredictable stress (Li et al., 2009).

### 6.3. Heterodimerization of 5-HT<sub>1A</sub> and 5-HT<sub>7</sub> receptors

Based on our findings (Figs. 20, 22), we have determined that changes in the 5-HT<sub>1A</sub>-5-HT<sub>7</sub> heterodimerization level are associated with the pathogenesis of depressive-like symptoms in C57BL/6J after CUS implementation. Noteworthy, the most pronounced decrease of the 5-HT<sub>1A</sub>-5-HT<sub>7</sub> heterodimers number was observed in the medial prefrontal cortex of the anhedonic rodents in comparison to the control and resilient animals. A higher level of 5-HT<sub>1A</sub>-5-HT<sub>7</sub> heterodimers was detected in the dentate gyrus of the resilient mice compared to anhedonic mice. Previous studies (Renner et al., 2012) have shown that the 5-HT<sub>1A</sub>-5-HT<sub>7</sub> heterodimerization results in the inhibition of the 5-HT<sub>1A</sub> receptor-mediated activation of G<sub>i</sub>-protein without affecting the 5-HT<sub>7</sub> receptor-Gα<sub>s</sub> mediated signaling. Additionally, Prasad and colleagues (Prasad et al., 2019) have utilized indirect approach and demonstrated cAMP activation in living cells using CEpac biosensor upon the 5-HT<sub>1A</sub>-5-HT<sub>7</sub> heterooligomerization. The 5-HT<sub>1A</sub>-5-HT<sub>7</sub> complex signaling characteristics in cultured hippocampal neurons were characterized by modeling the kinetics of intracellular cAMP level changes in relation to the 5-HT<sub>7</sub>R:5-HT<sub>1A</sub>R stoichiometry, and the relative dissociation constants for the 5-HT<sub>1A</sub> and 5-HT<sub>7</sub> dimers were described as  $K_{1A-1A} > K_{1A-7} > K_{7-7}$  (0.11 > 0.04 > 0.02). In this regard, we suggest that within physiological conditions (control unstressed rodents) higher 5-HT<sub>1A</sub>-5-HT<sub>7</sub> heterodimerization is accompanied by activation of the 5-HT<sub>7</sub> receptor-Gα<sub>s</sub>/AC mediated signaling and cAMP formation. In line with the above-mentioned, numerous antidepressants (amitriptyline, desipramine, and iprindole) actions are mainly mediated via Gα<sub>s</sub>-signaling pathway and activation of adenylyl cyclase (Senese et al., 2018; De Montis et al., 1990; Menkes et al., 1983; Ozawa and Rasenick, 1991). In addition to antidepressant treatment, chronic electroconvulsive treatment facilitates Gα<sub>s</sub>-signaling and activation of adenylyl cyclase (Ozawa and Rasenick, 1991).

Taking into account previous findings (Renner et al., 2012), the 5-HT<sub>1A</sub>-5-HT<sub>7</sub> heterodimerization sufficiently decreased the ability of the 5-HT<sub>1A</sub> receptor to activate GIRK channels. Since there was observed the lower level of the 5-HT<sub>1A</sub>-5-HT<sub>7</sub> heterodimers in the prefrontal cortex and hippocampus of anhedonic animals, we suggest that it is accompanied by increase of the 5-HT<sub>1A</sub>R homodimers. As a consequence, 5-HT<sub>1A</sub>R homodimers mediate stronger opening of GIRK channels,

which in turn leads to membrane hyperpolarization and a decrease in neuronal input resistance. Interestingly, previous electrophysiological studies have shown the presence of the 5-HT<sub>1A</sub> receptors in the cortical pyramidal glutamatergic neurons and interneurons (Amargós-Bosch et al., 2004; Santana et al., 2004). Upon activation of the 5-HT<sub>1A</sub> receptors in glutamatergic neurons, NMDA currents were inhibited (Yuen et al., 2008) and CAMKII-induced AMPA phosphorylation reduced (Cai et al., 2002), which in turn led to the inhibition of neuronal activity. Taking into account the hypothesis (Albert et al., 2014) that suggests higher sensitivity of the 5-HT<sub>1A</sub> receptors on interneurons compared to relatively lower sensitivity on the glutamatergic pyramidal neurons, we speculate that the lower level of the 5-HT<sub>1A</sub>-5-HT<sub>7</sub> heterodimers, accompanied by the increase of the 5-HT<sub>1A</sub>R homodimerization in the medial prefrontal cortex of anhedonic mice leads to activation of the 5-HT<sub>1A</sub>R in interneurons, which in turn inhibits glutamatergic signaling.

Notably, previous studies have shown that GPCR functions are strongly affected upon post-translational modifications (Gorinski and Ponimaskin, 2013; Resh, 2006; Zheng et al., 2013). Thus, both 5-HT<sub>1A</sub>R (Papoucheva et al., 2004; Gorinski et al., 2019) and 5-HT<sub>7</sub>R (Kvachnina et al., 2009) are palmitoylated. In particular, the 5-HT<sub>1A</sub> receptor is irreversibly palmitoylated at cysteine residues Cys417 and Cys420 that is essential for G<sub>i</sub>-protein coupling. Palmitoylation increases the tendency of the 1A receptor to localize to lipid rafts of the plasma membrane, which in turn increases the effective surface density of the receptor (Woehler et al., 2009). Since the 5-HT<sub>1A</sub>R palmitoylation decreases in the prefrontal cortex upon stress (Gorinski et al., 2019), we suggest that lower 5-HT<sub>1A</sub>R-5-HT<sub>7</sub>R heterodimerization in this brain region is a consequence of decreased 5-HT<sub>1A</sub>R binding (Renner et al., 2007) with 5-HT<sub>7</sub>R due to artificial localization of the 5-HT<sub>1A</sub>R outside of the membrane subdomain and lower interaction probability with the 5-HT<sub>7</sub>R.

It should be taken into account that differences in relative concentration of 5-HT<sub>1A</sub>R and 5-HT<sub>7</sub>R heterodimers represent an intriguing possibility to explain receptors coupling to G proteins. In the present study, we have shown that in adulthood (Fig. 15) in the prefrontal cortex and hippocampus of C57Bl/6J mice, 5-HT<sub>1A</sub> receptors represent the dominant (postsynaptic) 5-HT<sub>1A</sub> receptor population in comparison to 5-HT<sub>7</sub> receptors. In line with previous studies (Duncan et al., 1999; Kobe et al., 2012; Renner

et al., 2012), we have shown that the expression ratio of 5-HT<sub>1A</sub>R and 5-HT<sub>7</sub>R is age-dependent. Thus, it has been demonstrated that the expression level of 5-HT<sub>7</sub> receptors in the hippocampus is progressively decreased during postnatal development, while expression of the 5-HT<sub>1A</sub> receptor remained relatively constant (Kobe et al., 2012; Renner et al., 2012). Noteworthy, Naumenko and colleagues (Naumenko et al., 2014) have suggested that under (normal) physiological conditions the amount of 5-HT<sub>1A</sub>R-5-HT<sub>7</sub>R heterodimers in the presynaptic serotonergic neurons is higher than in postsynaptic neurons, which in turn leads to differential 5-HT or SSRI-mediated internalization of the 5-HT<sub>1A</sub> autoreceptors. Upon depression, the ratio between 5-HT<sub>1A</sub>R-5-HT<sub>1A</sub>R homodimers and 5-HT<sub>1A</sub>R-5-HT<sub>7</sub>R heterodimers in the presynaptic 5-HT neurons becomes shifted toward 5-HT<sub>1A</sub>R-5-HT<sub>1A</sub>R homodimers that leads to 5-HT<sub>1A</sub> receptor-mediated inhibition of 5-HT release. On the postsynaptic neurons, a higher amount of 5-HT<sub>1A</sub>R-5-HT<sub>7</sub>R heterodimers is expected during depression. Consequently, it will lead to the increased neuronal excitability. Despite this idea, we could not verify the above-mentioned theory, since we observed a higher level of 5-HT<sub>1A</sub>R-5-HT<sub>7</sub>R heterodimers on the postsynaptic neurons compared to presynaptic neurons already under the basal conditions. Additionally, the number of 5-HT<sub>1A</sub>R-5-HT<sub>7</sub>R heterodimers in stress-susceptible animals was reduced in comparison to the control group.

We would like to emphasize that further studies are required in order to understand the exact mechanism of 5-HT<sub>1A</sub>R and 5-HT<sub>7</sub>R heterodimerization. In the present study, we gave rise to structural bases of 5-HT<sub>1A</sub>R and 5-HT<sub>7</sub>R heterodimerization in the mouse brain using *in situ* PLA. Noteworthy, the PLA protocol is limited to the use of fixed specimens both *in vitro* and *in situ*. Taking into account the data from the literature, micro-PET (Luker et al., 2002), BRET (De and Gambhir, 2005), and FRET (Stockholm et al., 2005) techniques are promising approaches for investigation of protein-protein interactions in living animals with respect to specific types of neuronal cells. Additionally, patch-clamp recordings from Sprague-Dawley rats have shown that 5-HT<sub>1A</sub> and NMDA receptors interaction differentially regulated PFC neuronal firing, and the complex effects of 5-HT receptors on excitability were selectively mediated under stressful conditions (Zhong et al., 2008). In this regard, further neurophysiological studies will shed light on the evaluation of the 5-HT<sub>1A</sub> and 5-HT<sub>7</sub> receptors heterodimerization consequences on the functional level.

## 7. SUMMARY AND CONCLUSIONS

To summarize, the findings presented in the thesis:

- ❖ Meta-analysis of the chronic unpredictable stress paradigm was evaluated for modeling depression in rodents based on the sucrose preference test. As a result, C57BL/6J mice were chosen for reproducing anhedonic phenotype.
- ❖ Expression of 5-HT<sub>1A</sub> and 5-HT<sub>7</sub> receptors in different brain regions was evaluated, especially in respect to heterodimerization between these serotonin receptors. The western blot analysis revealed that the 5-HT<sub>1A</sub>R protein level was upregulated in the prefrontal cortex and hippocampus compared to the raphe nuclei during the brain development. Additionally, the results of qRT-PCR experiments have demonstrated that the 5-HT<sub>1A</sub>Rs are dominant subpopulation in comparison to the 5-HT<sub>7</sub>Rs in the prefrontal cortex and hippocampus of adult animals.
- ❖ We have determined that 5-HT<sub>1A</sub>-5-HT<sub>7</sub> receptors heterodimerization is associated with the pathogenesis of depression. The most prominent changes in heterodimerization profile of 5-HT<sub>1A</sub> and 5-HT<sub>7</sub> receptors were observed in the medial prefrontal cortex of C57Bl/6J mice. We have shown an increase in the number of 5-HT<sub>1A</sub>R and 5-HT<sub>7</sub>R heterodimeric complexes in the unstressed control and stressed resilient in comparison to stressed anhedonic mice. No significant changes in the 5-HT<sub>1A</sub>R and 5-HT<sub>7</sub>R heterodimerization profile were detected in the dorsal raphe nuclei.

In conclusion, obtained results have shown that 5-HT<sub>1A</sub>-5-HT<sub>7</sub> heterodimerization in the prefrontal cortex and hippocampus is important for pathogenesis of depression.

## 8. REFERENCES

1. Adayev, T., Ray I., Sondhi, R., Sobocki T., and Banerjee, P. (2003). The G protein-coupled 5-HT<sub>1A</sub> receptor causes suppression of caspase-3 through MAPK and protein kinase Calpha. *Biochim Biophys Acta* 1640, 85–96.
2. Albert, P.R., and Robillard, L. (2002). G protein specificity: traffic direction required. *Cell Signal* 14, 407–418.
3. Albert, P.R., and Vahid-Ansari, F. (2019). The 5-HT<sub>1A</sub> receptor: signaling to behavior. *Biochimie* 161, 34–45.
4. Albert, P.R., Sajedi, N., Lemonde, S., and Ghahremani, M.H. (1999). Constitutive G<sub>(i2)</sub> -dependent activation of adenylyl cyclase type II by the 5-HT<sub>1A</sub> receptor. Inhibition by anxiolytic partial agonists. *J Biol Chem* 274, 35469–35474.
5. Albert, P.R., Vahid-Ansari, F., and Luckhart, C. (2014). Serotonin-prefrontal cortical circuitry in anxiety and depression phenotypes: pivotal role of pre- and post-synaptic 5-HT<sub>1A</sub> receptor expression. *Front Behav Neurosci* 8, 199.
6. Amargós-Bosch, M., Bortolozzi, A., Puig, M.V., Serrats, J., Adell, A., Celada, P., Toth, M., Mengod, G., and Artigas, F. (2004). Co-expression and in vivo interaction of serotonin<sub>1A</sub> and serotonin<sub>2A</sub> receptors in pyramidal neurons of prefrontal cortex. *Cereb Cortex* 14, 281–299.
7. Angers, S., Salahpour, A., and Bouvier, M. (2002). Dimerization: an emerging concept for G protein-coupled receptor ontogeny and function. *Annu Rev of Pharmacol Toxicol* 42, 409–435.
8. Arango, V., Underwood, M.D., Boldrini, M., Tamir, H., Kassir, S.A., Hsiung, S., Chen, J.J., and Mann, J.J. (2001). Serotonin 1A receptors, serotonin transporter binding and serotonin transporter mRNA expression in the brainstem of depressed suicide victims. *Neuropsychopharmacology* 25, 892–903.
9. Azmitia, E.C., Saccomano, Z.T., Alzoobae, M.F., Boldrini, M., and Whitaker-Azmitia, P.M. (2016). Persistent Angiogenesis in the Autism Brain: An Immunocytochemical Study of Postmortem Cortex, Brainstem and Cerebellum. *J Autism Dev Disord* 46, 1307–1318.
10. Bai, M. (2004). Dimerization of G-protein-coupled receptors: roles in signal transduction. *Cell Signal* 16, 175–186.
11. Baker, L.P., Nielsen, M.D., Impey, S., Metcalf, M.A., Poser, S.W., Chan, G., Obrietan, K., Hamblin, M.W., and Storm, D.R. (1998). Stimulation of type 1 and type 8 Ca<sup>2+</sup>/calmodulin-sensitive adenylyl cyclases by the G<sub>s</sub>-coupled 5-hydroxytryptamine subtype 5-HT<sub>7A</sub> receptor. *J Biol Chem* 273, 17469–17476.
12. Bard, J.A., Zgombick, J., Adham, N., Vaysse, P., Branchek, T.A., and Weinshank, R.L. (1993). Cloning of a novel human serotonin receptor (5-HT<sub>7</sub>) positively linked to adenylate cyclase. *J Biol Chem* 268, 23422–23426.
13. Barnes, N.M., and Sharp, T. (1999). A review of central 5-HT receptors and their function. *Neuropharmacology* 38, 1083–1152.
14. Belmaker, R.H., and Agam, G. (2008). Major depressive disorder. *N Engl J of Med* 358, 55–68.
15. Benelli, A., Filaferro, M., Bertolini, A., and Genedani, S. (1999). Influence of S-adenosyl-L-methionine on chronic mild stress-induced anhedonia in castrated rats. *Br J Pharmacol* 127, 645–654.
16. Benkelfat, C. (1994). Mood-lowering effect of tryptophan depletion. Enhanced susceptibility in young men at genetic risk for major affective disorders. *Arch Gen Psychiatry* 51, 687–697.
17. Berger, M., Gray, J.A., and Roth, B.L. (2009). The expanded biology of serotonin. *Annu Rev Med* 60, 355–366.
18. Bhagwagar, Z., Rabiner, E.A., Sargent, P.A., Grasby, P.M., and Cowen, P.J. (2004). Persistent reduction in brain serotonin<sub>1A</sub> receptor binding in recovered depressed men measured by positron emission tomography with [<sup>11</sup>C]WAY-100635. *Mol Psychiatry* 9, 386–392.
19. Bijata, M., Labus, J., Guseva, D., Stawarski, M., Butzlaff, M., Dzwonek, J., Schneeberg, J., Böhm, K., Michaluk, P., Rusakov, D.A., et al. (2017). Synaptic Remodeling Depends on Signaling between Serotonin Receptors and the Extracellular Matrix. *Cell Rep* 19, 1767–1782.

20. Blanchard, R.J., Hebert, M., Sakai, R.R., McKittrick, C., Henrie, A., Yudko, E., McEwen, B.S., and Blanchard, D.C. (1998). Chronic social stress: changes in behavioral and physiological indices of emotion. *Aggress Behav* 24, 307–321.
21. Bobińska, K., Szemraj, J., Czarny, P., and Gałecki, P. (2016). Expression and activity of metalloproteinases in depression. *Med Sci Monit* 22, 1334–1341.
22. Borroto-Escuela, D.O., Corrales, F., Narvaez, M., Oflijan, J., Agnati, L.F., Palkovits, M., and Fuxe, K. (2013). Dynamic modulation of FGFR1-5-HT<sub>1A</sub> heteroreceptor complexes. Agonist treatment enhances participation of FGFR1 and 5-HT<sub>1A</sub> homodimers and recruitment of  $\beta$ -arrestin2. *Biochem Biophys Res Commun* 441, 387–392.
23. Borroto-Escuela, D.O., Pérez-Alea, M., Narvaez, M., Tarakanov, A.O., Mudó, G., Jiménez-Beristain, A., Agnati, L.F., Ciruela, F., Belluardo, N., and Fuxe, K. (2015). Enhancement of the FGFR1 signaling in the FGFR1-5-HT<sub>1A</sub> heteroreceptor complex in midbrain raphe 5-HT neuron systems. Relevance for neuroplasticity and depression. *Biochem Biophys Res Commun* 463, 180–186.
24. Borroto-Escuela, D.O., Carlsson, J., Ambrogini, P., Narváez, M., Wydra, K., Tarakanov, A.O., Li, X., Millón, C., Ferraro, L., Cuppini, R., et al. (2017a). Understanding the Role of GPCR Heteroreceptor Complexes in Modulating the Brain Networks in Health and Disease. *Front Cell Neurosci* 11, 37.
25. Borroto-Escuela, D.O., DuPont, C.M., Li, X., Savelli, D., Lattanzi, D., Srivastava, I., Narváez, M., Di Palma, M., Barbieri, E., Andrade-Talavera, Y., et al. (2017b). Disturbances in the FGFR1-5-HT<sub>1A</sub> Heteroreceptor Complexes in the Raphe-Hippocampal 5-HT System Develop in a Genetic Rat Model of Depression. *Front Cell Neurosci* 11, 309.
26. Borroto-Escuela, D.O., Li, X., Tarakanov, A.O., Savelli, D., Narváez, M., Shumilov, K., Andrade-Talavera, Y., Jimenez-Beristain, A., Pomierny, B., Díaz-Cabiale, Z., et al. (2017c). Existence of Brain 5-HT<sub>1A</sub>–5-HT<sub>2A</sub> Isoreceptor Complexes with Antagonistic Allosteric Receptor–Receptor Interactions Regulating 5-HT<sub>1A</sub> Receptor Recognition. *ACS Omega* 2, 4779–4789.
27. Borroto-Escuela, D.O., Narváez, M., Ambrogini, P., Ferraro, L., Brito, I., Romero-Fernandez, W., Andrade-Talavera, Y., Flores-Burgess, A., Millon, C., Gago, B., et al. (2018). Receptor–Receptor Interactions in Multiple 5-HT<sub>1A</sub> Heteroreceptor Complexes in Raphe-Hippocampal 5-HT Transmission and Their Relevance for Depression and Its Treatment. *Molecules* 23, 1341.
28. Bortolato, M., Pivac, N., Muck Seler, D., Nikolac Perkovic, M., Pessia, M., and Di Giovanni, G. (2013). The role of the serotonergic system at the interface of aggression and suicide. *Neuroscience* 236, 160–185.
29. Bosaipo, N.B., Foss, M.P., Young, A.H., and Juruena, M.F. (2017). Neuropsychological changes in melancholic and atypical depression: A systematic review. *Neurosci Biobehav Rev* 73, 309–325.
30. Bouvier, M. (2001). Oligomerization of G-protein-coupled transmitter receptors. *Nat Rev Neurosci* 2, 274–286.
31. Breitwieser, G.E. (2004). G protein-coupled receptor oligomerization: implications for G protein activation and cell signaling. *Circ Res* 94, 17–27.
32. Bulenger, S., Marullo, S., and Bouvier, M. (2005). Emerging role of homo- and heterodimerization in G-protein-coupled receptor biosynthesis and maturation. *Trends Pharmacol Sci* 26, 131–137.
33. Burnet, P.W., Eastwood, S.L., Lacey, K., and Harrison, P.J. (1995). The distribution of 5-HT<sub>1A</sub> and 5-HT<sub>2A</sub> receptor mRNA in human brain. *Brain Res* 676, 157–168.
34. Cai, X., Gu, Z., Zhong, P., Ren, Y., and Yan, Z. (2002). Serotonin 5-HT<sub>1A</sub> receptors regulate AMPA receptor channels through inhibiting Ca<sup>2+</sup>/calmodulin-dependent kinase II in prefrontal cortical pyramidal neurons. *J Biol Chem* 277, 36553–36562.
35. Caine, S.B., Negus, S.S., Mello, N.K., and Bergman, J. (1999). Effects of dopamine D(1-like) and D(2-like) agonists in rats that self-administer cocaine. *J Pharmacol Exp Ther* 291, 353–360.
36. Cairncross, K.D., Cox, B., Forster, C., and Wren, A.F. (1978). A new model for the detection of antidepressant drugs: Olfactory bulbectomy in the rat compared with existing models. *J Pharmacol Methods* 1, 131–143.

37. Calebiro, D., and Sungkaworn, T. (2018). Single-Molecule Imaging of GPCR interactions. *Trends Pharmacol Sci* 39, 109–122.
38. Cassel, J.C., and Jeltsch, H. (1995). Serotonergic modulation of cholinergic function in the central nervous system: cognitive implications. *Neuroscience* 69, 1–41.
39. Chalmers, D.T., and Watson, S.J. (1991). Comparative anatomical distribution of 5-HT<sub>1A</sub> receptor mRNA and 5-HT<sub>1A</sub> binding in rat brain—a combined in situ hybridisation/in vitro receptor autoradiographic study. *Brain Res* 561, 51–60.
40. Chen, Y., and Penington, N.J. (1996). Differential effects of protein kinase C activation on 5-HT<sub>1A</sub> receptor coupling to Ca<sup>2+</sup> and K<sup>+</sup> currents in rat serotonergic neurones. *J Physiol* 496, 129–137.
41. Cifariello, A., Pompili, A., and Gasbarri, A. (2008). 5-HT<sub>7</sub> receptors in the modulation of cognitive processes. *Behav Brain Res* 195, 171–179.
42. Citri, A., and Malenka, R.C. (2008). Synaptic plasticity: multiple forms, functions, and mechanisms. *Neuropsychopharmacology* 33, 18–41.
43. Conn, P.J., Battaglia, G., Marino, M.J., and Nicoletti, F. (2005). Metabotropic glutamate receptors in the basal ganglia motor circuit. *Nat Rev Neurosci* 6, 787–798.
44. Coppen, A. (1967). The biochemistry of affective disorders. *Br J Psychiatry* 113, 1237–1264.
45. Costa, A.C.S., Stasko, M.R., Stoffel, M., and Scott-McKean, J.J. (2005). G-protein-gated potassium (GIRK) channels containing the GIRK2 subunit are control hubs for pharmacologically induced hypothermic responses. *J Neurosci* 25, 7801–7804.
46. Cryan, J.F., Mombereau, C., and Vassout, A. (2005). The tail suspension test as a model for assessing antidepressant activity: review of pharmacological and genetic studies in mice. *Neurosci Biobehav Rev* 29, 571–625.
47. Czéh, B., Fuchs, E., Wiborg, O., and Simon, M. (2016). Animal models of major depression and their clinical implications. *Prog Neuropsychopharmacol Biol Psychiatry* 64, 293–310.
48. D'Aquila, P.S., Newton, J., and Willner, P. (1997). Diurnal variation in the effect of chronic mild stress on sucrose intake and preference. *Physiol Behav* 62, 421–426.
49. Dauchy, R.T., Dauchy, E.M., Tirrell, R.P., Hill, C.R., Davidson, L.K., Greene, M.W., Tirrell, P.C., Wu, J., Sauer, L.A., and Blask, D.E. (2010). Dark-phase light contamination disrupts circadian rhythms in plasma measures of endocrine physiology and metabolism in rats. *Comp Med* 60, 348–356.
50. De, A., and Gambhir, S.S. (2005). Noninvasive imaging of protein-protein interactions from live cells and living subjects using bioluminescence resonance energy transfer. *FASEB J* 19, 2017–2019.
51. Degasperi, A., Birtwistle, M.R., Volinsky, N., Rauch, J., Kolch, W., and Kholodenko, B.N. (2014). Evaluating strategies to normalize biological replicates of Western blot data. *PLoS One* 9, e87293.
52. Devi, L.A. (2001). Heterodimerization of G-protein-coupled receptors: pharmacology, signaling and trafficking. *Trends Pharmacol Sci* 22, 532–537.
53. Di Matteo, V., Di Giovanni, G., Pierucci, M., and Esposito, E. (2008). Serotonin control of central dopaminergic function: focus on in vivo microdialysis studies. *Prog Brain Res* 172, 7–44.
54. Díaz-Cabiale, Z., Petersson, M., Narváez, J.A., Uvnäs-Moberg, K., and Fuxe, K. (2000). Systemic oxytocin treatment modulates alpha 2-adrenoceptors in telencephalic and diencephalic regions of the rat. *Brain Res* 887, 421–425.
55. Dogrul, A., and Seyrek, M. (2006). Systemic morphine produce antinociception mediated by spinal 5-HT<sub>7</sub>, but not 5-HT<sub>1A</sub> and 5-HT<sub>2</sub> receptors in the spinal cord. *Br J Pharmacol* 149, 498–505.
56. Drevets, W.C., Frank, E., Price, J.C., Kupfer, D.J., Greer, P.J., and Mathis, C. (2000). Serotonin type-1A receptor imaging in depression. *Nucl Med Biol* 27, 499–507.
57. Duman, C.H. (2010). Models of depression. *Vitam Horm* 82, 1–21.
58. Duncan, M.J., and Congleton, M.R. (2010). Neural mechanisms mediating circadian phase resetting by activation of 5-HT<sub>7</sub> receptors in the dorsal raphe: roles of GABAergic and glutamatergic neurotransmission. *Brain Res* 1366, 110–119.
59. Duncan, M.J., Short, J., and Wheeler, D.L. (1999). Comparison of the effects of aging on 5-HT<sub>7</sub> and 5-HT<sub>1A</sub> receptors in discrete regions of the circadian timing system in hamsters. *Brain Res* 829, 39–45.

60. Errico, M., Crozier, R.A., Plummer, M.R., and Cowen, D.S. (2001). 5-HT(7) receptors activate the mitogen activated protein kinase extracellular signal related kinase in cultured rat hippocampal neurons. *Neuroscience* 102, 361–367.
61. Erspamer, V., and Asero, B. (1952). Identification of enteramine, the specific hormone of the enterochromaffin cell system, as 5-Hydroxytryptamine. *Nature* 169, 800–801.
62. Fairchild, G., Leitch, M.M., and Ingram, C.D. (2003). Acute and chronic effects of corticosterone on 5-HT<sub>1A</sub> receptor-mediated autoinhibition in the rat dorsal raphe nucleus. *Neuropharmacology* 45, 925–934.
63. Franco, R., Casadó, V., Cortés, A., Ferrada, C., Mallol, J., Woods, A., Lluís, C., Canela, E.I., and Ferré, S. (2007). Basic Concepts in G-protein-coupled receptor homo- and heterodimerization. *Scientific World Journal* 7, 48–57.
64. Furuyama, T., Inagaki, S., and Takagi, H. (1993). Distribution of type II adenylyl cyclase mRNA in the rat brain. *Brain Res Mol Brain Res* 19, 165–170.
65. Fuxe, K., Ferré, S., Canals, M., Torvinen, M., Terasmaa, A., Marcellino, D., Goldberg, S.R., Staines, W., Jacobsen, K.X., Lluís, C., et al. (2005). Adenosine A<sub>2A</sub> and dopamine D<sub>2</sub> heteromeric receptor complexes and their function. *J Mol Neurosci* 26, 209–220.
66. Fuxe, K., Marcellino, D., Rivera, A., Diaz-Cabiale, Z., Filip, M., Gago, B., Roberts, D.C.S., Langel, U., Genedani, S., Ferraro, L., et al. (2008). Receptor–receptor interactions within receptor mosaics. Impact on neuropsychopharmacology. *Brain Res Rev* 58, 415–452.
67. Ganguly, S., Clayton, A.H.A., and Chattopadhyay, A. (2011). Organization of higher-order oligomers of the serotonin<sub>1A</sub> receptor explored utilizing homo-FRET in live cells. *Biophys J* 100, 361–368.
68. Gellynck, E., Heynink, K., Andressen, K.W., Haegeman, G., Levy, F.O., Vanhoenacker, P., and Van Craenenbroeck, K. (2013). The serotonin 5-HT<sub>7</sub> receptors: two decades of research. *Exp Brain Res* 230, 555–568.
69. George, S.R., O’Dowd, B.F., and Lee, S.P. (2002). G-Protein-coupled receptor oligomerization and its potential for drug discovery. *Nat Rev Drug Discov* 1, 808–820.
70. Gomes, I., Jordan, B.A., Gupta, A., Trapaidze, N., Nagy, V., and Devi, L.A. (2000). Heterodimerization of mu and delta opioid receptors: A role in opiate synergy. *J Neurosci* 20, RC110.
71. González-Maeso, J., Ang, R.L., Yuen, T., Chan, P., Weisstaub, N.V., López-Giménez, J.F., Zhou, M., Okawa, Y., Callado, L.F., Milligan, G., et al. (2008). Identification of a serotonin/glutamate receptor complex implicated in psychosis. *Nature* 452, 93–97.
72. Goodfellow, N.M., Benekareddy, M., Vaidya, V.A., and Lambe, E.K. (2009). Layer II/III of the prefrontal cortex: Inhibition by the serotonin 5-HT<sub>1A</sub> receptor in development and stress. *J Neurosci* 29, 10094–10103.
73. Goodwin, G.M., Souza, R.J.D., Green, A.R., and Heal, D.J. (1987). The pharmacology of the behavioural and hypothermic responses of rats to 8-hydroxy-2-(di-n-propylamino)tetralin (8-OH-DPAT). *Psychopharmacology (Berl.)* 91(4), 506–11.
74. Gorinski, N., and Ponimaskin, E. (2013). Palmitoylation of serotonin receptors. *Biochem Soc Trans* 41, 89–94.
75. Gorinski, N., Kowalsman, N., Renner, U., Wirth, A., Reinartz, M.T., Seifert, R., Zeug, A., Ponimaskin, E., and Niv, M.Y. (2012). Computational and experimental analysis of the transmembrane domain 4/5 dimerization interface of the serotonin 5-HT<sub>1A</sub> receptor. *Mol Pharmacol* 82, 448–463.
76. Gorinski, N., Bijata, M., Prasad, S., Wirth, A., Abdel Galil, D., Zeug, A., Bazovkina, D., Kondaurova, E., Kulikova, E., Ilchibaeva, T., et al. (2019). Attenuated palmitoylation of serotonin receptor 5-HT<sub>1A</sub> affects receptor function and contributes to depression-like behaviors. *Nat Commun* 10, 3924.
77. Gross, C., Zhuang, X., Stark, K., Ramboz, S., Oosting, R., Kirby, L., Santarelli, L., Beck, S., and Hen, R. (2002). Serotonin<sub>1A</sub> receptor acts during development to establish normal anxiety-like behaviour in the adult. *Nature* 416, 396–400.
78. Guo, H., An, S., Ward, R., Yang, Y., Liu, Y., Guo, X.-X., Hao, Q., and Xu, T.R. (2017). Methods used to study the oligomeric structure of G-protein-coupled receptors. *Biosci Rep* 37, BSR2016054.

79. Guscott, M., Bristow, L.J., Hadingham, K., Rosahl, T.W., Beer, M.S., Stanton, J.A., Bromidge, F., Owens, A.P., Huscroft, I., Myers, J., (2005). Genetic knockout and pharmacological blockade studies of the 5-HT<sub>7</sub> receptor suggest therapeutic potential in depression. *Neuropharmacology* 48, 492–502.
80. Guthrie, C.R., Murray, A.T., Franklin, A.A., and Hamblin, M.W. (2005). Differential agonist-mediated internalization of the human 5-hydroxytryptamine 7 receptor isoforms. *J Pharmacol Exp Ther* 313, 1003–1010.
81. Halasy, K., Miettinen, R., Szabat, E., and Freund, T.F. (1992). GABAergic Interneurons are the Major Postsynaptic Targets of Median Raphe Afferents in the Rat Dentate Gyrus. *Eur J Neurosci* 4, 144–153.
82. Hall, H., Lundkvist, C., Halldin, C., Farde, L., Pike, V.W., McCarron, J.A., Fletcher, A., Cliffe, I.A., Barf, T., Wikström, H., et al. (1997). Autoradiographic localization of 5-HT<sub>1A</sub> receptors in the post-mortem human brain using [<sup>3</sup>H]WAY-100635 and [<sup>11</sup>C]way-100635. *Brain Res* 745, 96–108.
83. Han, X., Shao, W., Liu, Z., Fan, S., Yu, J., Chen, J., Qiao, R., Zhou, J., and Xie, P. (2015). iTRAQ-based quantitative analysis of hippocampal postsynaptic density-associated proteins in a rat chronic mild stress model of depression. *Neuroscience* 298, 220–292.
84. Hedlund, P.B. (2009). The 5-HT<sub>7</sub> receptor and disorders of the nervous system: an overview. *Psychopharmacology (Berl)* 206, 345–354.
85. Hedlund, P.B., Kelly, L., Mazur, C., Lovenberg, T., Sutcliffe, J.G., and Bonaventure, P. (2004). 8-OH-DPAT acts on both 5-HT<sub>1A</sub> and 5-HT<sub>7</sub> receptors to induce hypothermia in rodents. *Eur J Pharmacol* 487, 125–132.
86. Hedlund, P.B., Huitron-Resendiz, S., Henriksen, S.J., and Sutcliffe, J.G. (2005). 5-HT<sub>7</sub> receptor inhibition and inactivation induce antidepressant-like behavior and sleep pattern. *Biol Psychiatry* 58, 831–837.
87. Hedlund, P.B., Leopoldo, M., Caccia, S., Sarkisyan, G., Fracasso, C., Martelli, G., Lacivita, E., Berardi, F., and Perrone, R. (2010). LP-211 is a brain penetrant selective agonist for the serotonin 5-HT<sub>7</sub> receptor. *Neurosci Lett* 481, 12–16.
88. Heidmann, D.E., Szot, P., Kohen, R., and Hamblin, M.W. (1998). Function and distribution of three rat 5-hydroxytryptamine<sub>7</sub> (5-HT<sub>7</sub>) receptor isoforms produced by alternative splicing. *Neuropharmacology* 37, 1621–1632.
89. Hennessy, M.B., Heybach, J.P., Vernikos, J., and Levine, S. (1979). Plasma corticosterone concentrations sensitively reflect levels of stimulus intensity in the rat. *Physiol Behav* 22, 821–825.
90. Hesselgrave, N., and Parsey, R.V. (2013). Imaging the serotonin 1A receptor using [<sup>11</sup>C]WAY100635 in healthy controls and major depression. *Philos Tran R Soc Lon Biol Sci* 368, 20120004.
91. Hiley, E., McMullan, R., and Nurrish, S.J. (2006). The Galph<sub>12</sub>-RGS RhoGEF-RhoA signalling pathway regulates neurotransmitter release in *C. elegans*. *EMBO J* 25, 5884–5895.
92. Hjorth, S. (1985). Hypothermia in the rat induced by the potent serotonergic agent 8-OH-DPAT. *J Neural Transmission* 61, 131–135.
93. Holliday, N.D., Watson, S.-J., and Brown, A.J.H. (2011). Drug discovery opportunities and challenges at G protein coupled receptors for long chain free Fatty acids. *Front Endocrinol (Lausanne)* 2, 112.
94. Horisawa, T., Ishiyama, T., Ono, M., Ishibashi, T., and Taiji, M. (2013). Binding of lurasidone, a novel antipsychotic, to rat 5-HT<sub>7</sub> receptor: analysis by [<sup>3</sup>H]SB-269970 autoradiography. *Prog Neuropsychopharmacol Biol Psychiatry* 40, 132–137.
95. Hornigold, D.C., Mistry, R., Raymond, P.D., Blank, J.L., and Challiss, R.A.J. (2003). Evidence for cross-talk between M<sub>2</sub> and M<sub>3</sub> muscarinic acetylcholine receptors in the regulation of second messenger and extracellular signal-regulated kinase signalling pathways in Chinese hamster ovary cells. *Br J Pharmacol* 138, 1340–1350.
96. Horwitz, A.V., Wakefield, J.C., and Lorenzo-Luaces, L. (2017). History of depression. *The Oxford Handbook of Mood Disorders*, Oxford University Press, 11-23.
97. Hoyer, D., Hannon, J.P., and Martin, G.R. (2002). Molecular, pharmacological and functional diversity of 5-HT receptors. *Pharmacol Biochem and Behav* 71, 533–554.

98. Hsiung, S., Adlersberg, M., Arango, V., Mann, J.J., Tamir, H., and Liu, K. (2003). Attenuated 5-HT<sub>1A</sub> receptor signaling in brains of suicide victims: involvement of adenylyl cyclase, phosphatidylinositol 3-kinase, Akt and mitogen-activated protein kinase. *J Neurochem* 87, 182–194.
99. Israilova, M., Tanaka, T., Suzuki, F., Morishima, S., and Muramatsu, I. (2004). Pharmacological characterization and cross talk of alpha<sub>1a</sub>- and alpha<sub>1b</sub>-adrenoceptors coexpressed in human embryonic kidney 293 cells. *J Pharmacol Exp Ther* 309, 259–266.
100. Jeltsch-David, H., Koenig, J., and Cassel, J.-C. (2008). Modulation of cholinergic functions by serotonin and possible implications in memory: general data and focus on 5-HT(1A) receptors of the medial septum. *Behav Brain Res* 195, 86–97.
101. Johnson-Farley, N.N., Kertesz, S.B., Dubyak, G.R., and Cowen, D.S. (2005). Enhanced activation of Akt and extracellular-regulated kinase pathways by simultaneous occupancy of G<sub>q</sub>-coupled 5-HT<sub>2A</sub> receptors and G<sub>s</sub>-coupled 5-HT<sub>7A</sub> receptors in PC12 cells. *J Neurochem* 92, 72–82.
102. Jordan, B.A., Gomes, I., Rios, C., Filipovska, J., and Devi, L.A. (2003). Functional interactions between mu opioid and alpha 2A-adrenergic receptors. *Mol Pharmacol* 64, 1317–1324.
103. Kachroo, A., Orlando, L.R., Grandy, D.K., Chen, J.-F., Young, A.B., and Schwarzschild, M.A. (2005). Interactions between metabotropic glutamate 5 and adenosine A<sub>2A</sub> receptors in normal and parkinsonian mice. *J Neurosci* 25, 10414–10419.
104. Katz, R.J., Roth, K.A., and Carroll, B.J. (1981). Acute and chronic stress effects on open field activity in the rat: implications for a model of depression. *Neurosci Biobehav Rev* 5, 247–251.
105. Kaufman, J., Sullivan, G.M., Yang, J., Ogden, R.T., Miller, J.M., Oquendo, M.A., Mann, J.J., Parsey, R.V., and DeLorenzo, C. (2015). Quantification of the Serotonin 1A Receptor Using PET: Identification of a Potential Biomarker of Major Depression in Males. *Neuropsychopharmacology* 40, 1692–1699.
106. Keim, K.L., and Sigg, E.B. (1976). Physiological and biochemical concomitants of restraint stress in rats. *Pharmacol Biochem Behav* 4, 289–297.
107. Kirby, E.D., Muroy, S.E., Sun, W.G., Covarrubias, D., Leong, M.J., Barchas, L.A., and Kaufer, D. (2013). Acute stress enhances adult rat hippocampal neurogenesis and activation of newborn neurons via secreted astrocytic FGF2. *Elife* 2, e00362.
108. Kobe, F., Renner, U., Woehler, A., Wlodarczyk, J., Pampusheva, E., Bao, G., Zeug, A., Richter, D.W., Neher, E., and Ponimaskin, E. (2008). Stimulation and palmitoylation-dependent changes in oligomeric conformation of serotonin 5-HT<sub>1A</sub> receptors. *Biochim Biophys Acta* 1783, 1503–1516.
109. Kobe, F., Guseva, D., Jensen, T.P., Wirth, A., Renner, U., Hess, D., Müller, M., Medrihan, L., Zhang, W., Zhang, M., et al. (2012). 5-HT<sub>7R</sub>/G<sub>12</sub> signaling regulates neuronal morphology and function in an age-dependent manner. *J Neurosci* 32, 2915–2930.
110. Kobilka, B.K. (2007). G protein coupled receptor structure and activation. *Biochim Biophys Acta* 1768, 794–807.
111. Krishnan, V., and Nestler, E.J. (2010). Linking molecules to mood: new insight into the biology of depression. *Am J Psychiatry* 167, 1305–1320.
112. Krobert, K.A., Bach, T., Syversveen, T., Kvingedal, A.M., and Levy, F.O. (2001). The cloned human 5-HT<sub>7</sub> receptor splice variants: a comparative characterization of their pharmacology, function and distribution. *Naunyn Schmiedebergs Arch Pharmacol* 363, 620–632.
113. Krobert, K.A., Andressen, K.W., and Levy, F.O. (2006). Heterologous desensitization is evoked by both agonist and antagonist stimulation of the human 5-HT(7) serotonin receptor. *Eur J Pharmacol* 532, 1–10.
114. Kroeger, K.M., Pflieger, K.D.G., and Eidne, K.A. (2003). G-protein coupled receptor oligomerization in neuroendocrine pathways. *Front Neuroendocrinol* 24, 254–278.
115. Krzystyniak, A., Baczynska, E., Magnowska, M., Antoniuk, S., Roszkowska, M., Zareba-Kozioł, M., Das, N., Basu, S., Pikula, M., and Wlodarczyk, J. (2019). Prophylactic Ketamine Treatment Promotes Resilience to Chronic Stress and Accelerates Recovery: Correlation with Changes in Synaptic Plasticity in the CA3 Subregion of the Hippocampus. *Int J Mol Sci* 20, 1726.
116. Kushwaha, N., and Albert, P.R. (2005). Coupling of 5-HT<sub>1A</sub> autoreceptors to inhibition of mitogen-activated protein kinase activation via G beta gamma subunit signaling. *Eur J Neurosci* 21, 721–732.

117. Kvachnina, E. (2005). 5-HT7 receptor is coupled to G subunits of heterotrimeric G12-protein to regulate gene transcription and neuronal morphology. *J Neurosci* 25, 7821–7830.
118. Kvachnina, E., Dumuis, A., Włodarczyk, J., Renner, U., Cochet, M., Richter, D.W., and Ponimaskin, E. (2009). Constitutive Gs-mediated, but not G12-mediated, activity of the 5-hydroxytryptamine 5-HT7(a) receptor is modulated by the palmitoylation of its C-terminal domain. *Biochim Biophys Acta* 1793, 1646–1655.
119. Lanzenberger, R., Baldinger, P., Hahn, A., Ungersboeck, J., Mitterhauser, M., Winkler, D., Micskei, Z., Stein, P., Karanikas, G., Wadsak, W., et al. (2013). Global decrease of serotonin-1A receptor binding after electroconvulsive therapy in major depression measured by PET. *Mol Psychiatry* 18, 93–100.
120. Laporte, A.M., Lima, L., Gozlan, H., and Hamon, M. (1994). Selective in vivo labelling of brain 5-HT1A receptors by [3H]WAY 100635 in the mouse. *Eur J Pharmacol* 271, 505–514.
121. Latacz, G., Hogendorf, A.S., Hogendorf, A., Lubelska, A., Wierońska, J.M., Woźniak, M., Cieślik, P., Kieć-Kononowicz, K., Handzlik, J., and Bojarski, A.J. (2018). Search for a 5-CT alternative. In vitro and in vivo evaluation of novel pharmacological tools: 3-(1-alkyl-1H-imidazol-5-yl)-1H-indole-5-carboxamides, low-basicity 5-HT<sub>7</sub> receptor agonists. *Medchemcomm* 9, 1882–1890.
122. Lee, S.P., So, C.H., Rashid, A.J., Varghese, G., Cheng, R., Lança, A.J., O'Dowd, B.F., and George, S.R. (2004). Dopamine D1 and D2 receptor co-activation generates a novel phospholipase C-mediated calcium signal. *J Biol Chem* 279, 35671–35678.
123. Lenox, R.H., Kant, G.J., Sessions, G.R., Pennington, L.L., Mougey, E.H., and Meyerhoff, J.L. (1980). Specific hormonal and neurochemical responses to different stressors. *Neuroendocrinology* 30, 300–308.
124. Leopoldo, M., Lacivita, E., Berardi, F., Perrone, R., and Hedlund, P.B. (2011). Serotonin 5-HT7 receptor agents: structure-activity relationships and potential therapeutic applications in central nervous system disorders. *Pharmacol Ther* 129, 120–148.
125. Li, Y.-C., Wang, F.-M., Pan, Y., Qiang, L.-Q., Cheng, G., Zhang, W.-Y., and Kong, L.-D. (2009). Antidepressant-like effects of curcumin on serotonergic receptor-coupled AC-cAMP pathway in chronic unpredictable mild stress of rats. *Prog Neuropsychopharmacol Biol Psychiatry* 33, 435–449.
126. Li, Z., Li, B., Song, X., and Zhang, D. (2017). Dietary zinc and iron intake and risk of depression: A meta-analysis. *Psychiatry Res* 251, 41–47.
127. Lidow, M.S., Goldman-Rakic, P.S., Gallager, D.W., and Rakic, P. (1989). Quantitative autoradiographic mapping of serotonin 5-HT1 and 5-HT2 receptors and uptake sites in the neocortex of the rhesus monkey. *J Comp Neurol* 280, 27–42.
128. Lin, S.L., Johnson-Farley, N.N., Lubinsky, D.R., and Cowen, D.S. (2003). Coupling of neuronal 5-HT7 receptors to activation of extracellular-regulated kinase through a protein kinase A-independent pathway that can utilize Epac. *J Neurochem* 87, 1076–1085.
129. Liu, J., and Jordan, L.M. (2005). Stimulation of the parapyramidal region of the neonatal rat brain stem produces locomotor-like activity involving spinal 5-HT7 and 5-HT2A receptors. *J Neurophysiol* 94, 1392–1404.
130. Liu, H., Irving, H.R., and Coupar, I.M. (2001). Expression patterns of 5-HT7 receptor isoforms in the rat digestive tract. *Life Sci* 69, 2467–2475.
131. Liu, X.-Y., Chu, X.-P., Mao, L.-M., Wang, M., Lan, H.-X., Li, M.-H., Zhang, G.-C., Parelkar, N.K., Fibuch, E.E., Haines, M., et al. (2006). Modulation of D2R-NR2B interactions in response to cocaine. *Neuron* 52, 897–909.
132. Liu, Y.F., Ghahremani, M.H., Rasenick, M.M., Jakobs, K.H., and Albert, P.R. (1999). Stimulation of cAMP synthesis by Gi-coupled receptors upon ablation of distinct Galphai protein expression. Gi subtype specificity of the 5-HT1A receptor. *J Biol Chem* 274, 16444–16450.
133. Livak, K.J., and Schmittgen, T.D. (2001). Analysis of relative gene expression data using real-time quantitative PCR and the 2<sup>-ΔΔC<sub>T</sub></sup>. *Methods* 25, 402–408.
134. Llamosas, N., Bruzos-Cidón, C., Rodríguez, J.J., Ugedo, L., and Torrecilla, M. (2015). Deletion of GIRK2 Subunit of GIRK Channels Alters the 5-HT1A Receptor-Mediated Signaling and Results in a Depression-Resistant Behavior. *Int J Neuropsychopharmacol* 18, pyvo51.

135. Lo Iacono, L., and Gross, C. (2008). Alpha-Ca<sup>2+</sup>/calmodulin-dependent protein kinase II contributes to the developmental programming of anxiety in serotonin receptor 1A knock-out mice. *J Neurosci* 28, 6250–6257.
136. López-Figueroa, A.L., Norton, C.S., López-Figueroa, M.O., Armellini-Dodel, D., Burke, S., Akil, H., López, J.F., and Watson, S.J. (2004). Serotonin 5-HT<sub>1A</sub>, 5-HT<sub>1B</sub>, and 5-HT<sub>2A</sub> receptor mRNA expression in subjects with major depression, bipolar disorder, and schizophrenia. *Biol Psychiatry* 55, 225–233.
137. López-Gil, X., Artigas, F., and Adell, A. (2010). Unraveling monoamine receptors involved in the action of typical and atypical antipsychotics on glutamatergic and serotonergic transmission in prefrontal cortex. *Curr Pharm Des* 16, 502–515.
138. Lovenberg, T.W., Baron, B.M., de Lecea, L., Miller, J.D., Prosser, R.A., Rea, M.A., Foye, P.E., Racke, M., Slone, A.L., and Siegel, B.W. (1993). A novel adenylyl cyclase-activating serotonin receptor (5-HT<sub>7</sub>) implicated in the regulation of mammalian circadian rhythms. *Neuron* 11, 449–458.
139. Luker, G.D., Sharma, V., Pica, C.M., Dahlheimer, J.L., Li, W., Ochesky, J., Ryan, C.E., Piwnica-Worms, H., and Piwnica-Worms, D. (2002). Noninvasive imaging of protein–protein interactions in living animals. *Proc Natl Acad Sci USA* 99, 6961–6966.
140. Marsden, W.N. (2013). Synaptic plasticity in depression: molecular, cellular and functional correlates. *Prog Neuropsychopharmacol Biol Psychiatry* 43, 168–184.
141. Marshall, F.H., White, J., Main, M., Green, A., and Wise, A. (1999). GABA(B) receptors function as heterodimers. *Biochem Soc Trans* 27, 530–535.
142. Masi, G., and Brovedani, P. (2011). The hippocampus, neurotrophic factors and depression: possible implications for the pharmacotherapy of depression. *CNS Drugs* 25, 913–931.
143. Matar, M.A., Zohar, J., and Cohen, H. (2013). Translationally relevant modeling of PTSD in rodents. *Cell Tissue Res* 354, 127–139.
144. Matthiessen, L., Daval, G., Bailly, Y., Gozlan, H., Hamon, M., and Vergé, D. (1992). Quantification of 5-hydroxytryptamine<sub>1A</sub> receptors in the cerebellum of normal and X-irradiated rats during postnatal development. *Neuroscience* 51, 475–485.
145. Ménard, C., Pfau, M.L., Hodes, G.E., and Russo, S.J. (2017). Immune and Neuroendocrine Mechanisms of Stress Vulnerability and Resilience. *Neuropsychopharmacology* 42, 62–80.
146. Meyerhof, W., Obermüller, F., Fehr, S., and Richter, D. (1993). A novel rat serotonin receptor: primary structure, pharmacology, and expression pattern in distinct brain regions. *DNA Cell Biology* 12, 401–409.
147. Milligan, G. (2007). G protein-coupled receptor dimerization: molecular basis and relevance to function. *Biochim Biophys Acta* 1768, 825–835.
148. Milligan, G., Ulven, T., Murdoch, H., and Hudson, B.D. (2014). G-protein-coupled receptors for free fatty acids: nutritional and therapeutic targets. *Br J Nutr* 111 Suppl 1, S3–7.
149. Mogha, A., Guariglia, S.R., Debata, P.R., Wen, G.Y., and Banerjee, P. (2012). Serotonin 1A receptor-mediated signaling through ERK and PKC $\alpha$  is essential for normal synaptogenesis in neonatal mouse hippocampus. *Transl Psychiatry* 2, e66.
150. Muscat, R., and Willner, P. (1992). Suppression of sucrose drinking by chronic mild unpredictable stress: a methodological analysis. *Neurosci Biobehav Rev* 16, 507–517.
151. Naumenko, V.S., Popova, N.K., Lacivita, E., Leopoldo, M., and Ponimaskin, E.G. (2014). Interplay between serotonin 5-HT<sub>1A</sub> and 5-HT<sub>7</sub> receptors in depressive disorders. *CNS Neurosci Ther* 20, 582–590.
152. Nichols, D.E., and Nichols, C.D. (2008). Serotonin receptors. *Chem Rev* 108, 1614–1641.
153. Odio, M.R., and Maickel, R.P. (1985). Comparative biochemical responses of rats to different stressful stimuli. *Physiol Behav* 34, 595–599.
154. Overmier, J.B., and Seligman, M.E. (1967). Effects of inescapable shock upon subsequent escape and avoidance responding. *J Comp Physiol Psychol* 63, 28–33.
155. Pacák, K., Palkovits, M., Kvetnanský, R., Yadid, G., Kopin, I.J., and Goldstein, D.S. (1995). Effects of various stressors on in vivo norepinephrine release in the hypothalamic paraventricular nucleus and on the pituitary-adrenocortical axis. *Ann N Y Acad Sci* 771, 115–130.

156. Paila, Y.D., Kombrabail, M., Krishnamoorthy, G., and Chattopadhyay, A. (2011). Oligomerization of the serotonin(1A) receptor in live cells: a time-resolved fluorescence anisotropy approach. *J Phys Chem B* 115, 11439–11447.
157. Panetta, R., and Greenwood, M.T. (2008). Physiological relevance of GPCR oligomerization and its impact on drug discovery. *Drug Discov Today* 13, 1059–1066.
158. Papp, M. (2012). Models of affective illness: chronic mild stress in the rat. *Curr Protoc Pharmacol Chapter 5*, Unit 5.9.
159. Parsey, R.V., Ogden, R.T., Miller, J.M., Tin, A., Hesselgrave, N., Goldstein, E., Mikhno, A., Milak, M., Zanderigo, F., Sullivan, G.M., et al. (2010). Higher serotonin 1A binding in a second major depression cohort: modeling and reference region considerations. *Biol Psychiatry* 68, 170–178.
160. Pereira, A.C., Carvalho, M.C., and Padovan, C.M. (2019). Both serotonergic and noradrenergic systems modulate the development of tolerance to chronic stress in rats with lesions of the serotonergic neurons of the median raphe nucleus. *Behav Brain Res* 357–358, 39–47.
161. Piszczek, L., Piszczek, A., Kuczmanska, J., Audero, E., and Gross, C.T. (2015). Modulation of anxiety by cortical serotonin 1A receptors. *Front Behav Neurosci* 9, 48.
162. Plassat, J.L., Amlaiky, N., and Hen, R. (1993). Molecular cloning of a mammalian serotonin receptor that activates adenylate cyclase. *Mol Pharmacol* 44, 229–236.
163. Ponimaskin, E.G., Profirovic, J., Vaiskunaite, R., Richter, D.W., and Voyno-Yasenetskaya, T.A. (2002). 5-Hydroxytryptamine 4(a) receptor is coupled to the Galpha subunit of heterotrimeric G13 protein. *J Biol Chem* 277, 20812–20819.
164. Porsolt, R.D., Le Pichon, M., and Jalfre, M. (1977). Depression: a new animal model sensitive to antidepressant treatments. *Nature* 266, 730–732.
165. Prasad, S., Ponimaskin, E., and Zeug, A. (2019). Serotonin receptor oligomerization regulates cAMP-based signaling. *J. Cell. Sci.* 132, jcs230334.
166. Purkayastha, S., Ford, J., Kanjilal, B., Diallo, S., Del Rosario Inigo, J., Neuwirth, L., El Idrissi, A., Ahmed, Z., Wieraszko, A., Azmitia, E.C., et al. (2012). Clozapine functions through the prefrontal cortex serotonin 1A receptor to heighten neuronal activity via calmodulin kinase II-NMDA receptor interactions. *J Neurochem* 120, 396–407.
167. Puścian, A., Łęski, S., Kasprowicz, G., Winiarski, M., Borowska, J., Nikolaev, T., Boguszewski, P.M., Lipp, H.-P., and Knapska, E. (2016). Eco-HAB as a fully automated and ecologically relevant assessment of social impairments in mouse models of autism. *ELife* 5, e19532.
168. Qiao, H., An, S.-C., Ren, W., and Ma, X.-M. (2014). Progressive alterations of hippocampal CA3-CA1 synapses in an animal model of depression. *Behav Brain Res* 275, 191–200.
169. Rapport, M.M., Green, A.A., and Page, I.H. (1948). Crystalline serotonin. *Science* 108, 329–330.
170. Renaud, S. (1959). Improved restraint-technique for producing stress and cardiac necrosis in rats. *J Appl Physiol* 14, 868–869.
171. Renner, U., Glebov, K., Lang, T., Papusheva, E., Balakrishnan, S., Keller, B., Richter, D.W., Jahn, R., and Ponimaskin, E. (2007). Localization of the mouse 5-Hydroxytryptamine1A receptor in lipid microdomains depends on its palmitoylation and is involved in receptor-mediated signaling. *Mol Pharmacol* 72, 502–513.
172. Renner, U., Zeug, A., Woehler, A., Niebert, M., Dityatev, A., Dityateva, G., Gorinski, N., Guseva, D., Abdel-Galil, D., Fröhlich, M., et al. (2012). Heterodimerization of serotonin receptors 5-HT1A and 5-HT7 differentially regulates receptor signalling and trafficking. *J Cell Sci* 125, 2486–2499.
173. Resh, M.D. (2006). Palmitoylation of ligands, receptors, and intracellular signaling molecules. *Sci STKE* 2006, re14.
174. Riad, M., Garcia, S., Watkins, K.C., Jodoin, N., Doucet, E., Langlois, X., el Mestikawy, S., Hamon, M., and Descarries, L. (2000). Somatodendritic localization of 5-HT1A and preterminal axonal localization of 5-HT1B serotonin receptors in adult rat brain. *J Comp Neurol* 417, 181–194.
175. Rozenfeld, R., and Devi, L.A. (2010). Receptor heteromerization and drug discovery. *Trends Pharmacol Sci* 31, 124–130.

176. Ruat, M., Traiffort, E., Leurs, R., Tardivel-Lacombe, J., Diaz, J., Arrang, J.M., and Schwartz, J.C. (1993). Molecular cloning, characterization, and localization of a high-affinity serotonin receptor (5-HT<sub>7</sub>) activating cAMP formation. *Proc Natl Acad Sci USA* 90, 8547–8551.
177. Santana, N., Bortolozzi, A., Serrats, J., Mengod, G., and Artigas, F. (2004). Expression of serotonin<sub>1A</sub> and serotonin<sub>2A</sub> receptors in pyramidal and GABAergic neurons of the rat prefrontal cortex. *Cereb Cortex* 14, 1100–1109.
178. Sargent, P.A., Kjaer, K.H., Bench, C.J., Rabiner, E.A., Messa, C., Meyer, J., Gunn, R.N., Grasby, P.M., and Cowen, P.J. (2000). Brain serotonin<sub>1A</sub> receptor binding measured by positron emission tomography with [<sup>11</sup>C]WAY-100635: effects of depression and antidepressant treatment. *Arch Gen Psychiatry* 57, 174–180.
179. Savitz, J., Lucki, I., and Drevets, W.C. (2009). 5-HT<sub>1A</sub> receptor function in major depressive disorder. *Prog Neurobiol* 88, 17–31.
180. Scheltens, P. (1999). Early diagnosis of dementia: neuroimaging. *J Neurol* 246, 16–20.
181. Schildkraut, J.J. (1965). The catecholamine hypothesis of affective disorders: a review of supporting evidence. *Am J Psychiatry* 122, 509–522.
182. Schoeffter, P., Ullmer, C., Bobirnac, I., Gabbiani, G., and Lübbert, H. (1996). Functional, endogenously expressed 5-hydroxytryptamine 5-HT<sub>7</sub> receptors in human vascular smooth muscle cells. *Br J Pharmacol* 117, 993–994.
183. Schoenfeld, T.J., McCausland, H.C., Morris, H.D., Padmanaban, V., and Cameron, H.A. (2017). Stress and Loss of Adult Neurogenesis Differentially Reduce Hippocampal Volume. *Biol Psychiatry* 82, 914–923.
184. Schwarzschild, M.A., Agnati, L., Fuxe, K., Chen, J.-F., and Morelli, M. (2006). Targeting adenosine A<sub>2A</sub> receptors in Parkinson's disease. *Trends Neurosci* 29, 647–654.
185. Senese, N.B., Rasenick, M.M., and Traynor, J.R. (2018). The Role of G-proteins and G-protein Regulating Proteins in Depressive Disorders. *Front Pharmacol* 9.
186. Shen, Y., Monsma, F.J., Metcalf, M.A., Jose, P.A., Hamblin, M.W., and Sibley, D.R. (1993). Molecular cloning and expression of a 5-hydroxytryptamine<sub>7</sub> serotonin receptor subtype. *J Biol Chem* 268, 18200–18204.
187. Shimizu, M., Nishida, A., Zensho, H., and Yamawaki, S. (1996). Chronic antidepressant exposure enhances 5-hydroxytryptamine<sub>7</sub> receptor-mediated cyclic adenosine monophosphate accumulation in rat frontocortical astrocytes. *J Pharmacol Exp Ther* 279, 1551–1558.
188. Shively, C.A., Friedman, D.P., Gage, H.D., Bounds, M.C., Brown-Proctor, C., Blair, J.B., Henderson, J.A., Smith, M.A., and Buchheimer, N. (2006). Behavioral depression and positron emission tomography-determined serotonin 1A receptor binding potential in cynomolgus monkeys. *Arch Gen Psychiatry* 63, 396–403.
189. Slattery, D.A., and Cryan, J.F. (2017). Modelling depression in animals: at the interface of reward and stress pathways. *Psychopharmacology (Berl)* 234, 1451–1465.
190. Speranza, L., Chambery, A., Di Domenico, M., Crispino, M., Severino, V., Volpicelli, F., Leopoldo, M., Bellenchi, G.C., di Porzio, U., and Perrone-Capano, C. (2013). The serotonin receptor 7 promotes neurite outgrowth via ERK and Cdk5 signaling pathways. *Neuropharmacology* 67, 155–167.
191. Steru, L., Chermat, R., Thierry, B., and Simon, P. (1985). The tail suspension test: a new method for screening antidepressants in mice. *Psychopharmacology (Berl)* 85, 367–370.
192. Stockholm, D., Bartoli, M., Sillon, G., Bourg, N., Davoust, J., and Richard, I. (2005). Imaging calpain protease activity by multiphoton FRET in living mice. *J Mol Biol* 346, 215–222.
193. Stockmeier, C.A., Shapiro, L.A., Dilley, G.E., Kolli, T.N., Friedman, L., and Rajkowska, G. (1998). Increase in serotonin-1A autoreceptors in the midbrain of suicide victims with major depression: postmortem evidence for decreased serotonin activity. *J Neurosci* 18, 7394–7401.
194. Storrington, J.M., Charest, A., Cheng, P., and Albert, P.R. (1999). TATA-driven transcriptional initiation and regulation of the rat serotonin 5-HT<sub>1A</sub> receptor gene. *J Neurochem* 72, 2238–2247.
195. Strekalova, T., and Steinbusch, H.W.M. (2010). Measuring behavior in mice with chronic stress depression paradigm. *Prog Neuropsychopharmacol Biol Psychiatry* 34, 348–361.

196. Takano, H., Ito, H., Takahashi, H., Arakawa, R., Okumura, M., Kodaka, F., Otsuka, T., Kato, M., and Suhara, T. (2011). Serotonergic neurotransmission in the living human brain: a positron emission tomography study using [<sup>11</sup>C]dasb and [<sup>11</sup>C]WAY100635 in young healthy men. *Synapse* 65, 624–633.
197. Takeda, H., Tsuji, M., Ikoshi, H., Yamada, T., Masuya, J., Imori, M., and Matsumiya, T. (2005). Effects of a 5-HT<sub>7</sub> receptor antagonist DR4004 on the exploratory behavior in a novel environment and on brain monoamine dynamics in mice. *Eur J Pharmacol* 518, 30–39.
198. Tang, W.J., and Gilman, A.G. (1991). Type-specific regulation of adenylyl cyclase by G protein beta gamma subunits. *Science* 254, 1500–1503.
199. Tang, Z.-Q., and Trussell, L.O. (2015). Serotonergic regulation of excitability of principal cells of the dorsal cochlear nucleus. *J Neurosci* 35, 4540–4551.
200. Thomas, D.R., Middlemiss, D.N., Taylor, S.G., Nelson, P., and Brown, A.M. (1999). 5-CT stimulation of adenylyl cyclase activity in guinea-pig hippocampus: evidence for involvement of 5-HT<sub>7</sub> and 5-HT<sub>1A</sub> receptors. *Br J Pharmacol* 128, 158–164.
201. Trifilieff, P., Rives, M.-L., Urizar, E., Piskorowski, R.A., Vishwasrao, H.D., Castrillon, J., Schmauss, C., Slättman, M., Gullberg, M., and Javitch, J.A. (2011). Detection of antigen interactions ex vivo by proximity ligation assay: endogenous dopamine D<sub>2</sub>-adenosine A<sub>2A</sub> receptor complexes in the striatum. *Biotechniques* 51, 111–118.
202. Tuladhar, B.R., Ge, L., and Naylor, R.J. (2003). 5-HT<sub>7</sub> receptors mediate the inhibitory effect of 5-HT on peristalsis in the isolated guinea-pig ileum. *Br J Pharmacol* 138, 1210–1214.
203. Twarog, B.M., and Page, I.H. (1953). Serotonin content of some mammalian tissues and urine and a method for its determination. *Am J Physiol* 175, 157–161.
204. Wacker, D., Wang, C., Katritch, V., Han, G.W., Huang, X.-P., Vardy, E., McCorvy, J.D., Jiang, Y., Chu, M., Siu, F.Y., et al. (2013). Structural features for functional selectivity at serotonin receptors. *Science* 340, 615–619.
205. Waldhoer, M., Fong, J., Jones, R.M., Lunzer, M.M., Sharma, S.K., Kostenis, E., Portoghese, P.S., and Whistler, J.L. (2005). A heterodimer-selective agonist shows in vivo relevance of G protein-coupled receptor dimers. *Proc Natl Acad Sci USA* 102, 9050–9055.
206. Wang, C., Jiang, Y., Ma, J., Wu, H., Wacker, D., Katritch, V., Han, G.W., Liu, W., Huang, X.-P., Vardy, E., et al. (2013). Structural basis for molecular recognition at serotonin receptors. *Science* 340, 610–614.
207. Wesolowska, A., Nikiforuk, A., Stachowicz, K., and Tatarczyńska, E. (2006). Effect of the selective 5-HT<sub>7</sub> receptor antagonist SB 269970 in animal models of anxiety and depression. *Neuropharmacology* 51, 578–586.
208. Willner, P. (1997). Validity, reliability and utility of the chronic mild stress model of depression: a 10-year review and evaluation. *Psychopharmacology (Berl)* 134, 319–329.
209. Willner, P. (2017). The chronic mild stress (CMS) model of depression: History, evaluation and usage. *Neurobiol Stress* 6, 78–93.
210. Wirth, A., Holst, K., and Ponimaskin, E. (2017). How serotonin receptors regulate morphogenic signalling in neurons. *Prog Neurobiol* 151, 35–56.
211. Woehler, A., Wlodarczyk, J., and Ponimaskin, E.G. (2009). Specific oligomerization of the 5-HT<sub>1A</sub> receptor in the plasma membrane. *Glycoconj J* 26, 749–756.
212. Woolley, D.W., and Shaw, E. (1954). A BIOCHEMICAL AND PHARMACOLOGICAL SUGGESTION ABOUT CERTAIN MENTAL DISORDERS. *Proc Natl Acad Sci USA* 40, 228–231.
213. Wright, D.E., Seroogy, K.B., Lundgren, K.H., Davis, B.M., and Jennes, L. (1995). Comparative localization of serotonin<sub>1A</sub>, <sub>1C</sub>, and <sub>2</sub> receptor subtype mRNAs in rat brain. *J Comp Neurol* 351, 357–373.
214. Yirmiya, R., and Goshen, I. (2011). Immune modulation of learning, memory, neural plasticity and neurogenesis. *Brain Behav Immun* 25, 181–213.
215. Yuen, E.Y., Jiang, Q., Chen, P., Gu, Z., Feng, J., and Yan, Z. (2005). Serotonin 5-HT<sub>1A</sub> receptors regulate NMDA receptor channels through a microtubule-dependent mechanism. *J Neurosci* 25, 5488–5501.

216. Yuen, E.Y., Jiang, Q., Chen, P., Feng, J., and Yan, Z. (2008). Activation of 5-HT<sub>2A/C</sub> receptors counteracts 5-HT<sub>1A</sub> regulation of n-methyl-D-aspartate receptor channels in pyramidal neurons of prefrontal cortex. *J Biol Chem* 283, 17194–17204.
217. Zheng, H., Loh, H.H., and Law, P.-Y. (2013). Posttranslation modification of G protein-coupled receptor in relationship to biased agonism. *Methods Enzymol* 522, 391–408.
218. Zhong, P., Yuen, E.Y., and Yan, Z. (2008). Modulation of neuronal excitability by serotonin-NMDA interactions in prefrontal cortex. *Mol Cell Neurosci* 38, 290–299.
219. Zoli, M., Agnati, L.F., Hedlund, P.B., Li, X.M., Ferré, S., and Fuxe, K. (1993). Receptor-receptor interactions as an integrative mechanism in nerve cells. *Mol Neurobiol* 7, 293–334.
220. Zunszain, P.A., Anacker, C., Cattaneo, A., Carvalho, L.A., and Pariante, C.M. (2011). Glucocorticoids, cytokines and brain abnormalities in depression. *Prog Neuropsychopharmacol Biol Psychiatry* 35, 722–729.

## CURRICULUM VITAE

<b>Name:</b>	Svitlana Antoniuk
<b>Birth:</b>	22/06/1991 (Kyiv district, Ukraine)
<b>Education:</b>	
<b>2008 – 2012</b>	Bachelor Degree: Biotechnology, National University of Food Technologies (Kyiv, Ukraine). Supervisor: Prof. Pyrog Tetiana Grade: Honors
<b>2012 – 2013</b>	Master degree: Biotechnology, National University of Food Technologies (Kyiv, Ukraine). Supervisor: Prof. Pyrog Tetiana Grade: Honors
<b>2015 – 2021</b>	PhD. Program: Bio4Med International PhD Program, Nencki Institute of Experimental Biology (Warsaw, Poland) Laboratory: Cell Biophysics Supervisors: Prof. J. Wlodarczyk, PhD, DSc. Prof. E. Ponimaskin, PhD, DSc.
<b>Apprenticeships:</b>	
<b>1/01/2017 – 30/05/2017</b> <b>1/06/2018 – 30/04/2020</b>	Department of Cellular Neurophysiology Hannover Medical School (Hannover, Germany) Supervisor: Prof. E. Ponimaskin, PhD, DSc.
<b>10 – 18/12/2018</b>	Department of Neuroscience Karolinska Institute (Stockholm, Sweden) Supervisor: Prof. Kjell Fuxe, PhD, DSc.

## PUBLICATIONS

1. **Antoniuk, S.**, Bijata, M., Ponimaskin, E., Wlodarczyk, J. (2019). Chronic unpredictable mild stress for modeling depression in rodents: Meta-analysis of model reliability. *Neurosci Biobehav Rev* 99, 101–116.
2. Krzystyniak, A., Baczynska, E., Magnowska, M., **Antoniuk, S.**, Roszkowska, M., Zareba-Kozioł, M., Das, N., Basu, S., Pikula, M., and Wlodarczyk, J. (2019) Prophylactic Ketamine Treatment Promotes Resilience to Chronic Stress and Accelerates Recovery: Correlation With Changes in Synaptic Plasticity in the CA3 Subregion of the Hippocampus. *Int J Mol Sci* 20 (7), 1726.
3. Müller, F.E., Schad, S.K., Cherkas, V., Stopper, L., Breithausen B., Minge, D., Varbanov, H., Wahl-Schott, C., **Antoniuk, S.**, Domingos, C., Compan, V., Kirchhoff, F., Henneberger, C., Ponimaskin, E., Zeug, A. (2021). Serotonin receptor 4 regulates hippocampal astrocyte morphology and function. *Glia* 69 (4), 872–889.